

PHYSICS IV 2016

Quantum Corrections in Left-Right Symmetric Seesaw Mechanisms

Ruihao Li

Supervisor: Dr. Michael Schmidt

Particle Physics Group,
School of Physics,
The University of Sydney.



THE UNIVERSITY OF
SYDNEY

Date: October 30, 2016

Abstract

Neutrinos are one of the most elusive particles in the Universe and they have tiny masses, as confirmed by oscillation experiments. The seesaw mechanism provides an appealing way to produce neutrino masses, which are associated with the dimension-5 Weinberg operator in the effective field theory. The seesaw mechanism is naturally embedded in the minimal left-right (LR) symmetric model, from which one can obtain a seesaw relation that relates the active neutrino masses to some other parameters in the LR symmetric model. However, these parameters may receive large quantum corrections when they evolve to lower energies, which will result in the violation of the seesaw relation. The quantum corrections are characterized by the renormalization group equations (RGEs), or β -functions.

In this project, we perform the RG analysis of the effective coupling of the Weinberg operator between the electroweak and the LR symmetry breaking scales. We consider the two-Higgs doublet model (2HDM) with the additional right-handed neutrinos and $SU(2)_L$ scalar triplet and derive the β -function for the effective coupling at one-loop level. We find that the antisymmetric part of the β -function contributes to the neutrino masses only via RG evolution, while the symmetric part contributes directly after spontaneous symmetry breaking. At the end, we emphasize the importance of this work by highlighting a few of its phenomenological implications.

Acknowledgements

First and foremost, I would like to thank my supervisor, Michael Schmidt, for so many things: introducing me to the field of particle physics from the third-year special project, providing lots of valuable advices related and unrelated to this project, proofreading my draft thesis for so many times, being very understanding when I sometimes didn't complete the task or had to reschedule our meeting, and most importantly, always taking his time to answer my questions, no matter how trivial they are. I would also like to thank the whole particle physics group, staff and students, for their support and great discussions about physics, particularly during the journal clubs. I also need to thank my friends, many of whom I could only reach via phone and Internet, for always motivating me to get better. Last but not least, I am extremely grateful to my parents for their continuous support and care over these years.

Statement of Student Contribution

This project was proposed by my supervisor, Michael Schmidt, and it mainly involves analytically evaluating one-loop Feynman diagrams and deriving the β -function for the effective vertex. In the past, the β -function for the effective vertex was derived for the Standard Model (SM), the Minimal Supersymmetric Standard Model (MSSM), and the Two Higgs Doublet Model (2HDM) with discrete \mathbb{Z}_2 symmetry. My project was to generalize this result for an n Higgs doublet model, plus the contributions from the right-handed (RH) neutrinos and the $SU(2)_L$ scalar triplet. This serves as the first step of the renormalization group (RG) analysis for the left-right symmetric model (LRSM), which has connections with grand unified theories (GUTs) and can generate neutrino masses via the seesaw mechanism. In this project, the specific work that I have done (with the aid of my supervisor) includes:

- Verified the effective Weinberg operator for the type-I seesaw mechanism by deriving the equations of motion for the RH neutrinos. It is shown in Section 3.2
- Derived the Feynman rules for the Higgs self-interaction and the effective vertex in the general 2HDM. Most of the other Feynman rules can be generalized in a straightforward way from the ones for the SM. This is shown in Appendix D.
- Determined the relevant Feynman diagrams in the 2HDM and calculated the corrections to the wavefunctions of the Higgs doublets and the lepton doublets, as well as to the effective vertex. This is shown in Section 4.2.
- Generalized the original β -function derivation to make it applicable to tensorial quantities with two different sets of indices, and derived the β -function for the effective coupling specifically. Part of it was cross-checked by Michael to ensure the correctness. I also determined the symmetric and antisymmetric parts of the β function. This is shown in Section 4.3.
- Calculated the contributions from the RH neutrinos and the $SU(2)_L$ scalar triplet to the effective coupling β -function. This is shown in Section 4.4.

*I certify that this report contains work carried out
by myself except where otherwise acknowledged.*

Signed

Date: October 30, 2016

Contents

1	Introduction	1
2	Survey of the Subject	3
2.1	Neutrino Masses	3
2.1.1	Experimental developments in neutrino masses and mixings	3
2.1.2	Origins of the small neutrino masses	5
2.2	Renormalization	6
2.2.1	Regularization methods	7
2.2.2	Renormalization schemes	8
2.2.3	Renormalization group equations	9
3	General Framework	10
3.1	Fermion Mass Terms	10
3.1.1	Helicity and chirality	10
3.1.2	Particle-antiparticle conjugation and charge conjugation	11
3.1.3	Dirac and Majorana mass terms	13
3.2	Seesaw Mechanisms	14
3.3	Left-Right Symmetry	17
3.3.1	Gauge left-right symmetry	17
3.3.2	Discrete left-right symmetry	19
4	RG Evolution of the Effective Coupling	21
4.1	Relevant Particles	21
4.2	Renormalization of the 2HDM	22
4.2.1	Higgs wavefunction renormalization	23
4.2.2	Left-handed lepton wavefunction renormalization	26
4.2.3	Effective vertex renormalization	27
4.3	Calculation of the β -Function	30
4.4	Beyond the 2HDM	33
5	Conclusion	35
	Bibliography	36
A	The Standard Model (SM) and the Left-Right Symmetric Model (LRSM)	44
A.1	Particle Contents of the SM	44

A.2 Particle Contents of the LRSM	45
B Dimensional Regularization	46
B.1 Feynman Parameters	46
B.2 Wick Rotations	46
B.3 Dimensional Regularization	47
B.4 Passarino-Veltman Functions	48
C Seesaw Mechanisms in Feynman Diagrams	51
D Summary of the Relevant Feynman Rules	53
Acronyms	56

Chapter 1

Introduction

The aim of particle physics is to understand the fundamental building blocks of the Universe, known as elementary particles, and their interactions. In the quest for a coherent and elegant mathematical framework that captures basic physical laws which govern these particles in a unified way, the Standard Model (SM), is arguably one of the most splendid triumphs in particle physics that fulfilled this goal. Over the past few decades, it has become one of the most well-tested physical theories and a fundamental paradigm. It describes the three fundamental interactions (the electromagnetic, weak and strong interactions) between all elementary particles known to date, including leptons, quarks, gauge bosons and the Higgs boson¹ [1]. Mathematically, the SM is a gauge theory based on the gauge symmetry group $G_{SM} = SU(3)_C \times SU(2)_L \times U(1)_Y$ ², where $SU(2)_L \times U(1)_Y$ describes the electroweak interaction (the unification of electromagnetic and weak interactions) between leptons and quarks, and $SU(3)_C$ encapsulates the strong interaction between the colored quarks [2]. Throughout the years, the SM has explained most of experimental results in particle physics and faithfully predicted multiple phenomena to high accuracy, for example, the prediction of W^\pm and Z^0 bosons including their masses were first experimentally confirmed in 1983 [3, 4, 5, 6]. More recently, the discovery of the Higgs boson [7, 8] offers another cogent piece of evidence that validates the SM.

Despite the overall success of the Standard Model, it also leaves some open questions which cannot be answered within its framework, one of which is regarding the origin of neutrino masses. The neutrinos are assumed to be massless in the SM, i.e. they do not obtain masses via the Higgs mechanism³ as other fermions in the SM do. However, the evidence for neutrino flavor oscillations initially reported by the Super-Kamiokande (Super-K) experiment [10] suggests that neutrinos have non-zero masses. To explain the active neutrino masses, we need to seek for new theories beyond the SM. One of the simplest and most appealing solutions is the so-called seesaw mechanism [11]. The electrically neutral nature of neutrinos raises the possibility that they may be Majorana fermions, which are their own antiparticles. In the conventional seesaw mechanism, neutrinos naturally contain Majorana mass terms in the Lagrangian and their small masses can be realized through the exchange of heavy particles at some high energy scale. Three types of seesaw mechanism are often considered, depending on what kind of heavy particle is introduced.

The other problem that the SM bears is that the theory itself contains too many free parameters, such as masses of different particles, mixing angles and coupling constants, making it unlikely to be the ‘ultimate’ complete theory of nature. As the work by Glashow, Weinberg and Salam (known as the GWS theory) [12, 13, 14] showed that the electromagnetic and weak forces can be unified into a single electroweak force at a sufficiently high energy scale, it is rational to speculate that at an even higher energy scale, the strong and electroweak interactions can also be unified, thus reducing the number of independent parameters in the theory. Such theories are called the Grand Unified Theories (GUTs). In the language of group theory, this means that there exists a larger symmetry group which contains the SM gauge group G_{SM} . Two of the earliest candidates of this kind are $SU(5)$, first proposed by Georgi and Glashow [15], and $SO(10)$, appeared in a paper by Georgi [16] shortly after the proposal of $SU(5)$. In relation to neutrino mass generation, the GUT

¹The particle contents of the Standard Model (SM) and their transformation properties under the SM gauge group are summarized in Appendix A.

²Here C is used to designate the color charge of quarks and gluons, whose symmetry is represented by the $SU(3)$ group. L represents the left-handed weak isospin which is associated with the symmetry group $SU(2)$. Y is known as the hypercharge that has $U(1)$ symmetry.

³The Higgs mechanism was developed from the idea of spontaneous symmetry breaking (SSB). It is used to explain the mass generation for the SM particles. For a detailed illustration of the Higgs mechanism, refer to [9].

group $SO(10)$ in particular, was found to encompass the a modest extension of the SM called the left-right (LR) symmetric model⁴ [17] due to its additional $B - L$ gauge symmetry⁵. In the LR symmetric framework, the right-handed neutrinos and the triplet Higgs are naturally present and thus can induce active neutrino masses via type-I and type-II seesaw mechanisms.

Due to its interesting nature and potential for providing an economical solution to both issues of the SM, various LR symmetric seesaw scenarios had been investigated in the past [18, 19, 20]. In the work by Akhmedov and Frigerio [21], they obtained a simplified LR symmetric seesaw relation by imposing a discrete LR symmetry, the charge conjugation symmetry, in addition to the gauge LR symmetry. They demonstrated that this seesaw relation is analytically solvable. The technique developed in their papers was found to be applicable in various specific models with renormalizable Yukawa couplings, for example, $SO(10)$ [22]. Albeit its significant implications in model building, it should be noted that different parameters in the LR symmetric seesaw relation will receive different loop corrections, i.e. quantum corrections when the renormalization group (RG) evolution runs to lower energies. Therefore, the discrete LR symmetry must be broken at some energy scale and below this scale, their results will need to be modified.

Our aim is to study how the quantum corrections up to one loop will alter the LR symmetric seesaw relation below the discrete LR symmetry breaking scale. As the first step towards this aim, in this thesis we will inspect the RG evolution of the effective vertex, which is related to the SM neutrino masses, from the electroweak scale to higher energy scales. In Chapter 2, we will give a brief overview of the subject matter, including the current experimental states of neutrino masses and mixings, various proposals for neutrino mass generation, and a concise introduction to the notion of regularization and renormalization. In Chapter 3, we will first attempt to clarify a few relevant concepts for the discussion of later parts. Then the seesaw mechanism and the left-right symmetric model (LRSM), which form the framework of this study, will be introduced. We will also show the connections between them and how the LR symmetric seesaw relation is obtained. The importance of the quantum corrections to this model is emphasized at the end and we shall see why RG analysis is needed. Then in Chapter 4, we will first identify the relevant particles for the RG evolution from the electroweak scale up to the LR symmetry breaking scale, and argue that the quantum corrections in this regime mainly affects the effective operator for the neutrino masses. Then based on the previous analysis, we will present the results of the one-loop renormalization in the two Higgs doublet model (2HDM). After obtaining corrections for the relevant renormalization constants, we will apply them to derive the β -function of the effective coupling, which essentially determines how the coupling evolves with energy. We will also add the right-handed neutrinos and the $SU(2)_L$ scalar triplet into the model as the first step to go beyond the 2HDM, i.e. to higher energies, and determine their contributions to the β -function of the effective coupling. At the end, we will investigate the implication of this β -function to the neutrino mass in general. First, as we shall, it is associated with the symmetric and antisymmetric parts of β -function. Second, by examining the structure of the β -function, we can make certain simplifications of it based on some experimental facts. Finally, in Chapter 5, we will summarize the work that is presented in the thesis and give an outlook to complete the RG analysis of the LRSM. We again emphasize the importance of this work in various theoretical and experimental studies.

⁴It is more modest than a GUT theory in the sense that instead of using a single group that contains the entire SM gauge group, the LR symmetric model only extends the SM electroweak sector into $SU(2)_L \times SU(2)_R \times U(1)_{B-L}$.

⁵ B is the known as the baryon number, which is defined as one-third of the difference between the number of quarks and the number of antiquarks. L is the lepton number defined as the difference between the number of the leptons and the number of antileptons.

Chapter 2

Survey of the Subject

2.1 Neutrino Masses

2.1.1 Experimental developments in neutrino masses and mixings

The neutrinos, first proposed by Wolfgang Pauli in 1930 [23] and later discovered in the Cowan-Reines experiment in 1956 [24], are weakly interacting leptons that were suspected to be massless for a long time, as in the SM. However, the report from the Super-Kamiokande (Super-K) experiment gave the first compelling piece of evidence for atmospheric neutrino oscillations [10]. A few years later, the SNO experiment [25, 26] confirmed the solar neutrino oscillations¹. More recently, various long-baseline experiments such as K2K [27] and MINOS [28] also showed consistent observations. This indicates that the neutrinos must be massive, which can be seen from the transition probability from a neutrino flavor state α with energy E to the final state β ($\beta \neq \alpha$) after traveling a distance L in vacuum,

$$P(\nu_\alpha \rightarrow \nu_\beta) = |\langle \nu_\beta | \nu_\alpha(t) \rangle|^2 = \sin^2(2\theta) \sin^2\left(\frac{\Delta m_{12}^2}{4E} L\right), \quad (2.1)$$

where θ is the mixing angle between the neutrino flavor eigenstates ($\nu_\alpha, \alpha \in \{e, \mu, \tau\}$) and the mass eigenstates ($\nu_i, i \in \{1, 2, 3\}$), which is associated with the Pontecorvo-Maki-Nakagawa-Sakata (PMNS) matrix², and Δm_{12}^2 is the squared difference between the two mass eigenstates. The mass dependence of the neutrino oscillations is thus manifest in Eq. (2.1). Assuming neutrinos to be Majorana particles³, that is, if they are their own antiparticles, the PMNS matrix can be parameterized as [29]:

$$U_{\text{PMNS}} = \begin{pmatrix} c_{12}c_{13} & s_{12}c_{13} & s_{13}e^{-i\delta} \\ -s_{12}c_{23} - c_{12}s_{13}e^{i\delta} & c_{12}c_{23} - s_{12}s_{13}s_{23}e^{i\delta} & c_{12}s_{23} \\ s_{12}s_{23} - c_{12}s_{13}e^{i\delta} & -c_{12}s_{23} - s_{12}s_{13}c_{23}e^{i\delta} & c_{13}c_{23} \end{pmatrix} \times \text{Diag}(e^{-i\varphi_1/2}, e^{-i\varphi_2/2}, 1), \quad (2.2)$$

where $c_{ij} = \cos \theta_{ij}$, $s_{ij} = \sin \theta_{ij}$, δ is the Dirac CP (charge-parity) violating phase and φ_1, φ_2 are the two Majorana CP violating phases. Hence, to characterize neutrino oscillations, we need to determine the three mixing angles ($\theta_{12}, \theta_{23}, \theta_{13}$) and the two mass-squared splittings ($\Delta m_{21}^2, |\Delta m_{31(32)}^2|$). To date, the sign of the mass-squared splitting Δm_{21}^2 has been measured but the sign of Δm_{31}^2 is still unclear. This results in two different orderings of neutrino mass eigenvalues [1]:

$$\Delta m_{21}^2 \ll (\Delta m_{32}^2 \simeq \Delta m_{31}^2 > 0); \quad (2.3)$$

$$\Delta m_{21}^2 \ll -(\Delta m_{31}^2 \simeq \Delta m_{32}^2 < 0). \quad (2.4)$$

The first one (2.3) implies $m_1 < m_2 < m_3$ and is called Normal Ordering (NO). The second one (2.4) implies $m_3 < m_1 < m_2$ and is called Inverted Ordering (IO). This is known as the neutrino mass hierarchy problem. To determine the mass hierarchy is fundamentally important because it has effects on a wide range of processes in particle physics and cosmology. For example, the observations

¹This work, along with the Super-K experiment, was awarded the 2015 Nobel Prize in Physics.

²Analogous to the more familiar Cabibbo-Kobayashi-Maskawa (CKM) matrix that determines the flavor mixing of quarks, PMNS matrix is the unitary flavor mixing matrix for neutrinos.

³The nature of neutrinos, whether they are Majorana or Dirac fermions, is still unknown. If they are Dirac fermions, they are not their own antiparticles, just like the other fermions in the SM. In the seesaw mechanism, which is the only mechanism we consider in this thesis to generate neutrino masses, neutrinos are assumed to be Majorana fermions.

Table 2.1: Global fits of 3-neutrino oscillation parameters based on solar, atmospheric, accelerator and reactor neutrino analyses. The best-fit values (within 1σ) and 3σ allowed ranges are shown. Note that $\Delta m_{3l}^2 \equiv \Delta m_{31}^2 > 0$ for NO and $\Delta m_{3l}^2 \equiv \Delta m_{32}^2 < 0$ for IO. [50]

Parameters	Normal Ordering		Inverted Ordering	
	Best fit ($\pm 1\sigma$)	3σ range	Best fit ($\pm 1\sigma$)	3σ range
$\sin^2 \theta_{12}$	$0.308^{+0.013}_{-0.012}$	$0.273 \rightarrow 0.349$	$0.308^{+0.013}_{-0.012}$	$0.273 \rightarrow 0.349$
$\sin^2 \theta_{23}$	$0.574^{+0.026}_{-0.144}$	$0.390 \rightarrow 0.639$	$0.579^{+0.022}_{-0.029}$	$0.400 \rightarrow 0.637$
$\sin^2 \theta_{13}$	$0.0217^{+0.0013}_{-0.0010}$	$0.0187 \rightarrow 0.0250$	$0.0221^{+0.0010}_{-0.0010}$	$0.0190 \rightarrow 0.0251$
Δm_{21}^2 [10^{-5}eV^2]	$7.94^{+0.19}_{-0.17}$	$7.02 \rightarrow 8.08$	$7.49^{+0.19}_{-0.17}$	$7.02 \rightarrow 8.08$
Δm_{3l}^2 [10^{-5}eV^2]	$+2.484^{+0.045}_{-0.048}$	$+2.351 \rightarrow +2.618$	$-2.465^{+0.041}_{-0.043}$	$-2.594 \rightarrow -2.339$

of the neutral current effects from supernova will depend on the the type of mass hierarchy [30]. The sign of Δm_{31}^2 also influences the effective neutrino mass term in the neutrinoless double-beta ($0\nu\beta\beta$) decay, which is one way to test the possible Majorana nature of the active neutrinos⁴ [32].

Experimentally, the mixing parameters have been measured by different neutrino oscillation experiments using different sources in the past decade or so. Currently available data include, for example, solar observations from Super-K [33, 34, 35], SNO [36, 37], atmospheric results from Super-K [38, 39], accelerator results from MINOS [40, 41], T2K [42, 43], and reactor results from KamLAND [44, 45], Daya Bay [46, 47] and RENO [48, 49]. Moreover, the development of global analyses on these experimental data allow us to obtain upper and lower bounds of these three-mixing parameters to increasingly higher precision [50, 51]. The most recent bounds from NuFIT [50] (based on global data in May 2016) are summarized in Table 2.1. The Dirac CP violating phase is not shown because it is still fully unconstrained, i.e. the value of it can be anywhere between 0 and 2π within the 3σ range. Nevertheless, the preliminary hints from T2K [52] and NO ν A [53] that $\sin \delta < 0$ encourages physicists to continue to improve the measurements in future long-baseline experiments.

Although the mass-squared splittings between the neutrino mass eigenstates were determined quite accurately from the oscillation experiments, the absolute mass scale of neutrinos remains largely unknown [54]. Despite this, we know that it is very small from constraints obtained by various other experiments. For instance, the combination of cosmological probes such as the Lyman- α (Ly- α) forest power spectrum data from the Baryon Oscillation Spectroscopic Survey (BOSS) and Planck 2015 cosmic microwave background (CMB) data sets an upper bound for the sum of neutrino masses, $m_\nu \equiv \sum_i m_i < 0.12$ eV (95% C.L.) [55]. However, the cosmological constraint is largely dependent on the specific models that one uses. Another feasible probe for neutrino masses is the $0\nu\beta\beta$ experiment if the active neutrinos are assumed to be Majorana fermions, because the effective Majorana mass $m_{ee} \equiv |\sum_i m_i U_{ei}^2|$ is related to m_i [56]. Recent $0\nu\beta\beta$ searches including the GERDA experiment [57], KamLAND-Zen [58] and EXO-200 [59] gave a limit on the effective mass, $m_{ee} \leq 0.2 - 0.4$ eV. Furthermore, the least model-dependent probe for the effective electron (anti-)neutrino mass $m_e \equiv \sum_i m_i^2 |U_{ei}|^2$ is the tritium β -decay experiments, currently providing a limit of $m_e \leq 2.05$ eV (95% C.L.) by the Troitsk experiment [60] and $m_e < 2.3$ eV (95% C.L.) by the Mainz experiment [61]. But this limit is expected to be greatly improved to $m_e \sim 0.20$ eV by the KATRIN experiment [62] in the near future.

⁴The term “active” is used here for the SM neutrinos to distinguish it from the sterile neutrinos, which are hypothetical particles that do not participate in any fundamental interaction in the SM. The sterile neutrinos are also known as right-handed neutrinos, which can take part in the type-I seesaw mechanism, or serve as a viable candidate for dark matter [31].

2.1.2 Origins of the small neutrino masses

As suggested by the experimental constraints of the neutrino masses mentioned above, the active neutrinos in the SM have tiny masses. They are in general much lighter than the other fermions in the SM. To explain the smallness of neutrino masses is yet another interesting open question in particle physics. Throughout the years, physicists have come up with different theories or models to explain this puzzle. A recapitulatory but by no means comprehensive list of possible origins of the small neutrino masses is shown below [54, 63].

- Small coupling constant.** In this scenario, neutrinos are postulated to be Dirac fermions and the right-handed (RH) neutrinos are added to the SM. This then allows for a neutrino-Higgs Yukawa coupling which translates into the Dirac neutrino mass after the electroweak symmetry breaking. However, the tiny mass of a neutrino requires a correspondingly tiny Yukawa coupling compared with those for the other fermions. This small coupling constant can be realized by positing extra dimensions of spacetime. The simplest way is to supplement the 4-dimensional spacetime, referred to as “3-brane”, with an extra n -dimensional compact space ($n \geq 2$) [64, 65]. The RH neutrinos, along with gravity, reside in the extra-dimensional space, while all the SM particles are stuck on the 3-brane. This mechanism makes the effective neutrino-Higgs Yukawa coupling typically small because of the exponentially small overlap of their wavefunctions in different dimensions. Additionally, instead of being flat, the extra-dimensional space can be “warped”, which has some distinct features. This is known as the Randall–Sundrum model [66].
- Seesaw mechanisms.** In the seesaw scenarios, the neutrinos are Majorana particles and their masses are generated at the tree level by adding extra heavy particles at high energy scales, as shown in Fig. 2.1(a). At low energies, these particles get “integrated out”⁵ and the interactions can be effectively described by a series of operators with dimensions⁶ greater than 4. The dominant one is the dimension-5 Weinberg operator $\mathcal{L}_5 \sim \kappa \ell_L \ell_L \phi \phi$ [68], where ℓ_L and ϕ are the lepton and Higgs doublets in the SM and κ is the effective coupling that can be written in terms of a dimensionless coupling λ and some large effective energy scale Λ , $\kappa = \lambda/\Lambda$. Typically, we can introduce three kinds of particles that will give rise to the Weinberg operator in the low-energy limit. In the type-I seesaw mechanism [18, 69, 70, 71, 72], the SM is extended by n generations of the RH neutrinos N_R , which are singlets under the SM gauge group. In the type-II seesaw mechanism [73, 74, 75, 76], a charged $SU(2)_L$ scalar triplet Δ , is added to the SM. And finally, the type-III seesaw mechanism [77, 78] is very similar to type-I, but with RH fermion triplets Σ_R added. The high-energy seesaw mechanisms avoid the need for minuscule Yukawa couplings, so they are less *ad hoc*. They also naturally show up in some GUT models because the mass of the heavy particles can be generated close to the GUT scale. For example, the type-I and/or type-II seesaw mechanisms are native in $SO(10)$ GUTs [79, 80] as well as LR symmetric models [19, 81]. The type-III seesaw mechanism can also be implemented in $SU(5)$ theories [78, 82].
- Radiative mass models.** While the seesaw mechanisms generate neutrino masses at the tree level, the radiative models are proposed to be fulfilled at the loop level, that is, at higher orders in perturbation theory. An example of this is shown in Fig. 2.1(b). Apart from the loop suppression factor of order $(16\pi^2)^n$, where n is the number of loops needed to generate the Weinberg operator, the smallness of the neutrino masses is also attributed to the additional couplings between the active neutrinos and the new particles in the loop [54]. Examples of such models include the earliest Zee model [83], the Zee-Babu model [85, 84, 86], the scotogenic model [87] etc. A summary of radiative mass models is presented in this short review [88].

⁵This reflects the main idea of the Effective Field Theory (EFT) [67], whose principle is to approximate a theory at a certain energy scale with some effective degrees of freedom, while ignoring the substructure and the degrees of freedom associated with higher energies, for example, the mass of a heavy particle in the low-momentum limit.

⁶“Dimension” refers to the mass dimension. The dimension of a Lagrangian density in a four-dimensional spacetime is 4 because an action is dimensionless. Therefore, a bosonic field has dimension of 1 and a fermionic field has a dimension of 3/2.

where $\frac{3}{2}$ arises as a symmetry factor due to the $SU(2)$ structure and λ is the Higgs self-coupling strength. A common trick to help evaluate such an integral is the Wick rotation⁷, which takes the substitution $k^0 \rightarrow ik_E^0$. The spatial components of k stay the same but let us rename them as $k_E^i \equiv k^i$, where $i = 1, 2, 3$. Now we have

$$k^2 = (k^0)^2 - (k^i)^2 \rightarrow -(k_E^0)^2 - (k_E^i)^2 = -k_E^2, \quad (2.6)$$

where k_E is called the Euclidean momentum because the Wick rotation essentially corresponds to a transformation from the Minkowski space to the Euclidean space. Without needing to bother with the original poles in the denominator of the integrand, we now can rewrite the vertex function as

$$\begin{aligned} i\Sigma_\phi &= -i\frac{3}{2}\lambda \int \frac{d^4 k_E}{(2\pi)^4} \frac{1}{k_E^2 + m^2} = -i\frac{3}{32\pi^4}\lambda \int d\Omega_4 \int_0^\infty dk_E \frac{k_E^3}{k_E^2 + m^2} \\ &= -i\frac{3}{32\pi^2} [k_E^2 - m^2 \ln(k_E^2 + m^2)]_0^\infty, \end{aligned} \quad (2.7)$$

where we have introduced the spherical coordinates and used the surface area of the Euclidean 4-sphere $\int d\Omega_4 = 2\pi^2$. In the last step, it can be clearly seen that the integral is ultraviolet (UV) divergent. Therefore, to calculate such a diagram, we first need to regularize it.

2.2.1 Regularization methods

The purpose of regularization is to tame a divergent integral by introducing an auxiliary parameter called regulator. A regulator is merely a tool to make such an integral convergent and the final physical results should be independent of it. In different regularization methods, different regulators are employed. For example, the simplest way to make UV divergent integrals well-behaved is by imposing a hard cutoff Λ as the upper limit of the integration. This cutoff is often interpreted as the scale above which the physics becomes irrelevant. However, imposing a hard UV cutoff will violate all the gauge symmetries and the Lorentz symmetry. Therefore, it is not suitable for gauge theories. Alternatively, one can introduce one or multiple ghost particles which are much heavier than the other particles in the theory. This method is called the Pauli-Villars regularization [100]. These ghost particles are unphysical because they have wrong spin-statistics. So they are just a mathematical tool invented to cancel the divergences in the loop integrals of the physical particles at asymptotically large momenta. But this method quickly becomes unfeasible when a large number of such fictitious particles are needed for higher-order corrections.

The dimensional regularization (DR) method proposed by 't Hooft and Veltman [101] is perhaps the most popular scheme in modern applications. It utilizes the fact that some integrals such as the one in Eq. (2.7) diverge in $d = 4$ dimensions but converge in $d < 4$. Therefore, we first evaluate the integral in the dimension of $d = 4 - \epsilon$. After renormalization, the regulator is removed by analytically continuing to $d = 4$, i.e. taking $\epsilon \rightarrow 0$. Moreover, to keep the coupling dimensionless by convention, one often introduces an arbitrary mass scale μ and replace λ by $\mu^\epsilon \lambda$ in d dimensions. The technical details about DR can be found in Appendix B. Here we simply jot down the result for our example:

$$i\Sigma_\phi = \frac{3}{2}\mu^\epsilon \lambda \int \frac{d^d k}{(2\pi)^d} \frac{1}{k^2 - m^2 + i\varepsilon} = i\frac{3}{32\pi^2}\lambda m^2 \left[\frac{2}{\epsilon} + \ln \frac{4\pi\mu^2}{m^2} - \gamma_E + 1 + \mathcal{O}(\epsilon) \right], \quad (2.8)$$

We see that by performing the DR, the divergent term, $\frac{1}{\epsilon}$, is separated from the other finite terms. The terms of order ϵ and higher are irrelevant because they vanish as $\epsilon \rightarrow 0$. Moreover, as we will see, DR makes the renormalization process very simple. Thus, in this thesis, we will stick to the DR method.

⁷In Wick rotation, we assume that integrating over the real axis is equivalent to integrating over the imaginary axis. This is justified by the Cauchy's integral theorem in complex analysis.

2.2.2 Renormalization schemes

In the renormalization process, we define a series of renormalized quantities with different renormalization constants. The divergent parts isolated by regularization are then subtracted and absorbed into the renormalization constants. For our example, a way to define the relations between the bare quantities (labelled with subscript B) and the renormalized ones (with no label) in d dimensions is

$$\phi_B = Z_\phi^{1/2} \phi \quad (2.9a)$$

$$m_B^2 = Z_\phi^{-1}(m^2 + \delta m^2) \quad (2.9b)$$

$$\lambda_B = \mu^\epsilon Z_\phi^{-2} Z_\lambda \lambda, \quad (2.9c)$$

where the renormalization constants Z_ϕ , δm^2 and Z_λ contain the divergences. Sometimes δm^2 is also called the mass counterterm. To one-loop order, we can expand the renormalization constants as

$$Z_i = 1 + \delta Z_i, \quad (2.10)$$

where Z_i ($i = \phi, \lambda$) are the field and coupling counterterms. In the perturbative renormalization theory, these counterterms appear as interactions in the Lagrangian with defined Feynman rules.

There are a few common renormalization, or subtraction schemes used to determine the renormalization constants. The first one is called the on-shell scheme. In this scheme, we identify the renormalized mass as the physical mass of the particle, which is the pole of the renormalized propagator. Then the finite parts of the counterterms are chosen to meet this requirement. The next one is the minimal subtraction (MS) scheme [102, 103] and is particularly useful when used along with DR. The counterterms under this scheme are defined to cancel only the divergences. To see this, let us look at the renormalized Higgs 2-point Green function. At the one-loop level, if we consider the Higgs self-coupling as the only correction, then the renormalized 2-point function can be written as a sum of the bare propagator, the bare one-loop correction, and the 2-point counterterm:

$$\begin{aligned}
 & \text{Diagram 1} = \text{Diagram 2} + \text{Diagram 3} \quad (2.11) \\
 & = i + i\Sigma_\phi + i(p^2\delta Z_\phi - \delta m^2) \stackrel{!}{=} \text{UV finite},
 \end{aligned}$$

where in the second line we have written down the vertex function for each diagram and the last term comes from the Feynman rule (see Appendix C). The first term is finite. Therefore, in the MS scheme, the counterterm are to cancel the divergent part of $i\Sigma_\phi$:

$$p^2\delta Z_\phi - \delta m^2 + \frac{3}{16\pi^2} \lambda m^2 \frac{1}{\epsilon} = 0, \quad (2.12)$$

which gives

$$\delta Z_\phi = 0, \quad \delta m^2 = \frac{3}{16\pi^2} \lambda m^2 \frac{1}{\epsilon}. \quad (2.13)$$

In a similar fashion, we can determine the counterterm δZ_λ by considering the 4-point Green functions. As we see, the MS scheme is very efficient once the divergent part of a diagram has been isolated via DR. Another feature of it is that the renormalization constants are independent of the renormalization scale, making it more suitable for the renormalization group evolution. Due to its advantages, we will use the MS scheme for renormalization in this thesis.

Another widely used scheme is the modified minimal subtraction ($\overline{\text{MS}}$) scheme [104], which is just a variant of the MS scheme. In this scheme, in addition to the divergent part of Eq. (2.15), the finite term $(\ln 4\pi - \gamma_E)$ is also subtracted because they always show up in the divergent integrals.

2.2.3 Renormalization group equations

One of the most important realizations from renormalization is that the renormalized quantities such as masses and couplings depend on the renormalization scale⁸, while the bare quantities do not. This means that a change of renormalization scheme does not change a theory itself but only the values of its renormalized parameters. The evolution of the renormalized parameters with the renormalization scale, governed by the RGEs, is called running and has practical implications in comparing theoretical predictions and experimental results. The idea of renormalization group (RG) running was first envisioned in the 1950s [105, 106]. Its application in particle physics was later found in the early 1970s through the work of Callan [107] and Symanzik [108].

To derive the RGEs, we first consider the n -point Green function for the Higgs field ϕ , with mass m and self-coupling λ . In momentum space, the bare Green function is given by

$$G_B^{(n)}(\{p_i\}, \lambda_B, m_B, \epsilon) \equiv \langle 0 | T[\phi_B(p_1) \cdots \phi_B(p_n)] | 0 \rangle, \quad (2.14)$$

where T is the time-ordering operator of the fields and $|0\rangle$ is the vacuum state of the theory. The parameter ϵ implies the use of DR, which allows for an arbitrary dimension of spacetime. Using the wavefunction renormalization given by (2.9a), the relation between the renormalized Green function and the bare one is simply given by

$$G_B^{(n)}(\{p_i\}, \lambda_B, m_B, \epsilon) = Z_\phi^{n/2} G^{(n)}(\{p_i\}, \lambda, m, \epsilon, \mu), \quad (2.15)$$

where the renormalized Green function is defined in terms of the renormalized fields,

$$G^{(n)}(\{p_i\}, \lambda, m, \epsilon, \mu) \equiv \langle 0 | T[\phi(p_1) \cdots \phi(p_n)] | 0 \rangle. \quad (2.16)$$

Since the bare quantities remain constant as we alter the renormalization scale μ , the bare Green function is independent of μ . Therefore, taking the total derivative of the left hand side of Eq. (2.15) with respect to $\ln \mu$ gives zero,

$$\frac{d}{d \ln \mu} G_B^{(n)}(\{p_i\}, \lambda, m, \epsilon) = \mu \frac{d}{d \mu} G_B^{(n)}(\{p_i\}, \lambda, m, \epsilon) = 0. \quad (2.17)$$

On the other hand, the renormalized quantities depend on the renormalization scale, and the total derivative of the renormalized Green function with respect to $\ln \mu$ can be written in terms of partial derivatives using the chain rule. Then Eqs. (2.15) and (2.17) together imply

$$\left[\mu \frac{\partial}{\partial \mu} + \beta \frac{\partial}{\partial \lambda} - \gamma_m m \frac{\partial}{\partial m} + \frac{n}{2} \gamma \right] G^{(n)}(\{p_i\}, \lambda, m, \epsilon, \mu) = 0. \quad (2.18)$$

This is known as the Callan-Symanzik equation. It contains a set of renormalization group equations

$$\beta \equiv \mu \frac{d\lambda}{d\mu}, \quad (2.19a)$$

$$\gamma_m \equiv -\frac{1}{m} \mu \frac{dm}{d\mu}, \quad (2.19b)$$

$$\gamma \equiv \frac{1}{Z_\phi} \mu \frac{dZ_\phi}{d\mu}, \quad (2.19c)$$

where β is called the β -function for the coupling and γ_m , γ are referred to as the anomalous dimensions of the mass and the field, respectively. These RGEs describe the running of all the renormalized parameters in our example.

⁸In dimensional regularization, this scale is implicitly set by the dimensionful parameter μ . See Section 2.2.1.

Chapter 3

General Framework

3.1 Fermion Mass Terms

3.1.1 Helicity and chirality

In previous chapters, we referred to the “handedness” of particles (e.g. right-handed neutrinos) without explaining what it really means. There are generally two concepts used to describe the handedness of a particle, helicity and chirality.

The helicity of a particle is the projection of its angular momentum onto its momentum. The total angular momentum of the particle is the sum of the orbital angular momentum and the spin angular momentum, with the orbital angular momentum given by $\vec{L} = \vec{r} \times \vec{p}$. Since the orbital angular momentum \vec{L} is perpendicular to the 3-momentum \vec{p} , it does not contribute to helicity. Therefore, the helicity of a particle can be defined as the normalized component of its spin angular momentum \vec{S} along the direction it travels,

$$H_p \equiv \frac{\vec{S} \cdot \vec{p}}{|\vec{p}|}. \quad (3.1)$$

For instance, the two possible helicity states for a spin-1/2 fermion are called left-handed (LH) and right-handed (RH) helicity states, corresponding to $H_p = -1/2$ and $H_p = +1/2$, respectively. For a free particle, helicity is conserved because it can be shown that the helicity operator commutes with the free Hamiltonian operator [109]. However, helicity is not a Lorentz-invariant quantity for massive particles. This can be easily demonstrated by considering a massive fermion whose spin aligns with its momentum in the initial reference frame of an observer. In this frame, $H_p = +1/2$. If we now Lorentz boost the observer to a reference frame that moves faster than the fermion, the particle is now moving in the opposite direction from the observer’s perspective. Then the momentum direction is reversed. Since the spin of the fermion does not change, this results in an opposite helicity, $H_p = -1/2$. For massless particles, helicity is Lorentz invariant because there is no such a boost that can make a reference frame move faster than the speed of light.

On the other hand, chirality is a Lorentz invariant quantity for all particles. It is determined by whether a particle transforms in a LH or RH representation of the Lorentz group. For a four-component spinor, the chirality of it is associated with the matrix γ^5 , sometimes called the chirality matrix, which is defined as

$$\gamma^5 \equiv i\gamma^0\gamma^1\gamma^2\gamma^3, \quad (3.2)$$

where $\gamma^0, \gamma^1, \gamma^2$ and γ^3 are the conventional 4×4 γ -matrices in the Clifford algebra. A few useful properties of the γ^5 matrix include:

$$(\gamma^5)^\dagger = \gamma^5; \quad (3.3a)$$

$$(\gamma^5)^2 = 1; \quad (3.3b)$$

$$\{\gamma^5, \gamma^\mu\} = 0. \quad (3.3c)$$

The chiral projection operators for the fermion fields are defined as

$$P_L \equiv \frac{1 - \gamma^5}{2}, \quad P_R \equiv \frac{1 + \gamma^5}{2}. \quad (3.4)$$

They project out the LH and RH chiral components of a fermionic spinor ψ , respectively:

$$\psi_L = P_L \psi, \quad \psi_R = P_R \psi. \quad (3.5)$$

Some typical properties of the projection operators are:

$$P_L^2 = P_L, \quad P_R^2 = P_R; \quad (3.6a)$$

$$P_L P_R = P_R P_L = 0; \quad (3.6b)$$

$$P_L + P_R = 1. \quad (3.6c)$$

In summary, chirality and helicity are two different concepts. Chirality is a more intrinsic property of particles in the sense that it does not depend on the reference frame (i.e. Lorentz invariant), while helicity does. So we will use chirality to refer to a particle's handedness in this thesis. However, they can be used interchangeably for massless particles.

3.1.2 Particle-antiparticle conjugation and charge conjugation

Another two important concepts that the literature is replete with but are often carelessly treated are the particle-antiparticle conjugation and charge conjugation, as suggested in [110]. As we will see, although these two operators have the same effect on fermions that have both LH and RH components, they are not equivalent when acting on chiral fields. So we should distinguish them to avoid confusions.

Let us first look at the particle-antiparticle conjugation operator \mathcal{C} . Under its operation, a fermion field ψ and its Dirac adjoint $\bar{\psi}$ transform as

$$\mathcal{C}: \quad \psi \longrightarrow \psi^c \equiv C \bar{\psi}^T = -\gamma^0 C \psi^*, \quad (3.7a)$$

$$\mathcal{C}: \quad \bar{\psi} \longrightarrow \bar{\psi}^c = \overline{C \bar{\psi}^T} = -\psi^T C^\dagger, \quad (3.7b)$$

where C is the charge conjugation matrix satisfying

$$C^\dagger = C^T = C^{-1} = -C, \quad (3.8a)$$

$$C \gamma_\mu^T C^{-1} = -\gamma_\mu. \quad (3.8b)$$

In the standard representation, $C = i\gamma^2\gamma^0$, and thus $\psi^c = i\gamma^2\psi^*$. To grasp the physical meaning of the operator \mathcal{C} , we first consider its effect on a quantized Dirac field, whose mode expansion can be written as

$$\psi(x) = \int \frac{d^3p}{(2\pi)^3 \sqrt{2E_p}} \sum_{s=1}^2 \left[c_s(\vec{p}) u_s(\vec{p}) e^{-ip \cdot x} + d_s^\dagger(\vec{p}) v_s(\vec{p}) e^{ip \cdot x} \right], \quad (3.9)$$

where $c_s(\vec{p})$ is the annihilation operator of particles, $d_s^\dagger(\vec{p})$ is the creation operator of antiparticles and s is the spin of the field. Similarly, the Dirac adjoint of this field is quantized as

$$\bar{\psi}(x) = \int \frac{d^3p}{(2\pi)^3 \sqrt{2E_p}} \sum_{s=1}^2 \left[c_s^\dagger(\vec{p}) \bar{u}_s(\vec{p}) e^{ip \cdot x} + d_s(\vec{p}) \bar{v}_s(\vec{p}) e^{-ip \cdot x} \right]. \quad (3.10)$$

By explicit calculation, one can shown that the basis spinors in the mode expansions satisfy the following identities

$$C \bar{u}_s^T(\vec{p}) = v_s(\vec{p}), \quad (3.11a)$$

$$C \bar{v}_s^T(\vec{p}) = u_s(\vec{p}). \quad (3.11b)$$

Then if we implement the particle-antiparticle conjugation using a unitary operator U_c (with $U_c^\dagger = U_c^{-1}$) and ignoring the phase factor for simplicity,

$$U_c \psi(x) U_c^\dagger = \psi^c(x) = C \bar{\psi}^T(x), \quad (3.12)$$

the field $\psi(x)$ with mode expansion (3.9) transforms as

$$\begin{aligned} U_c \psi(x) U_c^\dagger &= \int \frac{d^3 p}{(2\pi)^3 \sqrt{2E_p}} \sum_{s=1}^2 \left[\left(U_c c_s(\vec{p}) U_c^\dagger \right) u_s(\vec{p}) e^{-ip \cdot x} + \left(U_c d_s^\dagger(\vec{p}) U_c^\dagger \right) v_s(\vec{p}) e^{ip \cdot x} \right] \\ &= \int \frac{d^3 p}{(2\pi)^3 \sqrt{2E_p}} \sum_{s=1}^2 \left[\left(U_c c_s(\vec{p}) U_c^\dagger \right) C \bar{v}_s^T(\vec{p}) e^{-ip \cdot x} + \left(U_c d_s^\dagger(\vec{p}) U_c^\dagger \right) C \bar{u}_s^T(\vec{p}) e^{ip \cdot x} \right] \\ &= C \int \frac{d^3 p}{(2\pi)^3 \sqrt{2E_p}} \sum_{s=1}^2 \left[\left(U_c c_s(\vec{p}) U_c^\dagger \right) \bar{v}_s(\vec{p}) e^{-ip \cdot x} + \left(U_c d_s^\dagger(\vec{p}) U_c^\dagger \right) \bar{u}_s(\vec{p}) e^{ip \cdot x} \right]^T \\ &\stackrel{!}{=} C \bar{\psi}^T(x), \end{aligned} \quad (3.13)$$

where we have used the identities (3.11a) and (3.11b) in the second line and the transpose in the third line only acts on the spinor space. Then comparing with Eq. (3.10), we see that the last equality holds if and only if

$$U_c c_s(\vec{p}) U_c^\dagger = d_s(\vec{p}), \quad (3.14a)$$

$$U_c d_s^\dagger(\vec{p}) U_c^\dagger = c_s^\dagger(\vec{p}). \quad (3.14b)$$

Therefore, the particle-antiparticle conjugation interchanges the annihilation and creation operators of particles and their own antiparticles. This is exactly what its name suggests.

But this is not the whole story. If we consider the left-handed component of a fermion field ψ , which is projected out by the chiral projection operator P_L , and apply the particle-antiparticle conjugation operator \mathcal{C} to it, we can show that

$$(\psi_L)^c = C(\overline{P_L \psi})^T = P_R \psi^c \equiv (\psi^c)_R, \quad (3.15)$$

where we need to use Eqs. (3.3a) and (3.3c). Similarly, if we apply the operator \mathcal{C} to the right-handed component, we obtain

$$(\psi_R)^c = (\psi^c)_L. \quad (3.16)$$

We therefore see that this operator also changes the chirality, i.e. it turns a LH spinor field into a RH spinor field and vice versa. As a result, under the particle-antiparticle conjugation, the antiparticle of a LH fermion is RH, and vice versa.

On the other hand, the charge conjugation operator \mathcal{C} interchanges particles and their own antiparticles without changing the chirality. When acting on chiral fermion fields, it is defined as

$$\mathcal{C}: \quad \psi_L \longrightarrow \hat{\psi}_L \equiv (\psi^c)_L, \quad (3.17a)$$

$$\mathcal{C}: \quad \psi_R \longrightarrow \hat{\psi}_R \equiv (\psi^c)_R. \quad (3.17b)$$

Hence, we see that under the charge conjugation, the antiparticle of a LH fermion remains LH, and the antiparticle of a RH fermion remains RH. For a massive fermion which contains LH and RH components, the particle-antiparticle conjugation \mathcal{C} and the charge conjugation \mathcal{C} coincide:

$$\mathcal{C}: \quad \psi = \psi_L + \psi_R \longrightarrow (\psi)^c = (\psi_L)^c + (\psi_R)^c = (\psi^c)_R + (\psi^c)_L, \quad (3.18a)$$

$$\mathcal{C}: \quad \psi = \psi_L + \psi_R \longrightarrow \hat{\psi} = \hat{\psi}_L + \hat{\psi}_R \equiv (\psi^c)_L + (\psi^c)_R. \quad (3.18b)$$

Hence, often in the literature, they are used interchangeably.

3.1.3 Dirac and Majorana mass terms

Now we are ready to write the fermion mass terms. Recall from QFT that the Dirac Lagrangian for a free massive fermion is

$$\mathcal{L} = \bar{\psi}(i\gamma^\mu\partial_\mu - m)\psi, \quad (3.19)$$

which leads to the famous Dirac equation. For a general fermion field with left- and right-chiral components, the mass term of this Lagrangian can be written as

$$\begin{aligned} \mathcal{L}_m &= -m\bar{\psi}\psi = -m(\bar{\psi}_L + \bar{\psi}_R)(\psi_L + \psi_R) \\ &= -m(\bar{\psi}_L\psi_L + \bar{\psi}_R\psi_R + \bar{\psi}_L\psi_R + \bar{\psi}_R\psi_L). \end{aligned} \quad (3.20)$$

Using the properties of the γ^5 matrix and the projection operators listed in Sec. 3.1.1, one can show

$$\bar{\psi}_L = \bar{P}_L\psi_L = \bar{\psi}_L P_R. \quad (3.21)$$

Then the term $\bar{\psi}_L\psi_L$ becomes

$$\bar{\psi}_L\psi_L = \bar{\psi}_L \underbrace{P_R P_L}_{=0} \psi_L = 0. \quad (3.22)$$

Similarly, $\bar{\psi}_R\psi_R = 0$. Thus, only the cross terms survive and the fermion mass term is simplified to

$$\mathcal{L}_m = -m(\bar{\psi}_L\psi_R + \bar{\psi}_R\psi_L). \quad (3.23)$$

There are two different types of mass term that can arise from Eq. (3.23). First, if the RH component of the fermion field is completely independent of the LH one, this is a Dirac field. A Dirac mass term has exactly the same form as Eq. (3.23):

$$\mathcal{L}_D = -m_D(\bar{\psi}_L\psi_R + \bar{\psi}_R\psi_L). \quad (3.24)$$

Second, if the RH component is related to the LH one by the particle-antiparticle conjugate (\mathcal{C}),

$$\psi_R = (\psi_L)^c = (\psi^c)_R, \quad (3.25)$$

or

$$\psi = \psi_L + (\psi^c)_R = \psi_L + (\psi_L)^c. \quad (3.26)$$

In this case, such a field is called a Majorana field, which is constructed via only one chiral field ψ_L . Similarly, one can also construct a Majorana field via the RH field ψ_R only:

$$\psi = \psi_R + (\psi^c)_L = \psi_R + (\psi_R)^c. \quad (3.27)$$

Then it immediately follows from Eqs. (3.26) and (3.27) that the particle-antiparticle conjugate of a Majorana field coincide with itself:

$$\psi^c = \psi. \quad (3.28)$$

This is known as the Majorana condition. It implies that Majorana fermions must be neutral because they are their own antiparticles. In order to simplify the notation, we define

$$\psi_L^c \equiv (\psi_L)^c, \quad \psi_R^c \equiv (\psi_R)^c. \quad (3.29)$$

Then the most general Majorana mass term can be written as

$$\mathcal{L}_M = -\frac{1}{2}m_L(\bar{\psi}_L^c\psi_L + \bar{\psi}_L\psi_L^c) - \frac{1}{2}m_R(\bar{\psi}_R^c\psi_R + \bar{\psi}_R\psi_R^c). \quad (3.30)$$

For n fermion flavors ($n > 1$), the fields ψ_L and ψ_R are vectors in the flavor space and the masses m_D , m_L and m_R are all $n \times n$ matrices. In general, the matrices are non-diagonal, which leads to

flavor mixings (e.g. neutrino oscillations), and complex. The only restriction is that the Majorana matrices must be symmetric. Since the Lagrangian is a scalar, we have, for example,

$$\overline{\psi_L^c} m_L \psi_L \stackrel{!}{=} (\overline{\psi_L^c} m_L \psi_L)^T \stackrel{(3.7b)}{=} (-\psi_L^T C^\dagger m_L \psi_L)^T = \psi_L^T C^* m_L^T \psi_L = \overline{\psi_L^c} m_L^T \psi_L, \quad (3.31)$$

where we have used the anticommutation property of fermion fields. This then leads to $m_L^T = m_L$. And similarly, $m_R^T = m_R$. In the most general case, the Dirac and Majorana mass terms can be present at the same time, so the general fermion mass term is a combination of (3.24) and (3.30).

3.2 Seesaw Mechanisms

As discussed in Chapter 2, the seesaw mechanism provides a natural and attractive explanation for the small active neutrino masses because it is simple and is potentially associated with some high-energy theories such as GUTs and LR symmetric models. It also offers a simple explanation for the observed baryon asymmetry in our universe - baryogenesis via leptogenesis [112].

The basic idea of the seesaw mechanism is to extend the SM with some heavy particle(s) associated with an energy scale called the seesaw scale, usually of order 10^{14} - 10^{16} GeV [111]. This is much higher than the electroweak scale $v_{EW} \simeq 246$ GeV, at which all the other fermions in the SM obtain their masses via the Higgs mechanism. At low energies, the active neutrino masses are suppressed by the heavy mass and therefore small.

The simplest way to realize the seesaw mechanism is by adding to the SM the RH neutrinos $N_R \sim (1, 1, 0)$, which are singlets under $SU(3)_C$ and $SU(2)_L$ and have hypercharge $Y = 0$. Assuming they are Majorana fermions, both the Majorana mass term and the Dirac-type Yukawa couplings are allowed in the Lagrangian

$$\mathcal{L} \supset -\frac{1}{2} \overline{N_R^c} M_N N_R - \frac{1}{2} \overline{N_R} M_N N_R^c - \overline{N_R} y_N \tilde{\phi}^\dagger \ell_L - \overline{\ell_L} \tilde{\phi} y_N^\dagger N_R, \quad (3.32)$$

where M_N is the Majorana mass matrix of the RH neutrinos, y_N is the Yukawa coupling matrix and $\tilde{\phi} \equiv i\tau_2 \phi^*$, with τ_2 being the second Pauli spin matrix. After electroweak symmetry breaking, the neutral component of the Higgs doublet obtains a vacuum expectation value (VEV). In the unitary gauge, it can be written as

$$\langle \tilde{\phi} \rangle = i\tau_2 \begin{pmatrix} 0 \\ v \end{pmatrix} = \begin{pmatrix} v \\ 0 \end{pmatrix}, \quad (3.33)$$

where $v \equiv (1/\sqrt{2})v_{EW} \simeq 174$ GeV. Then the Yukawa couplings in (3.32) turn into the Dirac mass terms for neutrinos and the whole neutrino mass term can be written as

$$\mathcal{L}_m = -\frac{1}{2} (\overline{\nu_L^c} \quad \overline{N_R}) \begin{pmatrix} 0 & m_D \\ m_D^T & M_N \end{pmatrix} \begin{pmatrix} \nu_L \\ N_R^c \end{pmatrix} + \text{h.c.}, \quad (3.34)$$

where

$$m_D = v \cdot y_N^T \quad (3.35)$$

is the Dirac mass matrix for neutrinos. So the complete neutrino mass matrix is

$$\mathcal{M} = \begin{pmatrix} 0 & m_D \\ m_D^T & M_N \end{pmatrix}. \quad (3.36)$$

Block-diagonalization of this matrix leads to two eigenvalues [113]:

$$m_1 \simeq -m_D M_N^{-1} m_D^T, \quad (3.37a)$$

$$m_2 \simeq M_N, \quad (3.37b)$$

where it is assumed that the eigenvalues of M_N are much larger than those of m_D because the RH neutrinos are heavy, so only the terms up to $\mathcal{O}(m_D/M_N)$ are kept. The mass matrix m_1 is much smaller than m_2 due to the inverse power of M_N . Consequently, the eigenvalues of m_1 should serve the purpose of the mass eigenvalues of the light active neutrinos, while the eigenvalues of m_2 correspond to those of the heavy RH neutrinos and are associated with the seesaw scale. This is known as the type-I seesaw mechanism. The type-I seesaw relation is therefore given by Eq. (3.37a):

$$m_\nu = -m_D M_N^{-1} m_D^T = -v^2 y_N^T M_N^{-1} y_N, \quad (3.38)$$

The other way to obtain the seesaw relation (3.38) is to derive the effective Lagrangian for type-I seesaw model. The effective field theory (EFT) provides a useful tool to approximate a full high-energy theory at low energy scales by “integrating out” the degrees of freedom associated with higher energies. Perhaps the best-known example of an EFT is the 4-Fermi theory for the β -decay:

$$n \rightarrow p + e^- + \bar{\nu}_e. \quad (3.39)$$

In the 1930s, in order to describe this phenomenon, Fermi first proposed a model with an interaction term involving only the 4 particles in the β -decay,

$$\mathcal{L}_F = G_F \bar{\psi}_p \psi_n \bar{\psi}_e \psi_\nu, \quad (3.40)$$

where G_F is now known as the Fermi constant, which can be extracted from experiments. This simple model had great phenomenological success, for example, in predicting the β -decay rate. Today, we know from the SM that this decay arises from the weak interaction, which is mediated via the exchange of a W^- boson between an u - d pair and an e - $\bar{\nu}_e$ pair. Therefore, the 4-Fermi theory can be regarded as an effective description of this more fundamental interaction at energies much lower than the W boson mass (~ 80 GeV). In this effective field theory, the W boson is integrated out and the interaction is described by an effective Lagrangian (3.40).

Similarly, the RH neutrinos can be integrated out when we consider the active neutrino masses, which are generated at an energy scale much lower than the seesaw scale. One way to integrate out the RH neutrinos is to use the Euler-Lagrange equation¹

$$\frac{\partial \mathcal{L}}{\partial \psi} - \partial_\mu \left(\frac{\partial \mathcal{L}}{\partial (\partial_\mu \psi)} \right) = 0 \quad (3.41)$$

to derive the equations of motion for both N_R and \bar{N}_R from the original Lagrangian (3.32). Then N_R and \bar{N}_R can be written in terms of the other fields (ℓ_L, ϕ etc.). When putting these two expressions back into (3.32), we arrive at an effective Lagrangian without the RH neutrino fields [68]

$$\mathcal{L}_\kappa = \frac{1}{4} \kappa_{\beta\alpha} \bar{\ell}_{Lc}^\beta \varepsilon_{cd} \phi_d \ell_{Lb}^\alpha \varepsilon_{ba} \phi_a + \text{h.c.}, \quad (3.42)$$

where $\varepsilon \equiv i\tau_2$, a, b, c, d are $SU(2)$ indices, α, β are lepton flavor indices, and κ is the effective coupling defined by

$$\kappa \equiv 2y_N^T M_N^{-1} y_N. \quad (3.43)$$

The effective Lagrangian (3.42) is the well-known dimension-5 Weinberg operator that gives the active neutrinos ν_L Majorana masses after electroweak symmetry breaking. This is easy to see. Again, when the Higgs doublet gets a VEV v , the effective Lagrangian becomes

$$\mathcal{L}_\kappa = \frac{1}{2} \left(\frac{v^2}{2} \kappa \right) \bar{\nu}_L^c \nu_L + \text{h.c.}, \quad (3.44)$$

¹The process of integrating out the heavy particles can also be easily understood from Feynman diagrams, from which we can derive the effective coupling. Appendix C summarizes this approach for the type-I and II seesaw mechanisms.

which is exactly a Majorana mass term for ν_L [cf. Eq. (3.30)]. Therefore, the active neutrino mass matrix is given by

$$m_\nu = -\frac{v^2}{2}\kappa = -v^2 y_N^T M_N^{-1} y_N, \quad (3.45)$$

which is the same as Eq. (3.38). We have retrieved the type-I seesaw relation from the effective field theory analysis.

Apart from the type-I seesaw mechanism, where the RH neutrinos have been added into the SM, we can also consider the SM extended by a charged $SU(2)_L$ scalar triplet $\Delta \sim (1, 3, 2)$ with mass M_Δ , which will generate the same dimension-5 Weinberg operator in the low-energy limit. This is called the type-II seesaw mechanism. In the $SU(2)$ adjoint representation, using the Pauli spin matrices τ^i , this triplet can be written as [114]

$$\Delta = \frac{\tau^i \Delta^i}{\sqrt{2}} = \begin{pmatrix} \Delta^+/\sqrt{2} & \Delta^{++} \\ \Delta^0 & -\Delta^+/\sqrt{2} \end{pmatrix}, \quad (3.46)$$

where

$$\Delta^0 \equiv (\Delta^1 + i\Delta^2)/\sqrt{2}, \quad \Delta^+ \equiv \Delta^3, \quad \Delta^{++} \equiv (\Delta^1 - i\Delta^2)/\sqrt{2}. \quad (3.47)$$

The addition of this particle gives rise to additional terms in the Lagrangian. For example, it can interact with the SM Higgs doublet, which is characterized by the coupling Λ ,

$$\mathcal{L}_{\Delta,\phi} = -\Lambda \left(\phi^T i\tau_2 \Delta^\dagger \phi \right) + \text{h.c.} \quad (3.48)$$

It also induces a Yukawa interaction with the lepton doublets, which has the Yukawa coupling f_Δ ,

$$\mathcal{L}_{\Delta,\ell_L} = -f_\Delta (\ell_L^T C i\tau_2 \Delta \ell_L) + \text{h.c.} \quad (3.49)$$

Therefore, with the relevant Lagrangian of the $SU(2)_L$ triplet

$$\mathcal{L}_\Delta \supset -M_\Delta^2 \text{Tr}(\Delta^\dagger \Delta) - \Lambda \left(\phi^T i\tau_2 \Delta^\dagger \phi \right) - f_\Delta (\ell_L^T C i\tau_2 \Delta \ell_L) + \text{h.c.}, \quad (3.50)$$

we can derive the equation of motion for Δ from Eq. (3.41) and re-express it in terms of other fields, similar to what is done for the type-I seesaw mechanism. Then putting this expression back into (3.50), we arrive at the same effective operator (3.42), with the effective coupling defined as

$$\kappa = -2 \frac{\Lambda}{M_\Delta^2} f_\Delta. \quad (3.51)$$

After electroweak symmetry breaking, the mass matrix for the active neutrinos is then given by

$$m_\nu = -\frac{v^2}{2}\kappa = \left(\frac{\Lambda v^2}{M_\Delta^2} \right) f_\Delta. \quad (3.52)$$

This is the type-II seesaw relation. Again, the active neutrino masses are suppressed by the heavy triplet M_Δ and thereby small. The seesaw relation (3.52) can be slightly simplified by recognizing the term in the bracket is exactly the VEV of the neutral component of the triplet (v_Δ) after symmetry breaking, which results from its interaction with the SM Higgs, as described by the Lagrangian (3.48). Then the type-II seesaw relation can be simply written as

$$m_\nu = v_\Delta f_\Delta. \quad (3.53)$$

There is one more way to achieve the effective Weinberg operator with introducing only one new particle species. We can extend the SM by the $SU(2)_L$ fermion triplets $\Sigma_R \sim (1, 3, 0)$. This is called the type-III seesaw mechanism. Since the type-III seesaw cannot be embedded in the minimal

left-right symmetric model that will be discussed in Section 3.3, we will not dive into the details of it. However, it should be noted that these three types of seesaw mechanism are not isolated from each other. Some combination of them can be present in the same context. For example, in the “hybrid seesaw mechanism” [115, 116], which is based on the $SU(5)$ GUT, both the type-I and type-III seesaw mechanism contribute to the neutrino masses because the corresponding particles live in the same adjoint representation of $SU(5)$.

3.3 Left-Right Symmetry

The particle content of the SM tells us that the LH fields are $SU(2)_L$ doublets, while the RH fields are $SU(2)_L$ singlets, which do not change under $SU(2)$ transformations. It reflects the fact that the weak interaction is chiral, i.e. only the LH particles play a role in the weak interaction. This immediately tells us that parity is violated in the weak interaction, which was first demonstrated by the β -decay experiment of ^{60}Co about 60 years ago [117]. However, due to its various drawbacks, the SM may not be the complete theory of nature, but rather an effective theory valid below a certain energy scale. From this perspective, parity may be a fundamental symmetry in a complete theory beyond the SM but is broken at low energies. The left-right symmetric model (LRSM) [118, 119, 120, 121] turns out to be an appealing extension of the SM that can restore parity. Therefore, the LRSM gives a natural explanation for parity violation in the weak interaction, which cannot be explained by the SM itself. Indeed, the parity consideration was originally one of the most important motivations for studying the LRSM. The other motivation comes from the fact that it is naturally linked to the $SO(10)$ GUTs and can serve as an intermediate symmetry breaking step from $SO(10)$ to the SM gauge group [17]. The minimal LRSM is of our particular interest in this project because it is intimately related to neutrino mass generation. As will be shown below, both the type-I and II seesaw mechanisms are naturally embedded in this framework.

3.3.1 Gauge left-right symmetry

In the minimal LRSM, the complete gauge group is given by

$$G_{LR} = SU(3)_C \times SU(2)_L \times SU(2)_R \times U(1)_{B-L}. \quad (3.54)$$

Comparing this gauge group with the SM gauge group $G_{SM} = SU(3)_C \times SU(2)_L \times U(1)_Y$, we see that in the LRSM, an $SU(2)$ gauge group for the right-chiral fields is added and the $U(1)$ symmetry is associated with the baryon number minus the lepton number ($B - L$) instead of the hypercharge (Y). As this gauge group suggests, in the fermion sector, both the LH and RH fermions are doublets in the $SU(2)$ representation, which can be written as

$$Q_{L,R} = \begin{pmatrix} u \\ d \end{pmatrix}_{L,R}, \quad \ell_{L,R} = \begin{pmatrix} \nu \\ e \end{pmatrix}_{L,R}, \quad (3.55)$$

where Q stands for the quark doublets and ℓ stands for the lepton doublets. In a shorthand notation, neglecting the $SU(3)_C$ part, we write

$$Q_L \sim (2, 1, \tfrac{1}{3}), \quad Q_R \sim (1, 2, \tfrac{1}{3}); \quad (3.56a)$$

$$\ell_L \sim (2, 1, -1), \quad \ell_R \sim (1, 2, -1), \quad (3.56b)$$

where the three numbers are the quantum numbers of $SU(2)_L$, $SU(2)_R$ and $U(1)_{B-L}$, respectively. For example, the LH quark doublet Q_L transforms as a doublet under $SU(2)_L$, a singlet under $SU(2)_R$ and has $B - L$ quantum number of $1/3$. In this model, the RH neutrinos are naturally present, living in the $SU(2)_R$ doublets ℓ_R . The Higgs sector, on the other hand, contains a bi-

doublet $\Phi \sim (2, 2, 0)$ and two $SU(2)_{L,R}$ triplets², $\Delta_L \sim (3, 1, 2)$ and $\Delta_R \sim (1, 3, 2)$ [122]. They can be represented by matrices:

$$\Phi = \begin{pmatrix} \phi_1^0 & \phi_2^+ \\ \phi_1^- & \phi_2^0 \end{pmatrix}, \quad \Delta_{L,R} = \begin{pmatrix} \Delta^+/\sqrt{2} & \Delta^{++} \\ \Delta^0 & -\Delta^+/\sqrt{2} \end{pmatrix}_{L,R}. \quad (3.57)$$

There also exist the $SU(2)_R$ gauge bosons $W_{R\mu}^i$ ($i = 1, 2, 3$) and a $U(1)_{B-L}$ gauge boson A_μ , in addition to the $SU(2)_L$ gauge bosons $W_{L\mu}^i$ in the SM. They are strictly massless before spontaneous symmetry breaking.

To demonstrate how the seesaw mechanisms are embedded in this model, we consider the following Yukawa interactions in the Lagrangian [123],

$$\mathcal{L}_Y = -\frac{1}{2}f_L(\ell_L^T C i\tau_2 \Delta_L \ell_L) - \frac{1}{2}f_R(\ell_R^{cT} C i\tau_2 \Delta_R \ell_R^c) - y_1(\ell_L^T C \tau_2 \tilde{\Phi} \tau_2 \ell_R^c) - y_2(\ell_L^T C \tau_2 \Phi \tau_2 \ell_R^c) + \text{h.c.}, \quad (3.58)$$

where ℓ_L and $\ell_R^c \equiv C\bar{\ell}_R^T$ are the $SU(2)_L$ and $SU(2)_R$ lepton doublets³, respectively, and $\tilde{\Phi} \equiv \tau_2 \Phi^* \tau_2$. The first two terms in the Lagrangian correspond to the Majorana-type Yukawa couplings between the lepton doublets and the Higgs triplets $\Delta_{L,R}$, while the last two terms correspond to the Dirac-type Yukawa couplings between the lepton doublets and the Higgs bi-doublets Φ and $\tilde{\Phi}$. The LRSM undergoes spontaneous symmetry breaking twice [76], which can be summarized as

$$SU(2)_L \times SU(2)_R \times U(1)_{B-L} \xrightarrow{\langle \Delta_R \rangle} SU(2)_L \times U(1)_Y \xrightarrow{\langle \Phi \rangle, \langle \Delta_L \rangle} U(1)_{EM}. \quad (3.59)$$

The $SU(3)_C$ gauge group remains intact during both stages of symmetry breaking and therefore is neglected for simplicity. In the first stage, the neutral component of the $SU(2)_R$ triplet acquires a VEV

$$\Delta_R \rightarrow \langle \Delta_R \rangle = \begin{pmatrix} 0 & 0 \\ v_R & 0 \end{pmatrix}. \quad (3.60)$$

This breaks the $SU(2)_R$ symmetry, giving the RH neutrinos large Majorana masses due to the second term in the Lagrangian (3.58),

$$M_N = v_R f_R. \quad (3.61)$$

At the same time, three massive gauge bosons (W_R^\pm, Z_R^0), which are some linear combinations of the $SU(2)_R$ and $U(1)_{B-L}$ gauge bosons, are generated. There is also a combination that is massless, corresponding to the gauge boson of $U(1)_Y$. This is similar to the case of electroweak symmetry breaking in the SM. After this step, the LRSM gauge group G_{LR} reduces to the SM gauge group G_{SM} . Notice that due to the symmetry breaking of $SU(2)_R$, the components of the bi-doublet no longer transform as a bi-doublet but as two different Higgs doublets under $SU(2)_L$. In the second symmetry breaking stage, the two Higgs doublets get their VEVs⁴, which subsequently induces the $SU(2)_L$ triplet to acquire its VEV:

$$\Phi \rightarrow \langle \Phi \rangle = \begin{pmatrix} v_1 & 0 \\ 0 & v_2 \end{pmatrix}, \quad \Delta_L \rightarrow \langle \Delta_L \rangle = \begin{pmatrix} 0 & 0 \\ v_L & 0 \end{pmatrix}. \quad (3.62)$$

$\langle \Phi \rangle$ leads to mass generation for both the LH and RH fermions due to the last two terms in the Lagrangian (3.58). The couplings g and \tilde{g} can be combined to a single Dirac-type Yukawa coupling

²In some other versions of LRSM, two Higgs doublets are chosen instead of the triplets. We use the triplets because they will lead to type-II seesaw mechanism naturally and are naturally embedded in an $SO(10)$ GUT.

³To ease a potential confusion, we need to clarify one thing. The field $\ell_R^c = (\ell^c)_L$ is left-chiral, which means that it transforms in the left-handed representation of the Lorentz group. On the other hand, it is the $SU(2)_R$ lepton doublet, meaning that it transforms as a doublet under the right-handed $SU(2)$ gauge group.

⁴For convenience, we still write it as if the bi-doublet gets two VEVs in its neutral components. But the bi-doublet technically no longer exists after the first symmetry breaking.

matrix

$$y = \frac{v_1}{v} y_1 + \frac{v_2}{v} y_2, \quad (3.63)$$

where $v \equiv \sqrt{v_1^2 + v_2^2}$ and we have assumed that both v_1 and v_2 are real. Due to the presence of the heavy RH neutrinos after the first stage of symmetry breaking, the LH active neutrinos get their masses naturally via the type-I seesaw mechanism,

$$m_\nu^I = -m_D M_N^{-1} m_D^T = -v^2 y^T (v_R f_R)^{-1} y. \quad (3.64)$$

Also, since the $SU(2)_L$ triplet Δ_L gets its VEV at this stage, the LH neutrino masses gain an additional contribution from the type-II seesaw mechanism [cf. the first term in Lagrangian (3.58)],

$$m_\nu^{II} = v_L f_L. \quad (3.65)$$

Hence, the active neutrino mass matrix in the minimal LRSM is the combination of Eqs. (3.64) and (3.65),

$$m_\nu \simeq m_\nu^{II} + m_\nu^I = v_L f_L - v^2 y^T (v_R f_R)^{-1} y. \quad (3.66)$$

Finally, a few comments on the constraints of this model are in order. For the LRSM to be consistent with our current phenomenological observations, a certain hierarchy among the VEVs of the Higgs fields must exist. First, in order to generate the tiny active neutrino masses via the seesaw mechanism, the RH neutrinos must be heavy, implying that the symmetry breaking scale v_R needs to be much higher than the electroweak scale. Therefore, $v_R \gg v_1, v_2$. Second, $v_1 \gg v_2$ is required to suppress the mixing between the charged gauge bosons W_L and W_R [124]. By carefully matching the experimentally measured W boson masses, one can find that

$$v = \sqrt{v_1^2 + v_2^2} \simeq v_1 \simeq 174 \text{ GeV}, \quad (3.67)$$

which is the electroweak VEV [19]. Furthermore, since the VEV of the triplet Δ_L , v_L , also contributes to the W_L and Z_L boson masses, which have been measured to high accuracies, it is constraint by these experimental data. In short, the upper bound for v_L comes from the precision measurement of the ρ -parameter, which is defined as

$$\rho \equiv \frac{M_{W_L}^2}{(M_{Z_L} \cos \theta_W)^2}, \quad (3.68)$$

where θ_W is the Weinberg angle. The deviation of it, $\Delta\rho \simeq -2v_L^2/v^2$, should be within 1% of unity, suggesting $v \lesssim 14 \text{ GeV}$ [1].

3.3.2 Discrete left-right symmetry

In addition to the gauge LR symmetry (3.54), a discrete LR symmetry is often imposed on the model to make the LR symmetry complete. For example, to restore parity, we require the Lagrangian (3.58) to be invariant under the following particle exchanges:

$$\ell_L \leftrightarrow \ell_R, \quad \Delta_L \leftrightarrow \Delta_R^*, \quad \Phi \leftrightarrow \Phi^\dagger. \quad (3.69)$$

This condition then yields the following relations for the Yukawa coupling matrices,

$$f_L = f_R^*, \quad y = y^\dagger \quad (y_1 = y_1^\dagger, \quad y_2 = y_2^\dagger). \quad (3.70)$$

The implementation of the parity symmetry was studied extensively in the past due to historical reasons [118, 119, 120, 121]. However, there is another way in which the discrete LR symmetry can be realized, that is, the charge conjugation symmetry. The charge conjugation symmetry was less

studied but is more natural in the $SO(10)$ GUT, where it is automatically a gauge symmetry [125]. It requires the Lagrangian (3.58) to be invariant under

$$\ell_L \leftrightarrow \widehat{\ell}_L \equiv \ell_R^c, \quad \Delta_L \leftrightarrow \widehat{\Delta}_L \equiv \Delta_R, \quad \Phi \leftrightarrow \widehat{\Phi} \equiv \Phi^T, \quad (3.71)$$

where the hat indicates the charge conjugation operator [cf. Eqs. (3.17a) and (3.17b) for charge conjugation on chiral fermion fields]. Then this condition leads to

$$f_L = f_R \equiv f, \quad y = y^T \quad (y_1 = y_1^T, \quad y_2 = y_2^T), \quad (3.72)$$

i.e. the two Majorana-type Yukawa coupling matrices are the same, and the Dirac-type Yukawa coupling matrix is symmetric. In this case, the LR symmetric seesaw relation (3.66) simplifies to

$$m_\nu \simeq m_\nu^{II} + m_\nu^I = v_L f - \frac{v^2}{v_R} y f^{-1} y. \quad (3.73)$$

As a result of the additional symmetries, this type of LRSM contains fewer parameters than the more general one, making it more predictive. Moreover, a duality property that lies in Eq. (3.73) was identified [21]: if f is a solution to the above seesaw formula, so is

$$\widehat{f} = \frac{m_\nu}{v_L} - f, \quad (3.74)$$

provided that the Dirac-type Yukawa coupling matrix y is invertible.

This duality property has important implications. First, it makes it possible to analytically reconstruct the Majorana-type Yukawa coupling f by inverting the seesaw formula (3.73). The reason to do this is the following. As mentioned above, the electroweak VEV v is accurately known from precision tests and the $SU(2)_L$ triplet VEV v_L is constraint by the W_L and Z_L boson masses. Although there is essentially no upper bound on the $SU(2)_R$ triplet VEV v_R , by assuming a GUT origin of the model and demanding the RH neutrinos to be heavy, its order of magnitude can be estimated from m_ν ⁵, v_L and v . The Dirac-type Yukawa coupling y is not directly measurable, but in the context of GUTs, it is related to the known quark and/or charged lepton Yukawa couplings. On the contrary, the Majorana-type Yukawa coupling f is not directly accessible from any experiment. Hence, it is reasonable to reconstruct f from the LR symmetric seesaw relation, taking the other parameters that can be more or less inferred from experiments as inputs. Performing such a task can shed light on the underlying physics at the seesaw scale, which is highly characterized by the structure of f . A detailed phenomenological study of this can be found in [126]. Second, the existence of the duality implies that the solutions are degenerate. For instance, for three lepton generations, there are eight degenerate solutions in general. It means that for given Dirac-type Yukawa coupling y and VEVs v_L and v_R , all eight solutions of f lead to the same active neutrino mass matrix m_ν . Thus, it also presents an eight-fold ambiguity for this mass matrix. A study on lifting the degeneracy by considering the stability and leptogenesis criteria is presented in [127].

Despite providing critical insight into high-energy theories at the seesaw scale, the particular LR symmetric seesaw relation (3.73) cannot give an accurate account of the active neutrino masses at low energies. The reason is that below the discrete LR symmetry breaking scale v_{LR} , different parameters such as f_L and f_R may receive different quantum corrections under the renormalization group (RG) evolution. As a result, these corrections induce a difference between f_L and f_R and an asymmetry in y . In this case, the relations (3.72) no longer hold and the seesaw relation needs to be reevaluated by taking into account the quantum corrections for different parameters.

⁵See Section 2.1.1 for various experimental bounds on the active neutrino masses m_ν .

Chapter 4

RG Evolution of the Effective Coupling

4.1 Relevant Particles

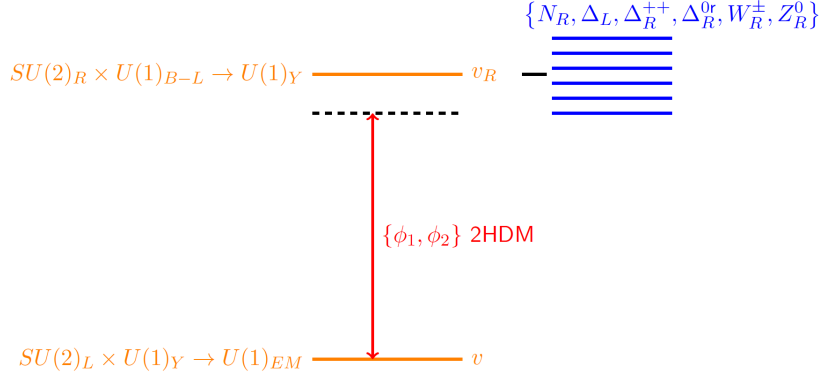


Figure 4.1: A schematic illustrating the symmetry breaking scales of the minimal LRSM and the particle spectrum. On the left, the two orange lines indicate the energy scales of the two stages of symmetry breaking in the LRSM, v_R and v . On the right, the blue lines are different mass thresholds of the different particles in the brackets. In the regime between v and the lowest mass threshold of the heavy particles, only the two Higgs doublets are relevant for the RG evolution in addition to the other SM particles. Such a scenario is called the two Higgs doublet model (2HDM).

To modify the seesaw relation (3.73) below the discrete LR symmetry breaking scale v_{LR} , we need to calculate how each of the different parameters evolves with energy, i.e. the renormalization scale μ . This is determined by the β -function of the corresponding parameter, as introduced in Section 2.2.3. In general, v_{LR} can be different from the $SU(2)_R$ symmetry breaking scale v_R [128], but for simplicity, we will assume these two symmetry breaking scales coincide, which is a reasonable expectation for the minimal LRSM.

Here, we take a bottom-up approach, where we consider the RG evolution from the electroweak scale v up to the discrete LR symmetry breaking scale v_{LR} . This approach is taken for the following reasons. First, we have a fairly good understanding of the low-energy physics at v as it is accessible from experiments. On the contrary, the high-energy physics at v_{LR} is largely unknown and it needs to be inferred from the low-energy phenomena. And the connection between them is exactly the RG running. Second, the particle spectrum at v_{LR} is fairly complicated, as illustrated in Fig. 4.1. After $SU(2)_R$ symmetry breaking, only the real part of Δ_R^0 (Δ_R^{0r}) and Δ_R^{++} remain, while the imaginary part Δ_R^{0i} and Δ_R^+ become the Goldstone bosons¹ that are “eaten” by the $SU(2)_R$ gauge bosons when they become massive [cf. (3.57) for the components of a scalar triplet]. Similarly, the RH neutrinos N_R also obtain their masses at this stage, as given in Eq. (3.61). Therefore, N_R , Δ_R^{++} , Δ_R^{0r} , and the $SU(2)_R$ gauge bosons W_R^\pm and Z_R^0 all have masses on the order of the $SU(2)_R$ symmetry breaking scale v_R , assuming their Yukawa couplings are of similar orders. The mass of Δ_L is of a similar order to that of Δ_R due to the discrete LR symmetry. Therefore, the mass thresholds of these particles, which are indicated by the blue lines in Fig. 4.1, are all on the order v_R but the exact spectrum is unknown. Below the lowest threshold, these particles are all integrated out in the EFT.

¹Goldstone bosons are the massless particles that arise when continuous symmetries are spontaneously broken, according to the Goldstone’s theorem [129, 130].

Then in between the electroweak scale and the lowest mass threshold, as indicated by the red arrow in the figure, the only relevant particles are the two Higgs doublets, ϕ_1 and ϕ_2 , that were originally embedded in the bi-doublet Φ before symmetry breaking, in addition to the other massless SM particles. In this regime, the most relevant parameter for the RG evolution is the effective coupling κ of the Weinberg operator [cf. Eq. (3.42)], which is associated with the active neutrino mass matrix m_ν in the seesaw formula. Therefore, the RG evolution of the effective coupling in the two Higgs doublet model (2HDM), which is characterized by its β -function, along with its implications, forms the main result of this thesis. The result also applies to a general n Higgs doublet model.

4.2 Renormalization of the 2HDM

In the 2HDM, the most general dimension-5 effective operator for neutrino mass is given by [68]

$$\mathcal{L}_\kappa = \frac{1}{4}(\kappa_1)_{\beta\alpha}^{ji}(\overline{\ell}_{Lc}^\beta \varepsilon_{cd}\phi_{dj})(\ell_{Lb}^\alpha \varepsilon_{ba}\phi_{ai}) + \frac{1}{4}(\kappa_2)_{\beta\alpha}^{ji}(\overline{\ell}_{Lc}^\beta \varepsilon_{cb}\ell_{Lb}^\alpha)(\phi_{dj}\varepsilon_{da}\phi_{ai}), \quad (4.1)$$

where a, b, c, d, \dots are the $SU(2)_L$ indices, α, β, \dots are the fermion flavor indices, and i, j, \dots are the Higgs flavor indices². The second term vanishes in the SM, where there is only one Higgs doublet, because the term is symmetric under the exchange of ϕ_d and ϕ_a , while the Levi-Civita symbol ε is antisymmetric. We can simplify this effective operator by exploiting the group theory identity

$$\varepsilon_{ab}\varepsilon_{cd} + \varepsilon_{ac}\varepsilon_{db} + \varepsilon_{ad}\varepsilon_{bc} = 0. \quad (4.2)$$

Then Eq. (4.1) can be written as

$$\mathcal{L}_\kappa = \frac{1}{4}\left[(\kappa_1)_{\beta\alpha}^{ji} + (\kappa_2)_{\beta\alpha}^{ji} - (\kappa_2)_{\beta\alpha}^{ij}\right](\overline{\ell}_{Lc}^\beta \varepsilon_{cd}\phi_{dj})(\ell_{Lb}^\alpha \varepsilon_{ba}\phi_{ai}). \quad (4.3)$$

Therefore, if we define a single effective coupling as $\kappa_{\beta\alpha}^{ji} \equiv (\kappa_1)_{\beta\alpha}^{ji} + (\kappa_2)_{\beta\alpha}^{ji} - (\kappa_2)_{\beta\alpha}^{ij}$, the most general effective operator is

$$\mathcal{L}_\kappa = \frac{1}{4}\kappa_{\beta\alpha}^{ji}(\overline{\ell}_{Lc}^\beta \varepsilon_{cd}\phi_{dj})(\ell_{Lb}^\alpha \varepsilon_{ba}\phi_{ai}). \quad (4.4)$$

It is noted that this Lagrangian is invariant under exchanging $i \leftrightarrow j$ and $\alpha \leftrightarrow \beta$ at the same time, so the effective coupling has the following symmetry:

$$\kappa_{\beta\alpha}^{ji} = \kappa_{\alpha\beta}^{ij}, \quad \text{i.e.} \quad \kappa^{ji} = (\kappa^{ij})^T, \quad (4.5)$$

where the transpose is acting on the fermion flavor space. The explicit connection between the effective coupling and the active neutrino mass matrix in the 2HDM is obtained when ϕ_i and ϕ_j ($i, j = 1, 2$) acquire their VEVs, denoted as v^i and v^j , after which the effective Lagrangian (4.4) turns into the Majorana mass term for ν_L [cf. Eq. (3.44)]. Then

$$m_\nu^{ij} = -\frac{\kappa^{ij}}{2}v^i v^j. \quad (4.6)$$

The effective coupling in general can be written in terms of its symmetric part $\kappa^{(ij)}$ ($\kappa^{(ji)} = \kappa^{(ij)}$) and the antisymmetric part $\kappa^{[ij]}$ ($\kappa^{[ji]} = -\kappa^{[ij]}$). At the tree level, only the symmetric part of κ contributes to the neutrino mass since Eq. (4.6) is symmetric under $i \leftrightarrow j$. In the LRSM, κ^{ij} is composed of the type-I and II seesaw contributions, i.e.

$$\kappa^{ij} = \kappa_I^{ij} + \kappa_{II}^{ij}, \quad (4.7)$$

²Here we can think of n different Higgs doublets as n flavors of the Higgs. Also, since the number of indices is getting a bit unmanageable, I will start using \mathcal{C} to label the particle-antiparticle conjugation to avoid confusion.

where the type-I effective vertex [cf. Eq. (3.43)] and the type-II effective vertex [cf. Eq. (3.51)] are given by

$$\kappa_I^{ij} = 2y_i^T M_N^{-1} y_j, \quad \kappa_{II}^{ij} = -2 \frac{\Lambda_L^{ij}}{M_{\Delta_L}^2} f_L. \quad (4.8)$$

It is worth noting that κ_I^{ij} contains both the symmetric and antisymmetric parts since $\kappa_I^{ij} \neq \kappa_I^{ji}$ in general, but only the symmetric part contributes to the neutrino mass. On the other hand, κ_{II}^{ij} is totally symmetric as $\Lambda_L^{ij} = \Lambda_L^{ji}$. It can be seen from the Feynman diagrams in (C.2) and (C.7).

We now consider the renormalization in the 2HDM. From Lagrangian (4.4), we see that the relevant parameters for the effective vertex renormalization are the wavefunction renormalizations of the Higgs and lepton doublets. They are defined as

$$\phi_B^i = (Z_\phi^{\frac{1}{2}})^{ij} \phi^j, \quad \ell_{LB}^\alpha = (Z_{\ell_L}^{\frac{1}{2}})_{\alpha\beta} \ell_L^\beta. \quad (4.9)$$

In a d -dimensional spacetime, we define the renormalization relation for the effective coupling as

$$(Z_{\ell_L}^{T\frac{1}{2}})_{\beta\beta'} (Z_\phi^{\frac{1}{2}})^{jj'} (\kappa_B)^{j'i'} (Z_\phi^{\frac{1}{2}})^{i'i} (Z_{\ell_L}^{\frac{1}{2}})_{\alpha'\alpha} = \mu^\epsilon [\kappa + \delta\kappa]_{\beta\alpha}^{ji}, \quad (4.10)$$

where $(\delta\kappa)_{\beta\alpha}^{ji}$ is the counterterm of the effective coupling. Then we can split the bare Lagrangian into the renormalized Lagrangian and the counterterm Lagrangian,

$$\mathcal{L}_{\kappa B} = \mathcal{L}_\kappa + \mathcal{C}_\kappa, \quad (4.11)$$

where \mathcal{L}_κ is given in Eq. (4.4), $\mathcal{L}_{\kappa B}$ has exactly the same form as \mathcal{L}_κ but with all the renormalized quantities replaced by the bare quantities, and the counterterm Lagrangian is given by

$$\mathcal{C}_\kappa = (\delta\kappa)_{\beta\alpha}^{ji} (\bar{\ell}_{Lc}^\beta \varepsilon_{cd} \phi_{dj}) (\ell_{Lb}^\alpha \varepsilon_{ba} \phi_{ai}). \quad (4.12)$$

4.2.1 Higgs wavefunction renormalization

We start by calculating the wavefunction renormalization of the Higgs fields. The relevant one-loop corrections to the Higgs 2-point function in the 2HDM are summarized in Fig. 4.2. Before evaluating the diagrams, we first take a look at the counterterm Lagrangian for the Higgs 2-point function. Its Feynman rule is given in Appendix D:

$$\text{---} \xrightarrow{\phi_i} \otimes \xrightarrow{\phi_j} \text{---} = i \left[p^2 (\delta Z_\phi)^{ij} - \delta m_{ij}^2 \right]. \quad (4.13)$$

It is clear that divergent terms that are absorbed into the Higgs wavefunction counterterm $(\delta Z_\phi)^{ij}$ should be proportional to p^2 . Those that are not proportional to p^2 are absorbed by the mass counterterm δm_{ij}^2 . If we consider the first Feynman diagram in Fig. 4.2, whose vertex function is given by Eq. (2.8), we see that the divergent part is related to the mass of the Higgs but not to its momentum³. So the first diagram does not contribute to the Higgs wavefunction renormalization.

We now consider the second diagram, where the loop consists of a RH electron and a LH lepton doublet. Using the DR method and the Feynman rules for the Yukawa vertices, we obtain

$$i(\Gamma_\phi^e)_{ab}^{ij} = \text{---} \xrightarrow{p} \text{---} \xrightarrow{p+k} \text{---} = (-1) \left[-i\mu^{\frac{d}{2}} (Y_e^j)_{\beta\alpha} \delta_{bc} \right] \left[-i\mu^{\frac{d}{2}} (Y_e^{i\dagger})_{\alpha\beta} \delta_{ca} \right] \int \frac{d^d k}{(2\pi)^d} \text{Tr} \left[P_L \frac{i(\not{p} + \not{k})}{(p+k)^2} P_R \frac{i\not{k}}{k^2} \right], \quad (4.14)$$

³To be precise, Eq. (2.8) is not the self-energy correction of Fig. 4.2(a). The reason is that in the 2HDM, the mass matrix of the Higgs is generally not diagonal. But since the divergent part of such a diagram is not proportional to p^2 , it does not contribute to the wavefunction renormalization.

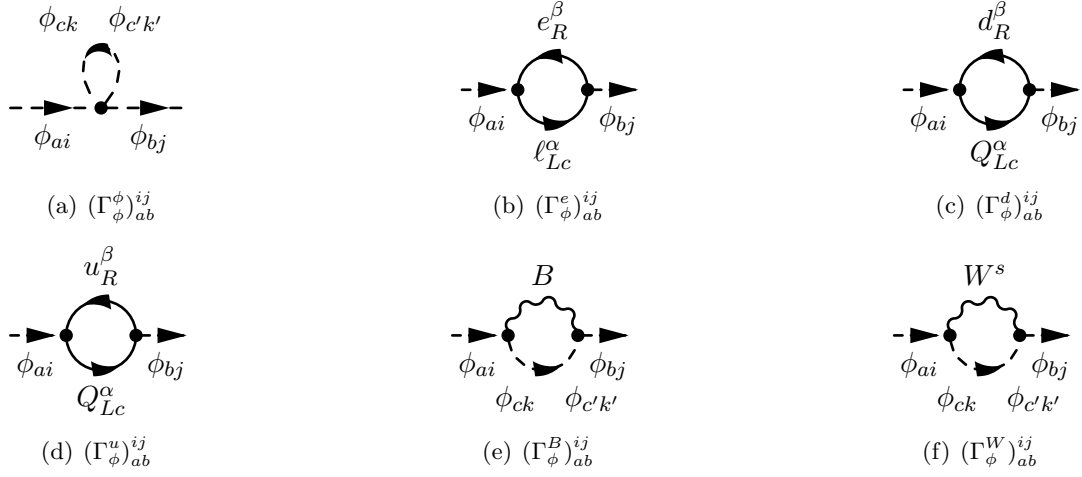


Figure 4.2: One-loop self-energy corrections to the Higgs fields in the 2HDM.

where the factor (-1) comes from the closed fermion loop, and Y_e^j , Y_e^i are the Yukawa couplings of the RH electron and LH lepton doublet with ϕ^j , ϕ^i (different Higgs flavors), respectively⁴. To evaluate the trace in the integral, we use the following useful identities from the Dirac algebra

$$\text{Tr} [\gamma^\mu \gamma^\nu] = 4g^{\mu\nu} \quad (4.15a)$$

$$\text{Tr} [\gamma^5] = \text{Tr} [\gamma^\mu] = \text{Tr} [\gamma^\mu \gamma^\alpha \gamma^\nu] = \text{Tr} [\text{odd } \# \text{ of } \gamma\text{-matrices}] = 0 \quad (4.15b)$$

as well as Eqs. (3.3a) and (3.3b). The trace is evaluated to be

$$\text{Tr} \left[P_L \frac{i(\not{p} + \not{k})}{(p+k)^2} P_R \frac{i\not{k}}{k^2} \right] = -\frac{2(p+k) \cdot k}{(p+k)^2 k^2}. \quad (4.16)$$

Then Eq. (4.14) becomes

$$\begin{aligned} i(\Gamma_\phi^e)^{ij}_{ab} &= -\frac{i}{16\pi^2} \delta_{ab} \text{Tr} (Y_e^{i\dagger} Y_e^j) \frac{\mu^\epsilon}{i\pi^2} \int d^d k \frac{2(p+k) \cdot k}{(p+k)^2 k^2} \\ &= -\frac{i}{8\pi^2} \delta_{ab} \text{Tr} (Y_e^{i\dagger} Y_e^j) [A_0(0) + p^2 B_1(p^2, 0, 0)] \\ &= \frac{i}{8\pi^2} \delta_{ab} \text{Tr} (Y_e^{i\dagger} Y_e^j) p^2 \frac{1}{\epsilon} + \text{UV finite}, \end{aligned} \quad (4.17)$$

where we have used the Passarino-Veltman functions [131] that are summarized in Appendix B to evaluate the integral in the first line. The other diagrams in Fig. 4.2 can be evaluated in a similar fashion with the aid of the Feynman rules in Appendix D. However, notice that the last two diagrams contain a Higgs propagator in the loop, whose mass matrix is non-diagonal in general. In a general mass basis, the Higgs propagator is given by

$$\text{---} \text{---} \text{---} \text{---} \text{---} \text{---} : iS_\phi(p) = i(p^2 \delta_{ij} - m_{ij}^2)^{-1} \delta_{ba}. \quad (4.18)$$

To go to a diagonal basis, we make the following transformation,

$$d^2 = U m^2 U^\dagger, \quad (4.19)$$

where U is a unitary matrix ($U^\dagger = U^{-1}$) and d^2 is a diagonal matrix. Then the propagator becomes

$$iS_\phi(p) = i \left[p^2 \delta_{ij} - (U^\dagger d^2 U)_{ij} \right]^{-1} \delta_{ba} = (U^\dagger)_{ik} \frac{i}{p^2 - d_{kk}^2 + i\epsilon} U_{kj} \delta_{ba} \quad (4.20)$$

⁴In connection to the 2HDM, we identify $Y_e^1 = y_1$ and $Y_e^2 = y_2$ [cf. Eq. (3.58)]. The similar connections can be made for Y_d and Y_u as the quark Yukawa couplings in the 2HDM have the same form as the lepton Yukawa couplings.

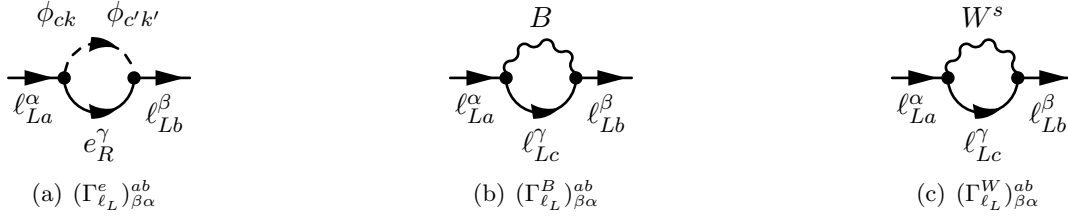


Figure 4.3: One-loop self-energy corrections to the lepton doublet fields in the 2HDM.

Note that there are technically diagrams which contain only gauge bosons in the loop that one needs to take into account. However, it can be easily shown that the divergent parts of these diagrams are proportional to the Passarino-Veltman function $A_0(0)$, that is,

$$\begin{array}{c} B/W^s \\ \text{---}\blacktriangleright \quad \bullet \quad \blacktriangleright\text{---} \\ \phi_{ai} \qquad \phi_{bj} \end{array} = k \cdot A_0(m^2=0) + \text{UV finite} = \text{UV finite}, \tag{4.25}$$

where k is a proportionality constant. Therefore, these diagrams are finite.

4.2.2 Left-handed lepton wavefunction renormalization

Next, we calculate the wavefunction renormalization for the LH lepton doublets. In the 2HDM, there are only three contributing Feynman diagrams, as shown in Fig. 4.3. Similar to what we did to obtain the corrections to the Higgs 2-point function, we evaluate each diagram in DR and extract the divergent parts. They are summarized in the following:

$$(\Gamma_{\ell_L}^e)^{ab}_{\beta\alpha} = \frac{1}{16\pi^2} \sum_{k=1}^2 \left(Y_e^{k\dagger} Y_e^k \right)_{\beta\alpha} \delta_{ab} \not{p}_L \frac{1}{\epsilon}; \quad (4.26a)$$

$$(\Gamma_{\ell_L}^B)^{ab}_{\beta\alpha} = \frac{1}{32\pi^2} \xi_1 g_1^2 \delta_{\beta\alpha} \delta_{ab} \not{P}_L \frac{1}{\epsilon}; \quad (4.26b)$$

$$(\Gamma_{\ell_L}^W)_{\beta\alpha}^{ab} = \frac{3}{32\pi^2} \xi_2 g_2^2 \delta_{\beta\alpha} \delta_{ab} \not{p}_L \frac{1}{\epsilon}. \quad (4.26c)$$

Again, demanding the renormalized 2-point function to be UV finite,

$$\begin{aligned}
\text{Diagram 1} &= \text{Diagram 2} + \text{Diagram 3} + \text{Diagram 4} \\
&+ \sum_{s=1}^3 \text{Diagram 5} + \text{Diagram 6} \\
&= i\delta_{\beta\alpha} + i \sum \text{all self-energy corrections} + i\cancel{p}(\delta Z_{\ell_L})_{\beta\alpha} P_L \\
&\stackrel{!}{=} \text{UV finite,}
\end{aligned}$$

we obtain the lepton doublet wavefunction counterterm

$$(\delta Z_{\ell_L})_{\beta\alpha} = -\frac{1}{16\pi^2} \left[\sum_{k=1}^2 \left(Y_e^{k\dagger} Y_e^k \right)_{\beta\alpha} + \frac{1}{2} \xi_1 g_1^2 \delta_{\beta\alpha} + \frac{3}{2} \xi_2 g_2^2 \delta_{\beta\alpha} \right] \frac{1}{\epsilon}. \quad (4.27)$$

4.2.3 Effective vertex renormalization

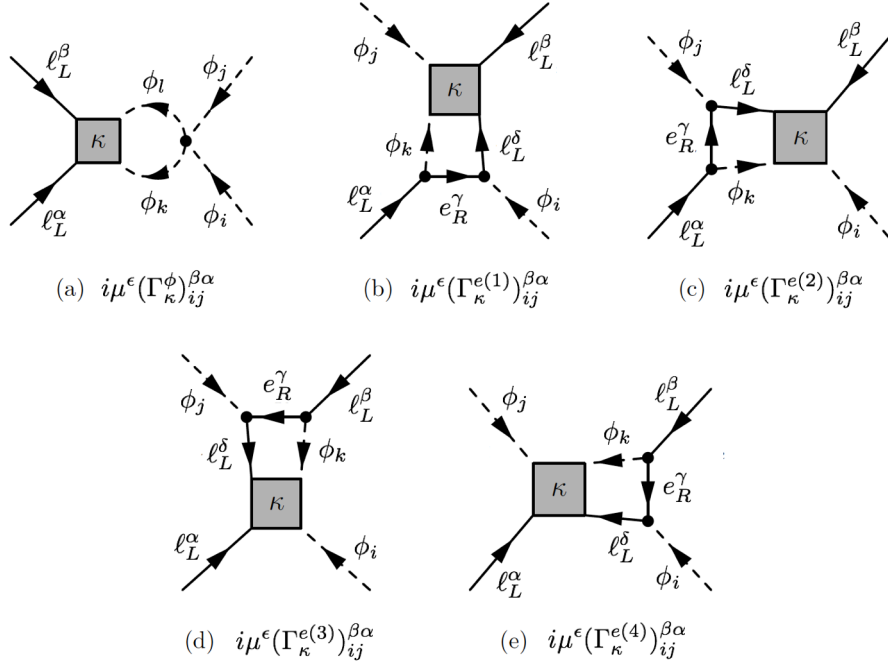


Figure 4.4: One-loop contributions to the renormalization of the effective vertex from fermions and/or scalars. The $SU(2)$ indices are omitted for simplicity. The assignment of them is the same as that in the effective vertex (D.10a).

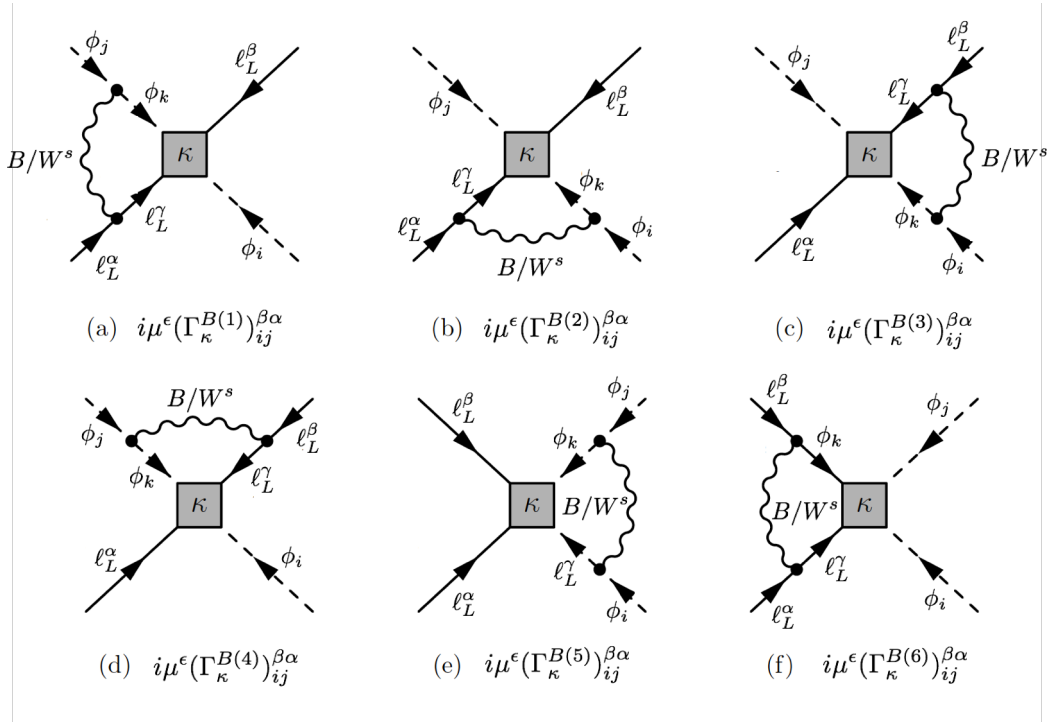


Figure 4.5: One-loop contributions to the renormalization of the effective vertex from $U(1)/SU(2)$ gauge bosons. The $SU(2)$ indices are omitted for simplicity.

Here we calculate all the effective vertex corrections up to one-loop order. First, we define the Lagrangian for the Higgs fields as

$$\mathcal{L}_\phi = (D_\mu \phi_i)^\dagger (D^\mu \phi_i) - m_{ij}^2 \phi_i^\dagger \phi_j - \frac{1}{4} \lambda_{ijkl} (\phi_i^\dagger \phi_j) (\phi_k^\dagger \phi_l). \quad (4.28)$$

Then using the Feynman rules, the first diagram in Fig. 4.4 yields

$$\left(\Gamma_{\kappa_{ij}}^\phi \right)_{\beta\alpha}^{abcd} = \frac{-1}{32\pi^2} \cdot \frac{1}{2} \sum_{k,l=1}^2 \left[\left(\kappa_{\beta\alpha}^{lk} \lambda_{kilj} + \kappa_{\beta\alpha}^{kl} \lambda_{kjli} \right) \epsilon_{cd} \epsilon_{ba} + \left(\kappa_{\beta\alpha}^{lk} \lambda_{kjli} + \kappa_{\beta\alpha}^{kl} \lambda_{kilj} \right) \epsilon_{ca} \epsilon_{bd} \right] P_L \frac{1}{\epsilon}. \quad (4.29)$$

Using the symmetry property $\lambda_{kilj} = \lambda_{ljki}$ and relabelling $l \leftrightarrow k$, we can write

$$\kappa_{\beta\alpha}^{lk} \lambda_{kilj} = \kappa_{\beta\alpha}^{lk} \lambda_{ljki} = \kappa_{\beta\alpha}^{kl} \lambda_{kjli} \quad (4.30)$$

Similarly, we also have

$$\kappa_{\beta\alpha}^{lk} \lambda_{kjli} = \kappa_{\beta\alpha}^{kl} \lambda_{kilj}. \quad (4.31)$$

Therefore, the vertex correction (4.29) simplifies to

$$\left(\Gamma_{\kappa_{ij}}^\phi \right)_{\beta\alpha}^{abcd} = \frac{-1}{16\pi^2} \cdot \frac{1}{2} \sum_{k,l=1}^2 \left(\kappa_{\beta\alpha}^{kl} \lambda_{kjli} \epsilon_{cd} \epsilon_{ba} + \kappa_{\beta\alpha}^{kl} \lambda_{kilj} \epsilon_{ca} \epsilon_{bd} \right) P_L \frac{1}{\epsilon}. \quad (4.32)$$

Next, if the loop contains a LH lepton doublet, a Higgs doublet, and a RH electron singlet, there are four diagrams, as shown in Fig. 4.4 (b)-(e). They give four vertex corrections:

$$\begin{aligned} \left(\Gamma_{\kappa_{ij}}^{e(1)} \right)_{\beta\alpha}^{abcd} &= \frac{1}{8\pi^2} \cdot \frac{1}{2} \sum_{k=1}^2 \left[\left(\kappa^{jk} Y_e^{i\dagger} Y_e^k \right)_{\beta\alpha} \epsilon_{cd} \epsilon_{ba} + \left(\kappa^{kj} Y_e^{i\dagger} Y_e^k \right)_{\beta\alpha} \epsilon_{cb} \epsilon_{da} \right] P_L \frac{1}{\epsilon} \\ &= \frac{1}{8\pi^2} \cdot \frac{1}{2} \sum_{k=1}^2 \left[\left(\kappa^{jk} Y_e^{i\dagger} Y_e^k + \kappa^{kj} Y_e^{i\dagger} Y_e^k \right)_{\beta\alpha} \epsilon_{cd} \epsilon_{ba} - \left(\kappa^{kj} Y_e^{i\dagger} Y_e^k \right)_{\beta\alpha} \epsilon_{ca} \epsilon_{bd} \right] P_L \frac{1}{\epsilon}; \end{aligned} \quad (4.33a)$$

$$\begin{aligned} \left(\Gamma_{\kappa_{ij}}^{e(2)} \right)_{\beta\alpha}^{abcd} &= \frac{1}{8\pi^2} \cdot \frac{1}{2} \sum_{k=1}^2 \left[\left(\kappa^{ik} Y_e^{j\dagger} Y_e^k \right)_{\beta\alpha} \epsilon_{ca} \epsilon_{bd} - \left(\kappa^{ki} Y_e^{j\dagger} Y_e^k \right)_{\beta\alpha} \epsilon_{cb} \epsilon_{da} \right] P_L \frac{1}{\epsilon} \\ &= \frac{1}{8\pi^2} \cdot \frac{1}{2} \sum_{k=1}^2 \left[- \left(\kappa^{ki} Y_e^{j\dagger} Y_e^k \right)_{\beta\alpha} \epsilon_{cd} \epsilon_{ba} + \left(\kappa^{ik} Y_e^{j\dagger} Y_e^k + \kappa^{ki} Y_e^{j\dagger} Y_e^k \right)_{\beta\alpha} \epsilon_{ca} \epsilon_{bd} \right] P_L \frac{1}{\epsilon}; \end{aligned} \quad (4.33b)$$

$$\begin{aligned} \left(\Gamma_{\kappa_{ij}}^{e(3)} \right)_{\beta\alpha}^{abcd} &= \frac{1}{8\pi^2} \cdot \frac{1}{2} \sum_{k=1}^2 \left[\left(Y_e^{kT} Y_e^{j*} \kappa^{ki} \right)_{\beta\alpha} \epsilon_{cd} \epsilon_{ba} + \left(Y_e^{kT} Y_e^{j*} \kappa^{ik} \right)_{\beta\alpha} \epsilon_{cb} \epsilon_{da} \right] P_L \frac{1}{\epsilon} \\ &= \frac{1}{8\pi^2} \cdot \frac{1}{2} \sum_{k=1}^2 \left[\left(Y_e^{kT} Y_e^{j*} \kappa^{ki} + Y_e^{kT} Y_e^{j*} \kappa^{ik} \right)_{\beta\alpha} \epsilon_{cd} \epsilon_{ba} - \left(Y_e^{kT} Y_e^{j*} \kappa^{ik} \right)_{\beta\alpha} \epsilon_{ca} \epsilon_{bd} \right] P_L \frac{1}{\epsilon}; \end{aligned} \quad (4.33c)$$

$$\begin{aligned} \left(\Gamma_{\kappa_{ij}}^{e(4)} \right)_{\beta\alpha}^{abcd} &= \frac{1}{8\pi^2} \cdot \frac{1}{2} \sum_{k=1}^2 \left[\left(Y_e^{kT} Y_e^{i*} \kappa^{kj} \right)_{\beta\alpha} \epsilon_{ca} \epsilon_{bd} - \left(Y_e^{kT} Y_e^{i*} \kappa^{jk} \right)_{\beta\alpha} \epsilon_{cb} \epsilon_{da} \right] P_L \frac{1}{\epsilon} \\ &= \frac{1}{8\pi^2} \cdot \frac{1}{2} \sum_{k=1}^2 \left[- \left(Y_e^{kT} Y_e^{i*} \kappa^{jk} \right)_{\beta\alpha} \epsilon_{cd} \epsilon_{ba} + \left(Y_e^{kT} Y_e^{i*} \kappa^{kj} + Y_e^{kT} Y_e^{i*} \kappa^{jk} \right)_{\beta\alpha} \epsilon_{ca} \epsilon_{bd} \right] P_L \frac{1}{\epsilon}; \end{aligned} \quad (4.33d)$$

where we have used the group theory identity Eq. (4.2) to rewrite new $SU(2)$ structure in terms of the old ones that show up in the Feynman rule for the effective vertex. Next, if the loop correction contains the B boson, there are six different configurations, as shown in Fig. 4.5, and they give the

following vertex corrections:

$$\left(\Gamma_{\kappa_{ij}}^{B(1)}\right)_{\beta\alpha}^{abcd} = \frac{1}{32\pi^2} \xi_1 g_1^2 \cdot \frac{1}{2} \left[\kappa_{\beta\alpha}^{ji} \epsilon_{cd} \epsilon_{ba} + \kappa_{\beta\alpha}^{ij} \epsilon_{ca} \epsilon_{bd} \right] P_L \frac{1}{\epsilon}; \quad (4.34a)$$

$$\left(\Gamma_{\kappa_{ij}}^{B(2)}\right)_{\beta\alpha}^{abcd} = \frac{1}{32\pi^2} \xi_1 g_1^2 \cdot \frac{1}{2} \left[\kappa_{\beta\alpha}^{ji} \epsilon_{cd} \epsilon_{ba} + \kappa_{\beta\alpha}^{ij} \epsilon_{ca} \epsilon_{bd} \right] P_L \frac{1}{\epsilon}; \quad (4.34b)$$

$$\left(\Gamma_{\kappa_{ij}}^{B(3)}\right)_{\beta\alpha}^{abcd} = \frac{1}{32\pi^2} \xi_1 g_1^2 \cdot \frac{1}{2} \left[\kappa_{\beta\alpha}^{ji} \epsilon_{cd} \epsilon_{ba} + \kappa_{\beta\alpha}^{ij} \epsilon_{ca} \epsilon_{bd} \right] P_L \frac{1}{\epsilon}; \quad (4.34c)$$

$$\left(\Gamma_{\kappa_{ij}}^{B(4)}\right)_{\beta\alpha}^{abcd} = \frac{1}{32\pi^2} \xi_1 g_1^2 \cdot \frac{1}{2} \left[\kappa_{\beta\alpha}^{ji} \epsilon_{cd} \epsilon_{ba} + \kappa_{\beta\alpha}^{ij} \epsilon_{ca} \epsilon_{bd} \right] P_L \frac{1}{\epsilon}; \quad (4.34d)$$

$$\left(\Gamma_{\kappa_{ij}}^{B(5)}\right)_{\beta\alpha}^{abcd} = \frac{-1}{32\pi^2} \xi_1 g_1^2 \cdot \frac{1}{2} \left[\kappa_{\beta\alpha}^{ji} \epsilon_{cd} \epsilon_{ba} + \kappa_{\beta\alpha}^{ij} \epsilon_{ca} \epsilon_{bd} \right] P_L \frac{1}{\epsilon}; \quad (4.34e)$$

$$\left(\Gamma_{\kappa_{ij}}^{B(6)}\right)_{\beta\alpha}^{abcd} = \frac{-1}{32\pi^2} (3 + \xi_1) g_1^2 \cdot \frac{1}{2} \left[\kappa_{\beta\alpha}^{ji} \epsilon_{cd} \epsilon_{ba} + \kappa_{\beta\alpha}^{ij} \epsilon_{ca} \epsilon_{bd} \right] P_L \frac{1}{\epsilon}. \quad (4.34f)$$

Moreover, for each configuration, we can replace the B boson by a W boson and thus they also contribute to the vertex correction:

$$\left(\Gamma_{\kappa_{ij}}^{W(1)}\right)_{\beta\alpha}^{abcd} = \frac{1}{32\pi^2} \xi_2 g_2^2 \cdot \frac{1}{2} \left[-\kappa_{\beta\alpha}^{ji} \epsilon_{cd} \epsilon_{ba} + \left(3\kappa_{\beta\alpha}^{ij} + 2\kappa_{\beta\alpha}^{ji} \right) \epsilon_{ca} \epsilon_{bd} \right] P_L \frac{1}{\epsilon}; \quad (4.35a)$$

$$\left(\Gamma_{\kappa_{ij}}^{W(2)}\right)_{\beta\alpha}^{abcd} = \frac{1}{32\pi^2} \xi_2 g_2^2 \cdot \frac{1}{2} \left[\left(3\kappa_{\beta\alpha}^{ji} + 2\kappa_{\beta\alpha}^{ij} \right) \epsilon_{cd} \epsilon_{ba} - \kappa_{\beta\alpha}^{ij} \epsilon_{ca} \epsilon_{bd} \right] P_L \frac{1}{\epsilon}; \quad (4.35b)$$

$$\left(\Gamma_{\kappa_{ij}}^{W(3)}\right)_{\beta\alpha}^{abcd} = \frac{1}{32\pi^2} \xi_2 g_2^2 \cdot \frac{1}{2} \left[-\kappa_{\beta\alpha}^{ji} \epsilon_{cd} \epsilon_{ba} + \left(3\kappa_{\beta\alpha}^{ij} + 2\kappa_{\beta\alpha}^{ji} \right) \epsilon_{ca} \epsilon_{bd} \right] P_L \frac{1}{\epsilon}; \quad (4.35c)$$

$$\left(\Gamma_{\kappa_{ij}}^{W(4)}\right)_{\beta\alpha}^{abcd} = \frac{1}{32\pi^2} \xi_2 g_2^2 \cdot \frac{1}{2} \left[\left(3\kappa_{\beta\alpha}^{ji} + 2\kappa_{\beta\alpha}^{ij} \right) \epsilon_{cd} \epsilon_{ba} - \kappa_{\beta\alpha}^{ij} \epsilon_{ca} \epsilon_{bd} \right] P_L \frac{1}{\epsilon}; \quad (4.35d)$$

$$\left(\Gamma_{\kappa_{ij}}^{W(5)}\right)_{\beta\alpha}^{abcd} = \frac{-1}{32\pi^2} \xi_2 g_2^2 \cdot \frac{1}{2} \left[\left(2\kappa_{\beta\alpha}^{ij} - \kappa_{\beta\alpha}^{ji} \right) \epsilon_{cd} \epsilon_{ba} + \left(2\kappa_{\beta\alpha}^{ji} - \kappa_{\beta\alpha}^{ij} \right) \epsilon_{ca} \epsilon_{bd} \right] P_L \frac{1}{\epsilon}; \quad (4.35e)$$

$$\left(\Gamma_{\kappa_{ij}}^{W(6)}\right)_{\beta\alpha}^{abcd} = \frac{-1}{32\pi^2} (3 + \xi_2) g_2^2 \cdot \frac{1}{2} \left[\left(2\kappa_{\beta\alpha}^{ij} - \kappa_{\beta\alpha}^{ji} \right) \epsilon_{cd} \epsilon_{ba} + \left(2\kappa_{\beta\alpha}^{ji} - \kappa_{\beta\alpha}^{ij} \right) \epsilon_{ca} \epsilon_{bd} \right] P_L \frac{1}{\epsilon}. \quad (4.35f)$$

According to the Feynman rule, the counterterm vertex is given by

$$\left(\Gamma_{\delta\kappa_{ij}}\right)_{\beta\alpha}^{abcd} = \frac{1}{2} \left(\delta\kappa_{\beta\alpha}^{ji} \epsilon_{cd} \epsilon_{ba} + \delta\kappa_{\beta\alpha}^{ij} \epsilon_{ca} \epsilon_{bd} \right) P_L. \quad (4.36)$$

In renormalization, we again demand all the divergences to be absorbed into the counterterm:

$$\left(\Gamma_{\kappa_{ij}}^{\phi}\right)_{\beta\alpha}^{abcd} + \sum_{t=1}^4 \left(\Gamma_{\kappa_{ij}}^{e(t)}\right)_{\beta\alpha}^{abcd} + \sum_{t=1}^6 \left(\Gamma_{\kappa_{ij}}^{B(t)}\right)_{\beta\alpha}^{abcd} + \sum_{t=1}^6 \left(\Gamma_{\kappa_{ij}}^{W(t)}\right)_{\beta\alpha}^{abcd} + \left(\Gamma_{\delta\kappa_{ij}}\right)_{\beta\alpha}^{abcd} = 0. \quad (4.37)$$

Therefore, $(\delta\kappa)_{\beta\alpha}^{ij}$ is determined by matching the coefficients in front of the $SU(2)$ structure $\epsilon_{ca} \epsilon_{bd}$. Using the Einstein summation convention and thereby dropping the summation signs, we arrive at

$$\begin{aligned} (\delta\kappa)_{\beta\alpha}^{ij} = & -\frac{1}{16\pi^2} \left\{ -\kappa_{\beta\alpha}^{kl} \lambda_{kilj} + 2 \left[-\kappa_{\beta\alpha}^{kj} Y_e^{i\dagger} Y_e^k + \left(\kappa_{\beta\alpha}^{ik} + \kappa_{\beta\alpha}^{ki} \right) Y_e^{j\dagger} Y_e^k \right. \right. \\ & \left. \left. - Y_e^{kT} Y_e^{j*} \kappa_{\beta\alpha}^{ik} + Y_e^{kT} Y_e^{i*} \left(\kappa_{\beta\alpha}^{kj} + \kappa_{\beta\alpha}^{jk} \right) \right] \right. \\ & \left. + \left(\xi_1 - \frac{3}{2} \right) g_1^2 \kappa_{\beta\alpha}^{ij} + \left(3\xi_2 + \frac{3}{2} \right) g_2^2 \kappa_{\beta\alpha}^{ij} - 3g_2^2 \kappa_{\beta\alpha}^{ji} \right\} \frac{1}{\epsilon}. \end{aligned} \quad (4.38)$$

Similarly, $(\delta\kappa)_{\beta\alpha}^{ji}$ can be determined by matching the coefficients for $\epsilon_{cd} \epsilon_{ba}$. And the result turns out to be have the same structure as $(\delta\kappa)_{\beta\alpha}^{ij}$, with i and j exchanged in each term in Eq. (4.38). This is exactly what we would expect.

4.3 Calculation of the β -Function

The general method for calculating the β -function of tensorial quantities with one set of indices was derived in [132]. Here, we generalize this method for quantities with two different set of indices and specifically derive the β -function for the effective coupling $\kappa_{\beta\alpha}^{ij}$.

Recall the renormalization relation for the effective coupling $\kappa_{\beta\alpha}^{ij}$ is given in Eq. (4.10), or

$$(\kappa_B)_{\beta\alpha}^{ij} = (Z_\phi^{-\frac{1}{2}})^{ii'} (Z_{\ell_L}^{T-\frac{1}{2}})_{\beta\beta'} \mu^{D_\kappa \epsilon} [\kappa + \delta\kappa]_{\beta'\alpha'}^{i'j'} (Z_{\ell_L}^{-\frac{1}{2}})_{\alpha'\alpha} (Z_\phi^{-\frac{1}{2}})^{j'j}, \quad (4.39)$$

where $D_\kappa = 1$ and the transpose is acting on the spinor space (corresponding to the $SU(2)_L$ indices which are omitted here). As in the derivation of the Callan-Symanzik equation, we make use of the fact that the bare quantity κ_B is independent of the renormalization scale, i.e.

$$\mu \frac{d\kappa_B}{d\mu} = 0. \quad (4.40)$$

Therefore, the total derivative of the right hand side of Eq. (4.39) with respect to μ also vanishes. We need to use the chain rule when taking the total derivative, and thus we must take into account of all the parameters that are μ -dependent:

$$\delta\kappa = \delta\kappa(\kappa, \lambda, Y_e^\dagger, Y_e, Y_e^T, Y_e^*, g_1, g_2) \equiv \delta\kappa(\kappa, \{V_\kappa\}), \quad (4.41a)$$

$$Z_\phi = Z_\phi(Y_e^\dagger, Y_e, Y_d^\dagger, Y_d, Y_u^\dagger, Y_u, g_1, g_2) \equiv Z_\phi(\{V_\phi\}), \quad (4.41b)$$

$$Z_{\ell_L}^T = Z_{\ell_L}^T(Y_e^T, Y_e^*, g_1, g_2) \equiv Z_{\ell_L}^T(\{V_{\ell 1}\}), \quad (4.41c)$$

$$Z_{\ell_L} = Z_{\ell_L}(Y_e^\dagger, Y_e, g_1, g_2) \equiv Z_{\ell_L}^T(\{V_{\ell 2}\}). \quad (4.41d)$$

One has to keep in mind that different parameters carry different indices and they are omitted in these expressions just for the sake of convenience. If we now take the total derivative of Eq. (4.39) with respect to μ , we obtain

$$\begin{aligned} 0 = & (Z_\phi^{-\frac{1}{2}})^{ii'} (Z_{\ell_L}^{T-\frac{1}{2}})_{\beta\beta'} \left\{ (\beta_\kappa)_{\beta'\alpha'}^{i'j'} + \left\langle \frac{d\delta\kappa}{d\kappa} \middle| \beta_\kappa \right\rangle_{\beta'\alpha'}^{i'j'} + \sum_{\{V_\kappa\}} \left\langle \frac{d\delta\kappa}{dV_\kappa} \middle| \beta_{V_\kappa} \right\rangle_{\beta'\alpha'}^{i'j'} \right. \\ & \left. + D_\kappa \epsilon [\kappa + \delta\kappa]_{\beta'\alpha'}^{i'j'} \right\} (Z_{\ell_L}^{-\frac{1}{2}})_{\alpha'\alpha} (Z_\phi^{-\frac{1}{2}})^{j'j} \\ & + \sum_{\{V_\phi\}} \left\langle \frac{d\delta Z_\phi^{-\frac{1}{2}}}{dV_\phi} \middle| \beta_{V_\phi} \right\rangle^{ii'} (Z_{\ell_L}^{T-\frac{1}{2}})_{\beta\beta'} [\kappa + \delta\kappa]_{\beta'\alpha'}^{i'j'} (Z_{\ell_L}^{-\frac{1}{2}})_{\alpha'\alpha} (Z_\phi^{-\frac{1}{2}})^{j'j} \\ & + (Z_\phi^{-\frac{1}{2}})^{ii'} \sum_{\{V_{\ell 1}\}} \left\langle \frac{d\delta Z_{\ell_L}^{T-\frac{1}{2}}}{dV_{\ell 1}} \middle| \beta_{V_{\ell 1}} \right\rangle_{\beta\beta'} [\kappa + \delta\kappa]_{\beta'\alpha'}^{i'j'} (Z_{\ell_L}^{-\frac{1}{2}})_{\alpha'\alpha} (Z_\phi^{-\frac{1}{2}})^{j'j} \\ & + (Z_\phi^{-\frac{1}{2}})^{ii'} (Z_{\ell_L}^{T-\frac{1}{2}})_{\beta\beta'} [\kappa + \delta\kappa]_{\beta'\alpha'}^{i'j'} \sum_{\{V_{\ell 2}\}} \left\langle \frac{d\delta Z_{\ell_L}^{-\frac{1}{2}}}{dV_{\ell 2}} \middle| \beta_{V_{\ell 2}} \right\rangle_{\alpha'\alpha} (Z_\phi^{-\frac{1}{2}})^{j'j} \\ & + (Z_\phi^{-\frac{1}{2}})^{ii'} (Z_{\ell_L}^{T-\frac{1}{2}})_{\beta\beta'} [\kappa + \delta\kappa]_{\beta'\alpha'}^{i'j'} (Z_{\ell_L}^{-\frac{1}{2}})_{\alpha'\alpha} \sum_{\{V_\phi\}} \left\langle \frac{d\delta Z_\phi^{-\frac{1}{2}}}{dV_\phi} \middle| \beta_{V_\phi} \right\rangle^{j'j}, \end{aligned} \quad (4.42)$$

where we have introduced the angle bracket notation for arbitrary tensors F , x and y ,

$$\left\langle \frac{dF}{dx} \middle| y \right\rangle_{\alpha \dots \beta}^{a \dots b} \equiv \frac{dF_{\alpha \dots \beta}^{a \dots b}}{dx_{\delta \dots \gamma}^{m \dots n}} y_{\delta \dots \gamma}^{m \dots n}. \quad (4.43)$$

The first term in Eq. (4.42) is obtained by taking the total derivative of $\mu^{D_\kappa \epsilon} [\kappa + \delta\kappa]_{\beta'\alpha'}^{i'j'}$ in Eq. (4.39) with respect to μ . The other four terms correspond to taking the derivative of the wavefunction renormalization constants in Eq. (4.39). By repeating these steps, one can also obtain analogous relations for the other parameters $\{V_A\}$ ($A = \kappa, \phi, \ell_1, \ell_2$). With the set of equations of the type (4.42), the β -functions can be determined by expanding all quantities in powers of ϵ and matching the coefficients. First, the β -functions are defined in terms of derivatives of the renormalized quantities and consequently are finite in the limit $\epsilon \rightarrow 0$, so they can be expanded as

$$\beta_\kappa = \beta_\kappa^{(0)} + \epsilon \beta_\kappa^{(1)} + \cdots + \epsilon^n \beta_\kappa^{(n)}, \quad (4.44a)$$

$$\beta_{V_A} = \beta_{V_A}^{(0)} + \epsilon \beta_{V_A}^{(1)} + \cdots + \epsilon^n \beta_{V_A}^{(n)}. \quad (4.44b)$$

Again, different β -functions carry different indices. On the other hand, the expansion of wavefunction renormalization constants follows from the MS renormalization scheme:

$$(Z_\phi^{-\frac{1}{2}})^{ij} = \delta_{ij} - \frac{1}{2}(\delta Z_{\phi,1})^{ij} \frac{1}{\epsilon} + \mathcal{O}(1/\epsilon^2), \quad (4.45a)$$

$$(Z_{\ell_L}^{T-\frac{1}{2}})_{\beta\alpha} = \delta_{\beta\alpha} - \frac{1}{2}(\delta Z_{\ell_L,1}^T)_{\beta\alpha} \frac{1}{\epsilon} + \mathcal{O}(1/\epsilon^2), \quad (4.45b)$$

$$(Z_{\ell_L}^{-\frac{1}{2}})_{\beta\alpha} = \delta_{\beta\alpha} - \frac{1}{2}(\delta Z_{\ell_L,1})_{\beta\alpha} \frac{1}{\epsilon} + \mathcal{O}(1/\epsilon^2). \quad (4.45c)$$

Finally, we also define

$$(\delta\kappa)_{\beta\alpha}^{ij} \equiv \sum_{k \geq 1} (\delta\kappa, k)_{\beta\alpha}^{ij} \frac{1}{\epsilon^k} = (\delta\kappa, 1)_{\beta\alpha}^{ij} \frac{1}{\epsilon} + \mathcal{O}(1/\epsilon^2). \quad (4.46)$$

If we substitute these expansions back into Eq. (4.42), we will find that for $n > 1$, the only term of order ϵ^n is $\epsilon^n (\beta_\kappa^{(n)})_{\beta\alpha}^{ij}$, since the terms in the angle brackets such as $\langle \frac{d\delta\kappa}{d\kappa} | \beta_\kappa \rangle_{\beta\alpha}^{ij}$ are of order ϵ^{n-1} . This then implies that $\beta_\kappa^{(n)}$ must be zero. By the same argument, the analogs of Eq. (4.42) tell us that all the other β -functions at the n th order vanish, $\beta_{V_A}^{(n)} = 0$. If we continue this process for the order ϵ^{n-1} , we will find that again, all the β -functions at this order vanish. In fact, they all vanish for the orders $k = 2, \dots, n$.

At the order ϵ^1 , there are two terms in Eq. (4.42), $\epsilon (\beta_\kappa^{(1)})_{\beta\alpha}^{ij}$ and $D_\kappa \epsilon \kappa_{\beta\alpha}^{ij}$. Therefore, the first non-vanishing term is $\beta_\kappa^{(1)} = -D_\kappa \kappa = -\kappa$. In an analogous way, we find $\beta_{V_A}^{(1)} = -D_{V_A} V_A$. Therefore, the expansions (4.44a) and (4.44b) become

$$\beta_\kappa = \beta_\kappa^{(0)} - D_\kappa \kappa \epsilon, \quad (4.47a)$$

$$\beta_{V_A} = \beta_{V_A}^{(0)} - D_{V_A} V_A \epsilon. \quad (4.47b)$$

Note that the terms of order ϵ^1 do not contribute in 4 dimensions since they vanish when $\epsilon \rightarrow 0$. So the only relevant β -functions are of order ϵ^0 . At this order, the terms in the angle brackets also contribute. For example,

$$\begin{aligned} \delta_{ii'} \delta_{\beta\beta'} \left\langle \frac{d\delta\kappa}{d\kappa} \middle| \beta_\kappa \right\rangle_{\beta'\alpha'}^{i'j'} \delta_{\alpha'\alpha} \delta_{j'j} &= \left\langle \frac{d\delta\kappa}{d\kappa} \middle| \beta_\kappa \right\rangle_{\beta\alpha}^{ij} \\ &= \left\langle \frac{d\delta\kappa, 1}{d\kappa} \frac{1}{\epsilon} + \mathcal{O}(1/\epsilon^2) \middle| \beta_\kappa^{(0)} - D_\kappa \kappa \epsilon \right\rangle_{\beta\alpha}^{ij} \\ &= - \left\langle \frac{d\delta\kappa, 1}{d\kappa} \middle| \kappa \right\rangle_{\beta\alpha}^{ij} + \mathcal{O}(1/\epsilon). \end{aligned} \quad (4.48)$$

Therefore, the final result is

$$\begin{aligned}
 (\beta_\kappa^{(0)})_{\beta\alpha}^{ij} &= \left\langle \frac{d\delta\kappa_{,1}}{d\kappa} \middle| \kappa \right\rangle_{\beta\alpha}^{ij} + \sum_{\{V_\kappa\}} D_{V_\kappa} \left\langle \frac{d\delta\kappa_{,1}}{dV_\kappa} \middle| V_\kappa \right\rangle_{\beta\alpha}^{ij} - (\delta\kappa_{,1})_{\beta\alpha}^{ij} \\
 &\quad - \frac{1}{2} \sum_{\{V_\phi\}} D_{V_\phi} \left\langle \frac{d\delta Z_{\phi,1}}{dV_\phi} \middle| V_\phi \right\rangle_{\beta\alpha}^{ii'} \kappa_{\beta\alpha}^{i'j} - \frac{1}{2} \sum_{\{V_{\ell 1}\}} D_{V_{\ell 1}} \left\langle \frac{d\delta Z_{\ell L,1}^T}{dV_{\ell 1}} \middle| V_{\ell 1} \right\rangle_{\beta\beta'} \kappa_{\beta'\alpha}^{ij} \\
 &\quad - \frac{1}{2} \kappa_{\beta\alpha'}^{ij} \sum_{\{V_{\ell 2}\}} D_{V_{\ell 2}} \left\langle \frac{d\delta Z_{\ell L,1}}{dV_{\ell 2}} \middle| V_{\ell 2} \right\rangle_{\alpha'\alpha} - \frac{1}{2} \kappa_{\beta\alpha}^{ij'} \sum_{\{V_\phi\}} D_{V_\phi} \left\langle \frac{d\delta Z_{\phi,1}}{dV_\phi} \middle| V_\phi \right\rangle_{\beta\beta'}^{j'j}.
 \end{aligned} \tag{4.49}$$

If we then substitute the counterterms (4.23), (4.27) and (4.38) into the master formula (4.49), with $D_\lambda = 1$, $D_{Y_i} = D_{g_1} = D_{g_2} = \frac{1}{2}$, we obtain the β -function for the effective coupling,

$$\begin{aligned}
 16\pi^2 \mu \frac{d\kappa^{ij}}{d\mu} &= 16\pi^2 (\beta_\kappa^{(0)})^{ij} = \left\{ \kappa^{kl} \lambda_{kilj} + 2 \left[\kappa^{kj} Y_e^{j\dagger} Y_e^k - (\kappa^{ik} + \kappa^{ki}) Y_e^{j\dagger} Y_e^k \right. \right. \\
 &\quad \left. \left. + Y_e^{kT} Y_e^{j*} \kappa^{ik} - Y_e^{kT} Y_e^{i*} (\kappa^{kj} + \kappa^{jk}) \right] + T^{ii'} \kappa^{i'j} + \kappa^{ij'} T^{j'j} \right. \\
 &\quad \left. + \kappa^{ij} S + S^T \kappa^{ij} - 3g_2^2 (2\kappa^{ij} - \kappa^{ji}) \right\},
 \end{aligned} \tag{4.50}$$

where

$$T^{ij} \equiv \text{Tr} \left(Y_e^{i\dagger} Y_e^j + 3Y_d^{i\dagger} Y_d^j + 3Y_u^{i\dagger} Y_u^j \right), \tag{4.51}$$

and

$$S \equiv \frac{1}{2} Y_e^{k\dagger} Y_e^k. \tag{4.52}$$

Eq. (4.50) is the RGE of the effective coupling associated with the dimension-5 Weinberg operator in the 2HDM, which governs the evolution of the active neutrino matrix m_ν above the electroweak scale. The result can be justified from the following perspectives. First, the gauge parameters ξ_1 and ξ_2 do not show up in (4.50), which is what is expected as the β -function should not depend on the gauges chosen. Second, our result matches the previous calculation given in [133], except the final term in (4.50) that is proportional to g_2^2 . In our result, this term contains both κ^{ij} and κ^{ji} , which are generally two different matrices related by transposition in the fermion flavor space, as shown in Eq. (4.5). In the previous result, the corresponding term is $-3g_2^2 \kappa^{ij}$. However, the authors did not make an explicit assumption that $\kappa^{ij} = \kappa^{ji}$. Therefore, we believe (4.50) is the most general form of the β -function for an n Higgs doublet model. Third, our result also coincides with the one for 2HDM with an additional \mathbb{Z}_2 symmetry [134], when taking the limit $i = j$. It also agrees with the result in [132] at the limit where there is only one Higgs species.

It is also interesting to inspect the symmetric and antisymmetric parts of the β -function, which determines the RG evolution of $\kappa^{(ij)}$ and $\kappa^{[ij]}$, respectively. By demanding $\beta_\kappa^{ij} = \beta_\kappa^{(ij)} + \beta_\kappa^{[ij]}$ and $\kappa^{ij} = \kappa^{(ij)} + \kappa^{[ij]}$, Eq. (4.50) can be decomposed into

$$\begin{aligned}
 16\pi^2 \mu \frac{d\kappa^{(ij)}}{d\mu} &= \left\{ \frac{1}{2} \kappa^{(kl)} (\lambda_{kilj} + \lambda_{kjli}) - \left(\kappa^{(ik)} Y_e^{j\dagger} Y_e^k + Y_e^{kT} Y_e^{j*} \kappa^{(ik)} + \kappa^{(jk)} Y_e^{i\dagger} Y_e^k + Y_e^{kT} Y_e^{i*} \kappa^{(jk)} \right) \right. \\
 &\quad \left. + \frac{1}{2} \left[\kappa^{(ik)} (T^{jk} + T^{kj}) + \kappa^{(jk)} (T^{ik} + T^{ki}) \right] + \kappa^{(ij)} S + S^T \kappa^{(ij)} - 3g_2^2 \kappa^{(ij)} \right. \\
 &\quad \left. + \frac{1}{2} \kappa^{[kl]} (\lambda_{kilj} + \lambda_{kjli}) - \left(\kappa^{[ik]} Y_e^{j\dagger} Y_e^k - Y_e^{kT} Y_e^{j*} \kappa^{[ik]} + \kappa^{[jk]} Y_e^{i\dagger} Y_e^k - Y_e^{kT} Y_e^{i*} \kappa^{[jk]} \right) \right. \\
 &\quad \left. + \frac{1}{2} \left[\kappa^{[ik]} (T^{kj} - T^{jk}) + \kappa^{[jk]} (T^{ki} - T^{ik}) \right] \right\},
 \end{aligned} \tag{4.53}$$

and

$$\begin{aligned}
16\pi^2 \mu \frac{d\kappa^{[ij]}}{d\mu} = & \left\{ \frac{1}{2} \kappa^{(kl)} (\lambda_{kilj} - \lambda_{kjli}) - \left(3\kappa^{(ik)} Y_e^{j\dagger} Y_e^k - 3Y_e^{kT} Y_e^{i*} \kappa^{(ik)} - 3\kappa^{(jk)} Y_e^{i\dagger} Y_e^k + 3Y_e^{kT} Y_e^{i*} \kappa^{(jk)} \right) \right. \\
& + \frac{1}{2} \left[\kappa^{(ik)} (T^{kj} - T^{jk}) + \kappa^{(jk)} (T^{ik} - T^{ki}) \right] \\
& + \left\{ \frac{1}{2} \kappa^{[kl]} (\lambda_{kilj} - \lambda_{kjli}) - \left(-\kappa^{[ik]} Y_e^{j\dagger} Y_e^k - Y_e^{kT} Y_e^{i*} \kappa^{[ik]} + \kappa^{[jk]} Y_e^{i\dagger} Y_e^k + Y_e^{kT} Y_e^{i*} \kappa^{[jk]} \right) \right. \\
& \left. \left. + \frac{1}{2} \left[\kappa^{[ik]} (T^{kj} + T^{jk}) - \kappa^{[jk]} (T^{ki} + T^{ik}) \right] + \kappa^{[ij]} S + S^T \kappa^{[ij]} - 9g_2^2 \kappa^{[ij]} \right\} \right. \\
& \left. \right\}. \tag{4.54}
\end{aligned}$$

As discussed in the beginning of Section 4.2, only the symmetric part of the effective coupling ($\kappa^{(ij)}$) contributes to the active neutrino mass matrix through the effective operator at the tree level. However, as we see from Eq. (4.53), the RG evolution of $\kappa^{(ij)}$ includes contributions from the symmetric $\kappa^{(ij)}$ (in the first two lines) as well as the antisymmetric $\kappa^{[ij]}$ (in the last two lines). This implies that when loop corrections are included, the antisymmetric part of the effective coupling ($\kappa^{[ij]}$) also implicitly contributes to the neutrino mass matrix because it is fed into the RG evolution of the symmetric part. Similarly, as shown in Eq. (4.54), the symmetric $\kappa^{(ij)}$ also contributes to the RG evolution of the antisymmetric $\kappa^{[ij]}$.

4.4 Beyond the 2HDM

As discussed in Section 4.1, the 2HDM is the first step of RG evolution from the electroweak scale towards the LR symmetry breaking scale, which is taken to be the same as the $SU(2)_R$ breaking scale in our model. Beyond the 2HDM, there exists a complicated particle spectrum at higher energies, as shown in Fig. 4.1. Once the renormalization scale is above the mass thresholds of these particles, they cannot be regarded as irrelevant in the EFT, and hence, they will contribute to the β -function of the effective coupling κ and other parameters. Incorporating all these particles at once will require some dedicated work, but the contributions from the RH neutrinos N_R and the $SU(2)_L$ triplet Δ_L are relatively easy to calculate. Therefore, here we consider adding these two particles as our first step beyond the 2HDM.

Fig. 4.6 shows all the additional one-loop self-energy corrections to the 2-point functions of the Higgs doublets and the lepton doublets. There are two contributions from the RH neutrinos and three contributions from the $SU(2)_L$ triplet. However, not all of these diagrams contribute to the wavefunction renormalizations, which are relevant for the β -function of the effective vertex. By evaluating these diagrams, one will find only Figs. 4.6(a), 4.6(d) and 4.6(e) are relevant to the wavefunction renormalizations, whereas the other two diagrams contribute to the mass renormalization of the Higgs fields. For convenience, we will work in the basis where the RH mass matrix M is real and diagonal at some high energy, as it will yield the same result as if we work in a general mass basis. Then the corresponding divergent parts of the self-energy corrections are⁵:

$$(\Gamma_\phi^N)^{ij}_{ab} = \frac{1}{8\pi^2} \delta_{ab} (Y_\nu^{i\dagger})_{\alpha\beta} (Y_\nu^j)_{\beta\alpha} (p^2 - 2M_\beta^2) \frac{1}{\epsilon}; \tag{4.55a}$$

$$(\Gamma_{\ell_L}^N)^{ab}_{\beta\alpha} = \frac{1}{16\pi^2} (Y_\nu^{k\dagger} Y_\nu^k)_{\beta\alpha} \delta_{ab} \not{p} P_L \frac{1}{\epsilon}; \tag{4.55b}$$

$$(\Gamma_{\ell_L}^\Delta)^{ab}_{\beta\alpha} = \frac{3}{16\pi^2} (Y_\Delta^\dagger Y_\Delta)_{\beta\alpha} \delta_{ab} \not{p} P_L \frac{1}{\epsilon}. \tag{4.55c}$$

Since these two new particles do not contribute to the effective vertex renormalization, its counterterm (4.38) stays the same. Therefore, with the RH neutrinos and the $SU(2)_L$ triplet present, the

⁵Again, in connection to the 2HDM, we identify $Y_\nu^1 = y_2$ and $Y_\nu^2 = y_1$ [cf. Eq. (3.58)].

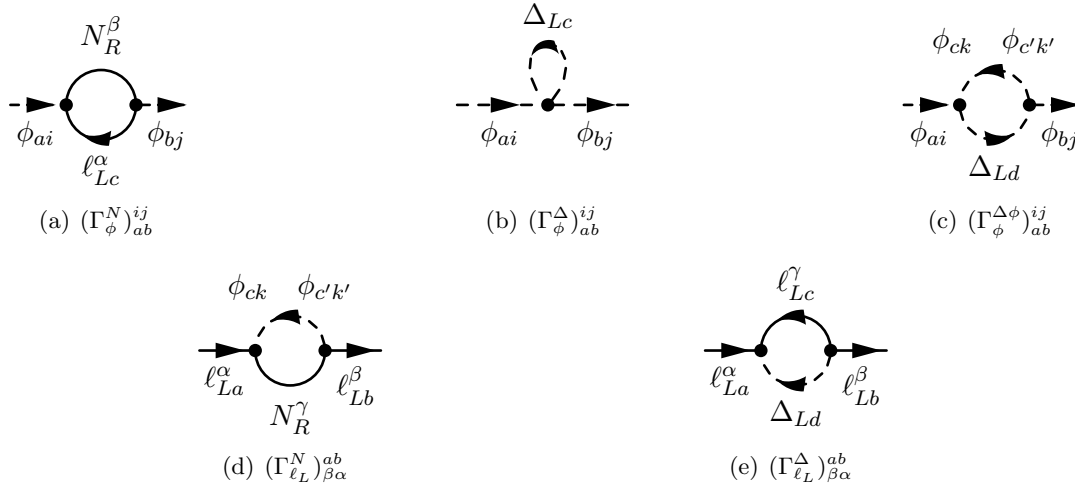


Figure 4.6: Additional one-loop self-energy corrections to 2-point function of the Higgs fields and the lepton doublet fields due to the RH neutrinos and the $SU(2)_L$ triplet.

β -function of the effective vertex stays in the same form as Eq. (4.50), with

$$T^{ij} = \text{Tr} \left(Y_\nu^{i\dagger} Y_\nu^j + Y_e^{i\dagger} Y_e^j + 3Y_d^{i\dagger} Y_d^j + 3Y_u^{i\dagger} Y_u^j \right), \quad (4.56)$$

and

$$S = \frac{1}{2} \left(Y_e^{k\dagger} Y_e^k + Y_\nu^{k\dagger} Y_\nu^k + 3Y_\Delta^\dagger Y_\Delta \right). \quad (4.57)$$

Therefore, compared to the RGE of the effective coupling for the 2HDM, only the trace T^{ij} and S are changed once we include the contributions from the RH neutrinos and the $SU(2)_L$ triplet, while the other terms remain the same. Specifically, there are one more trace term $\text{Tr} \left(Y_\nu^{i\dagger} Y_\nu^j \right)$ and two more terms in S , $\frac{1}{2} Y_\nu^{k\dagger} Y_\nu^k$ and $\frac{3}{2} Y_\Delta^\dagger Y_\Delta$.

As a final remark, we can make some approximations to the β -function (4.50) to simplify the actual calculation by identifying the dominant terms in the Yukawa couplings. For example, the quark Yukawa coupling matrices Y_u and Y_d , in the basis where they are diagonal, can be written as

$$Y_d = \text{diag}(y_d, y_s, y_b), \quad Y_u = \text{diag}(y_u, y_c, y_t). \quad (4.58)$$

Due to the mass hierarchy of the quarks, the (3,3)-component is always the dominant entry of the quark Yukawa coupling matrices and the other two diagonal entries can be neglected in the RG running. More specifically, in the 2HDM, the top quark mass is roughly given by $m_t \sim v_1 y_t^1 + v_2 y_t^2$, where v_1 and v_2 are the VEVs of the two Higgs doublets satisfying $\sqrt{v_1^2 + v_2^2} = v$, with $v \simeq 174$ GeV, and the superscripts of y_t denote the Higgs flavor. As argued previously in Section 3.3.1, there exists a prominent hierarchy of the two VEVs: $v_1 \gg v_2$ in order to suppress the unobserved W_L - W_R mixing. This then leads to $v_1 \simeq v$. Moreover, since the top quark mass $m_t \simeq v$, the top quark Yukawa coupling $y_t = (v_1/v) y_t^1 + (v_2/v) y_t^2 \sim 1$. To allow for perturbation expansion of the quantum corrections, we also require that $y_t^1, y_t^2 \lesssim 4\pi/\sqrt{3}$. Therefore, the dominant contribution to the top quark mass comes from the first term, i.e. $y_t \simeq (v_1/v) y_t^1$, with $y_t^1 \sim 1$. If $y_t^2 \sim y_t^1$, which is allowed, then both of the Yukawa couplings need to be considered in RG running. If, on the other hand, $y_t^2 \ll y_t^1$, then we would neglect y_t^2 and $\text{Tr} \left(3Y_u^{i\dagger} Y_u^j \right) \simeq 3y_t^{1\dagger} y_t^1 \delta^{i1} \delta^{j1}$. For the Yukawa couplings Y_e and Y_d , obviously y_τ and y_b dominates over the other entries, similar to the case of Y_u . However, in the 2HDM, $y_f^1 \ll y_f^2$ ($f = \tau, b$) is possible since the masses of the tauon and the bottom quark are much smaller than $v \simeq 174$ GeV. Then there are three limiting cases that one needs to consider. Finally, if we work in the basis where Y_e is diagonal, then Y_ν have non-diagonal entries because of leptonic mixings. These non-diagonal entries will contribute to the RG evolution and the sizes of these contributions are more difficult to estimate.

Chapter 5

Conclusion

The seminal work by Akhmedov and Frigerio [21] showed that by assuming a discrete LR symmetry, i.e. the charge conjugation symmetry in the LRSM, an analytically solvable seesaw relation can be obtained, which describes the active neutrino mass matrix as a combination of the type-I and II seesaw relations. However, due to quantum corrections, below the discrete LR symmetry breaking scale, the parameters in that seesaw relation evolve differently towards lower energies. Such an evolution with energy is characterized by the RGE, or the β -function of the corresponding parameter. In this thesis, we took a bottom-up approach, that is, we inspected the RG evolution from the low electroweak scale up to the high LR symmetry breaking scale. In this regime, the relevant particles are the two Higgs doublets that originate from the bi-doublet in the LRSM, as well as the massless SM particles. The most relevant parameter for the RG running of the active neutrino masses is the effective vertex κ^{ij} , which arises after integrating out the RH neutrinos N_R and the $SU(2)_L$ scalar triplet Δ_L below their mass thresholds. Therefore, by considering all the pertinent one-loop corrections, we arrived at the β -function of κ^{ij} in the 2HDM, which is given by Eq. (4.50) and forms the main result of the thesis. From the effective Lagrangian (4.4) of the 2HDM, we observed that only the symmetric part $\kappa^{(ij)}$ ($\kappa^{(ji)} = \kappa^{(ij)}$) contributes to the active neutrino masses. However, as we symmetrized and antisymmetrized the β -function of κ^{ij} , we found that the symmetric part of the β -function contains the symmetric $\kappa^{(ij)}$ as well as antisymmetric $\kappa^{[ij]}$ ($\kappa^{[ji]} = -\kappa^{[ij]}$). This interesting result implies that due to quantum corrections, the antisymmetric $\kappa^{[ij]}$ implicitly contributes to neutrino mass through the RG evolution. Moreover, as the first step beyond the 2HDM, we considered the additional contributions from N_R and Δ_L to the effective vertex renormalization because the incorporation of them is relatively straightforward. We found three relevant one-loop diagrams, which add three additional terms to the β -function correspondingly. The results we obtained are valid for a general n Higgs doublet model. At the end, we also made some simple arguments to simplify the RGE based on the structure of the Yukawa coupling matrices.

The work that is presented in this thesis is the first concrete step towards obtaining a full RG analysis of the LR symmetric seesaw relation (3.66) from the electroweak scale to the discrete LR symmetry breaking scale. This will open up a window for us to inspect the physics at high energies more carefully, based on the low-energy physics that is accessible from current experiments. Hence, as the second step, it is reasonable to add into the theory the remaining particles in the spectrum shown in Fig. 4.1, i.e. $\Delta_R^{0r}, \Delta_R^{++}, W_R^\pm$ and Z_R^0 , and determine their contributions to κ^{ij} . Next, once the running is above their mass thresholds, the RG evolution of other parameters such as f_L and f_R becomes important. Similarly, we also need to determine the RG evolution of the Yukawa couplings y_1 and y_2 . This step can be done on the software packages such as SARAH [135] and PyRØTE [136], which implement the general formulas for two-loop RG equations [137, 138, 139]. After the full set of RGEs are derived, one can perform a dedicated phenomenological study based on this model. Some phenomenological implications of the RG analysis may include the following. First, the evolved neutrino mass matrix can be used to extract the running of the mixing angles, phases, and mass eigenvalues, which are important parameters in flavor model building that is usually associated with a high energy scale. Second, as briefly mentioned before, the seesaw mechanism provides an attractive mechanism for generating the baryon asymmetry of our Universe through leptogenesis. Thus, analyzing the RG evolution in the LRSM, which has the seesaw mechanism embedded, can help us constrain leptogenesis better. Last but not least, it also provides insight into the GUTs since for example, as mentioned before, the LRSM can be embedded in $SO(10)$.

Bibliography

- [1] K. A. Olive *et al.* (Particle Data Group), Review of particle physics. *Chin. Phys. C*, **38**, 090001 (2014).
- [2] T. P. Cheng and L. F. Li, *Gauge theory of elementary particle physics*. Clarendon, 1988.
- [3] G. Arnison *et al.* (UA1 Collaboration), Experimental observation of isolated large transverse energy electrons with associated missing energy at $\sqrt{s} = 540$ GeV. *Phys. Lett. B*, **122**, 103 (1983).
- [4] M. Banner *et al.* (UA2 Collaboration), Observation of single isolated electrons of high transverse momentum in events with missing transverse energy at the CERN $\bar{p}p$ collider. *Phys. Lett. B*, **122**, 476 (1983).
- [5] G. Arnison *et al.* (UA1 Collaboration), Experimental observation of lepton pairs of invariant mass around 95 GeV/ c^2 at the CERN SPS collider. *Phys. Lett. B*, **126**, 398 (1983).
- [6] P. Bagnaia *et al.* (UA2 Collaboration), Evidence for $Z^0 \rightarrow e^+e^-$ at the CERN $\bar{p}p$ collider. *Phys. Lett. B*, **129**, 130 (1983).
- [7] ATLAS Collaboration, Observation of a new particle in the search for the Standard Model Higgs boson with the ATLAS detector at the LHC. *Phys. Lett. B*, **716**, 1 (2012) [arXiv:1207.7214 \[hep-ex\]](#).
- [8] CMS Collaboration, Observation of a new boson at a mass of 125 GeV with the CMS experiment at the LHC. *Phys. Lett. B*, **716**, 30 (2012) [arXiv:1207.7235 \[hep-ex\]](#).
- [9] V. A. Bednyakov, N. D. Giokaris and A. V. Bednyakov, On Higgs mass generation mechanism in the Standard Model. *Phys. Part. Nucl.*, **39**, 13 (2008) [arXiv:hep-ph/0703280](#).
- [10] Y. Fukuda *et al.* (Super-Kamiokande Collaboration), Evidence for oscillation of atmospheric neutrinos. *Phys. Rev. Lett.*, **81**, 1562 (1998) [arXiv:hep-ex/9807003](#).
- [11] S. F. King, Neutrino mass models. *Rept. Prog. Phys.*, **67**, 107 (2004) [arXiv:hep-ph/0310204](#).
- [12] S. L. Glashow, Partial symmetries of weak interactions. *Nucl. Phys.*, **22**, 579 (1961).
- [13] S. Weinberg, A model of leptons. *Phys. Rev. Lett.*, **19**, 1261 (1967).
- [14] A. Salam, Weak and electromagnetic interactions, in *Elementary Particle Theory*, Stockholm, 367 (1968).
- [15] H. Georgi and S. L. Glashow, Unity of all elementary-particle forces. *Phys. Rev. Lett.*, **32**, 438 (1974).
- [16] H. Georgi, The state of the art – gauge theories, in *Particles and Fields – 1974*, ed. Carl E. Carlson, AIP Conference Proceedings 23, 575 (1975).
- [17] R. N. Mohapatra, *Unification and Supersymmetry*. Springer, 1986.
- [18] R. N. Mohapatra and G. Senjanović, Neutrino mass and spontaneous parity violation. *Phys. Rev. Lett.*, **44**, 912 (1980).
- [19] N. G. Deshpande, J. F. Gunion, B. Kayser and F. Olness. Left-right-symmetric electroweak models with triplet Higgs field. *Phys. Rev. D*, **44**, 837 (1991).

- [20] P. F. Pérez, Type III seesaw and left-right symmetry. *JHEP*, **03**, 142 (2009) [arXiv:0809.1202 \[hep-ph\]](#).
- [21] E. K. Akhmedov and M. Frigerio, Duality in left-right symmetric seesaw mechanism. *Phys. Rev. Lett.*, **96**, 061802 (2006) [arXiv:hep-ph/0509299](#).
- [22] P. Hosteins, S. Lavignac and C. A. Savoy, Quark-lepton unification and eight-fold ambiguity in the left-right symmetric seesaw mechanism. *Nucl. Phys. B*, **755**, 137 (2006) [arXiv:hep-ph/0606078](#).
- [23] L. M. Brown, The idea of the neutrino. *Phys. Today*, **31**, 23 (1978).
- [24] C. L. Cowan *et al.*, Detection of the free neutrino: a confirmation. *Science*, **124**, 103 (1956).
- [25] Q. R. Ahmad *et al.* (SNO Collaboration), Measurement of the rate of $\nu_e + d \rightarrow p + p + e^-$ interactions produced by ^8B solar neutrinos at the Sudbury Neutrino Observatory. *Phys. Rev. Lett.*, **87**, 071301 (2001).
- [26] Q. R. Ahmad *et al.* (SNO Collaboration), Direct evidence for neutrino flavor transformation from neutral-current interactions in the Sudbury Neutrino Observatory. *Phys. Rev. Lett.*, **89**, 011301 (2002).
- [27] M. H. Ahn *et al.* (K2K Collaboration), Measurement of neutrino oscillation by the K2K experiment. *Phys. Rev. D*, **74**, 072003 (2006) [arXiv:hep-ex/0606032](#).
- [28] D. G. Michael *et al.* (MINOS Collaboration), Observation of muon neutrino disappearance with the MINOS detectors in the NuMI neutrino beam. *Phys. Rev. Lett.*, **97**, 191801 (2006) [arXiv:hep-ex/0607088](#).
- [29] S. Antusch, J. Kersten, M. Lindner, M. Ratz and M. A. Schmidt, Running neutrino mass parameters in see-saw scenarios. *JHEP*, **03**, 024 (2005) [arXiv:hep-ph/0501272](#).
- [30] A. S. Dighe and A. Y. Smirnov, Identifying the neutrino mass spectrum from a supernova neutrino burst. *Phys. Rev. D*, **62**, 033007 (2000) [arXiv:hep-ph/9907423](#).
- [31] K. Petraki and A. Kusenko, Dark-matter sterile neutrinos in models with a gauge singlet in the Higgs sector. *Phys. Rev. D*, **77**, 065014 (2008) [arXiv:0711.4646 \[hep-ph\]](#).
- [32] S. M. Bilenky, S. Pascoli and S. T. Petcov, Majorana neutrinos, neutrino mass spectrum, CP-violation and neutrinoless double beta-decay: I. The three-neutrino mixing case. *Phys. Rev. D*, **64**, 053010 (2001) [arXiv:hep-ph/0102265](#).
- [33] J. Hosaka *et al.* (Super-Kamiokande Collaboration), Solar neutrino measurements in Super-Kamiokande-I. *Phys. Rev. D*, **73**, 112001 (2006) [arXiv:hep-ex/0508053](#).
- [34] J. P. Cravens *et al.* (Super-Kamiokande Collaboration), Solar neutrino measurements in Super-Kamiokande-II. *Phys. Rev. D*, **78**, 032002 (2008) [arXiv:0803.4312 \[hep-ex\]](#).
- [35] K. Abe *et al.* (Super-Kamiokande Collaboration), Solar neutrino results in Super-Kamiokande-III. *Phys. Rev. D*, **83**, 052010 (2011) [arXiv:1010.0118 \[hep-ex\]](#).
- [36] B. Aharmim *et al.* (SNO Collaboration), Low-energy-threshold analysis of the Phase I and Phase II data sets of the Sudbury Neutrino Observatory. *Phys. Rev. C*, **81**, 055504 (2010) [arXiv:0910.2984 \[nucl-ex\]](#).
- [37] B. Aharmim *et al.* (SNO Collaboration), Combined analysis of all three phases of solar neutrino data from the Sudbury Neutrino Observatory. *Phys. Rev. C*, **88**, 025501 (2013) [arXiv:1109.0763 \[nucl-ex\]](#).

- [38] J. Hosaka *et al.* (Super-Kamiokande Collaboration), Three flavor neutrino oscillation analysis of atmospheric neutrinos in Super-Kamiokande. *Phys. Rev. D*, **74**, 032002 (2006) [arXiv:hep-ex/0604011](#).
- [39] R. Wendell *et al.* (Super-Kamiokande Collaboration), Atmospheric neutrino oscillation analysis with sub-leading effects in Super-Kamiokande I, II, and III. *Phys. Rev. D*, **81**, 092004 (2010) [arXiv:1002.3471 \[hep-ex\]](#).
- [40] P. Adamson *et al.* (MINOS Collaboration), Measurement of neutrino and antineutrino oscillations using beam and atmospheric data in MINOS. *Phys. Rev. Lett.*, **110**, 251801 (2013) [arXiv:1304.6335 \[hep-ex\]](#).
- [41] P. Adamson *et al.* (MINOS Collaboration), Combined analysis of ν_μ disappearance and $\nu_\mu \rightarrow \nu_e$ appearance in MINOS using accelerator and atmospheric neutrinos. *Phys. Rev. Lett.*, **112**, 191801 (2014) [arXiv:1403.0867 \[hep-ex\]](#).
- [42] K. Abe *et al.* (T2K Collaboration), Precise measurement of the neutrino mixing parameter θ_{23} from muon neutrino disappearance in an off-axis beam. *Phys. Rev. Lett.*, **112**, 181801 (2014) [arXiv:1403.1532 \[hep-ex\]](#).
- [43] K. Abe *et al.* (T2K Collaboration), Measurement of muon antineutrino oscillations with an accelerator-produced off-axis beam. *Phys. Rev. Lett.*, **116**, 181801 (2016) [arXiv:1512.02495 \[hep-ex\]](#).
- [44] S. Abe *et al.* (KamLAND Collaboration), Precision measurement of neutrino oscillation parameters with KamLAND. *Phys. Rev. Lett.*, **100**, 221803 (2008) [arXiv:0801.4589 \[hep-ex\]](#).
- [45] A. Gando *et al.* (KamLAND Collaboration), Reactor on-off antineutrino measurement with KamLAND. *Phys. Rev. D*, **88**, 033001 (2013) [arXiv:1303.4667 \[hep-ex\]](#).
- [46] F. P. An *et al.* (Daya Bay Collaboration), Observation of electron-antineutrino disappearance at Daya Bay. *Phys. Rev. Lett.*, **108**, 171803 (2012) [arXiv:1203.1669 \[hep-ex\]](#).
- [47] F. P. An *et al.* (Daya Bay Collaboration), New measurement of θ_{13} via neutron capture on hydrogen at Daya Bay. *Phys. Rev. D*, **93**, 072011 (2016) [arXiv:1603.03549 \[hep-ex\]](#).
- [48] J. K. Ahn *et al.* (RENO Collaboration), Observation of reactor electron antineutrinos disappearance in the RENO Experiment. *Phys. Rev. Lett.*, **108**, 191802 (2012) [arXiv:1204.0626 \[hep-ex\]](#).
- [49] J. H. Choi *et al.* (RENO Collaboration), Observation of energy and baseline dependent reactor antineutrino disappearance in the RENO Experiment. *Phys. Rev. Lett.*, **116**, 211801 (2016) [arXiv:1511.05849 \[hep-ex\]](#).
- [50] M. C. Gonzalez-Garcia, M. Maltoni and T. J. Schwetz, Updated fit to three neutrino mixing: status of leptonic CP violation. *JHEP*, **11**, 052 (2014) [arXiv:1409.5439 \[hep-ph\]](#).
- [51] F. Capozzi *et al.*, Neutrino masses and mixings: Status of known and unknown 3ν parameters *Nucl. Phys. B*, **908**, 218 (2016) [arXiv:1601.07777 \[hep-ph\]](#).
- [52] K. Abe *et al.* (T2K Collaboration), Measurements of neutrino oscillation in appearance and disappearance channels by the T2K experiment with 6.6×10^{20} protons on target. *Phys. Rev. D*, **91**, 072010 (2015) [arXiv:1502.01550 \[hep-ex\]](#).
- [53] P. Adamson *et al.* (NO ν A Collaboration), First measurement of electron neutrino appearance in NO ν A. *Phys. Rev. Lett.*, **116**, 151806 (2016) [arXiv:1601.05022 \[hep-ex\]](#).
- [54] R. Adhikari *et al.*, A white paper on keV sterile neutrino dark matter. [arXiv:1602.04816 \[hep-ph\]](#).

- [55] N. Palanque-Delabrouille *et al.*, Neutrino masses and cosmology with Lyman-alpha forest power spectrum. *JCAP*, **11**, 011 (2015) [arXiv:1506.05976 \[astro-ph.CO\]](#).
- [56] M. Lindner, A. Merle and W. Rodejohann, Improved limit on θ_{13} and implications for neutrino masses in neutrino-less double beta decay and cosmology. *Phys. Rev. D*, **73**, 053005 (2006) [arXiv:hep-ph/0512143](#).
- [57] M. Agostini *et al.* (GERDA Collaboration), Results on Neutrinoless Double- β decay of ^{76}Ge from phase I of the GERDA experiment. *Phys. Rev. Lett.*, **111**, 122503 (2013) [arXiv:1307.4720 \[nucl-ex\]](#).
- [58] A. Gando *et al.* (KamLAND-Zen Collaboration), Limit on neutrinoless $\beta\beta$ decay of ^{136}Xe from the first phase of KamLAND-Zen and comparison with the positive claim in ^{76}Ge . *Phys. Rev. Lett.*, **110**, 0622502 (2013) [arXiv:1211.3863 \[hep-ex\]](#).
- [59] J. B. Albert *et al.* (EXO-200 Collaboration), Search for Majorana neutrinos with the first two years of EXO-200 data. *Nature*, **510**, 229 (2014) [arXiv:1402.6956 \[nucl-ex\]](#).
- [60] V. N. Aseev *et al.*, Upper limit on the electron antineutrino mass from the Troitsk experiment. *Phys. Rev. D*, **84**, 112003 (2011) <http://arxiv.org/abs/1108.5034>.
- [61] Ch. Kraus *et al.*, Final results from phase II of the Mainz neutrino mass search in tritium β decay. *Eur. Phys. J.*, **C40**, 447 (2005) [arXiv:hep-ex/0412056](#).
- [62] K. Eitel *et al.* (KATRIN Collaboration), Direct neutrino mass experiments. *Nucl. Phys. Proc. Suppl.*, **143**, 197 (2005).
- [63] A. de Gouvêa, Neutrino mass models. *Annu. Rev. Nucl. Part. Sci.*, **66** (2016), DOI: [10.1146/annurev-nucl-102115-044600](#).
- [64] N. Arkani-Hamed, S. Dimopoulos and G. R. Dvali, The hierarchy problem and new dimensions at a millimeter. *Phys. Lett. B*, **429**, 263 (1998) [arXiv:hep-ph/9803315](#).
- [65] N. Arkani-Hamed, S. Dimopoulos, G. Dvali and J. March-Russell, Neutrino masses from large extra dimensions. *Phys. Rev. D*, **65**, 024032 (2001) [arXiv:hep-ph/9811448](#).
- [66] L. Randall and R. Sundrum, Large mass hierarchy from a small extra dimension. *Phys. Rev. Lett.*, **83**, 3370 (1999) [arXiv:hep-ph/9905221](#).
- [67] H. Georgi, Effective Field Theory. *Annu. Rev. Nucl. Part. Sci.*, **43**, 209 (1993).
- [68] S. Weinberg, Baryon- and lepton-nonconserving processes. *Phys. Rev. Lett.*, **43**, 1566 (1979).
- [69] P. Minkowski, $\mu \rightarrow e\gamma$ at a rate of one out of 10^9 muon decays? *Phys. Lett. B*, **67**, 421 (1977).
- [70] T. Yanagida, Horizontal symmetry and masses of neutrinos. *Conf. Proc. C*, **7902131**, 95 (1979).
- [71] M. Gell-Mann, P. Ramond and R. Slansky, Complex spinors and unified theories. *Conf. Proc. C*, **790927**, 315 (1979) [arXiv:1306.4669 \[hep-th\]](#).
- [72] S. L. Glashow, The future of elementary particle physics. *NATO Sci. Ser. B*, **61**, 687 (1980).
- [73] M. Magg and C. Wetterich, Neutrino mass problem and gauge hierarchy. *Phys. Lett. B*, **94**, 61 (1980).
- [74] G. Lazarides, Q. Shafi and C. Wetterich, Proton lifetime and fermion masses in an $SO(10)$ model. *Nucl. Phys. B*, **181**, 287 (1981).

- [75] J. Schechter and J. W. F. Valle, Neutrino masses in $SU(2) \times U(1)$ theories. *Phys. Rev. D*, **22**, 2227 (1980).
- [76] R. N. Mohapatra and G. Senjanović, Neutrino masses and mixings in gauge models with spontaneous parity violation. *Phys. Rev. D*, **23**, 165 (1981).
- [77] R. Foot, H. Lew, X. G. He and G. C. Joshi, Seesaw neutrino masses induced by a triplet of leptons. *Z. Phys. C*, **44**, 441 (1989).
- [78] E. Ma, Pathways to naturally small neutrino masses. *Phys. Rev. Lett.*, **81**, 1171 (1998) [arXiv:hep-ph/9805219](#).
- [79] R. Johnson, S. Ranfone and J. Schechter, The neutrino see-saw in $SO(10)$. *Phys. Lett. B*, **179**, 355 (1986).
- [80] H. S. Goh, R. N. Mohapatra and S. Nasri, $SO(10)$ symmetry breaking and type II seesaw formula. *Phys. Rev. D*, **70**, 075022 (2004) [arXiv:hep-ph/0408139](#).
- [81] G. Barenboim, M. Gorbahn, U. Nierste and M. Raidal, Higgs sector of the minimal left-right symmetric model. *Phys. Rev. D*, **65**, 095003 (2002) [arXiv:hep-ph/0107121](#).
- [82] B. Bajc and G. Senjanović, Seesaw at LHC. *JHEP*, **08**, 014 (2007) [arXiv:hep-ph/0612029](#).
- [83] A. Zee, A theory of lepton number violation, neutrino Majorana mass, and oscillation. *Phys. Lett. B*, **93**, 389 (1980).
- [84] A. Zee, Quantum numbers of Majorana neutrino masses. *Nucl. Phys. B*, **264**, 99 (1986).
- [85] T. P. Cheng and L. F. Li, Neutrino masses, mixings, and oscillations in $SU(2) \times U(1)$ models of electroweak interactions. *Phys. Rev. D*, **22**, 2860 (1980).
- [86] K. S. Babu, Model of ‘calculable’ Majorana neutrino masses. *Phys. Lett. B*, **203**, 132 (1988).
- [87] E. Ma, Verifiable radiative seesaw mechanism of neutrino mass and dark matter. *Phys. Rev. D*, **73**, 077301 (2006) [arXiv:hep-ph/0601225](#).
- [88] H. Sugiyama, Radiative Neutrino Mass Models. [arXiv:1505.01738 \[hep-ph\]](#).
- [89] A. Abada, C. Biggio, F. Bonnet, M. B. Gavela and T. Hambye, Low energy effects of neutrino masses. *JHEP*, **12**, 061 (2007) [arXiv:0707.4058 \[hep-ph\]](#).
- [90] M. B. Gavela, T. Hambye, D. Hernandez and P. Hernandez, Minimal flavour seesaw models. *JHEP*, **09**, 038 (2009) [arXiv:0906.1461 \[hep-ph\]](#).
- [91] L. M. Krauss, S. Nasri and M. Trodden, Model for neutrino masses and dark matter. *Phys. Rev. D*, **67**, 085002 (2003) [arXiv:hep-ph/0210389](#).
- [92] W. C. Huang and F. F. Deppisch, Dark matter origins of neutrino masses. *Phys. Rev. D*, **91**, 093011 (2015) [arXiv:1412.2027 \[hep-ph\]](#).
- [93] T. Tati and S. Tomonaga, A self-consistent subtraction method in the quantum field theory. I. *Progr. Theor. Phys.*, **3**, 391 (1948).
- [94] J. Schwinger, Quantum Electrodynamics. I. A Covariant Formulation. *Phys. Rev.*, **74**, 1439 (1948).
- [95] J. Schwinger, Quantum Electrodynamics. II. Vacuum Polarization and Self-Energy. *Phys. Rev.*, **75**, 651 (1949).
- [96] R. P. Feynman, Relativistic cut-off for quantum electrodynamics. *Phys. Rev.*, **74**, 1430 (1948).

- [97] S. Weinberg, *The Quantum Theory of Fields. Volume 1: Foundations*. Cambridge University Press, 1995.
- [98] G. 't Hooft, Renormalization of massless Yang-Mills fields. *Nucl. Phys. B*, **33**, 173 (1971).
- [99] G. 't Hooft, Renormalizable Lagrangians for massive Yang-Mills fields. *Nucl. Phys. B*, **35**, 167 (1971).
- [100] W. Pauli and F. Villars, On the invariant regularization in relativistic quantum theory. *Rev. Mod. Phys.*, **21**, 434 (1949).
- [101] G. 't Hooft and M. J. G. Veltman, Regularization and renormalization of gauge fields. *Nucl. Phys. B*, **44**, 189 (1972).
- [102] G. 't Hooft, Dimensional regularization and the renormalization group. *Nucl. Phys. B*, **61**, 455 (1973).
- [103] S. Weinberg, New approach to the renormalization group. *Phys. Rev. D*, 3497 (1973).
- [104] W. A. Bardeen, A. J. Buras, D. W. Duke and T. Muta, Deep inelastic scattering beyond the leading order in asymptotically free gauge theories. *Phys. Rev. D*, **18** (1978).
- [105] E.C.G. Stueckelberg and A. Petermann, Normalization of constants in the quanta theory. *Helv. Phys. Acta*, **26**, 499 (1953).
- [106] M. Gell-Mann and F. E. Low, Quantum electrodynamics at small distances. *Phys. Rev.*, **95**, 1300 (1954).
- [107] C. G. Callan, Broken scale invariance in scalar field theory. *Phys. Rev. D*, **2**, 1541 (1970).
- [108] K. Symanzik, Small distance behaviour in field theory and power counting. *Commun. Math. Phys.*, **18**, 227 (1970).
- [109] M. Thomson, *Modern Particle Physics*. Cambridge University Press, 2013.
- [110] E. Kh. Akhmedov, Neutrino physics. [arXiv:hep-ph/0001264](#).
- [111] W. Chao and M. J. Ramsey-Musolf, Hidden from view: Neutrino masses, dark matter, and TeV-scale leptogenesis in a neutrinophilic two-Higgs-doublet model. *Phys. Rev. D*, **89**, 033007 (2014) [arXiv:1212.5709 \[hep-ph\]](#).
- [112] M. Fukugita and T. Yanagida, Baryogenesis without grand unification. *Phys. Lett. B*, **174**, 45 (1986).
- [113] S. Ray, Renormalization group evolution of neutrino masses and mixing in seesaw models: A review. *Int. J. Mod. Phys. A*, **25**, 4339 (2010) [arXiv:1005.1938 \[hep-ph\]](#).
- [114] M. A. Schmidt, Renormalization group evolution in the type I + II seesaw model. *Phys. Rev. D*, **76**, 073010 (2007) [arXiv:0705.3841 \[hep-ph\]](#).
- [115] P. F. Pérez, Renormalizable adjoint $SU(5)$. *Phys. Lett. B*, **654**, 189 (2007) [arXiv:hep-ph/0702287](#).
- [116] P. F. Pérez, Supersymmetric adjoint $SU(5)$. *Phys. Rev. D*, **76**, 071701 (2007) [arXiv:0705.3589 \[hep-ph\]](#).
- [117] C. S. Wu, E. Ambler, R. W. Hayward, D. D. Hoppes and R. P. Hudson, Experimental test of parity conservation in beta decay. *Phys. Rev.*, **105**, 1413 (1957).
- [118] J. C. Pati and A. Salam, Lepton number as the fourth color. *Phys. Rev. D*, **10**, 275 (1974).

- [119] R. N. Mohapatra and J. C. Pati, “Natural” left-right symmetry. *Phys. Rev. D*, **11**, 2558 (1975).
- [120] G. Senjanović and R. N. Mohapatra, Exact left-right symmetry and spontaneous violation of parity. *Phys. Rev. D*, **12**, 1502 (1975).
- [121] G. Senjanović, Spontaneous breakdown of parity in a class of gauge theories. *Nucl. Phys. B*, **153**, 334 (1979).
- [122] G. Barenboim, M. Gorbahn, U. Nierste and M. Raidal, Higgs sector of the minimal left-right symmetric model. *Phys. Rev. D*, **65**, 095003 (2002) [arXiv:hep-ph/0107121](#).
- [123] M. Frigerio, Analysis of left-right symmetric seesaw. *JPCS*, **39**, 304 (2006).
- [124] M. A. B. Bég, R. V. Budny, R. N. Mohapatra and A. Sirlin, Manifest left-right symmetry and its experimental consequences. *Phys. Rev. Lett.*, **38**, 1252 (1977).
- [125] C. S. Aulakh, A. Melfo, A. Rašin and G. Senjanović, Supersymmetry and large scale left-right symmetry. *Phys. Rev. D*, **58**, 115007 (1998) [arXiv:hep-ph/9712551](#).
- [126] E. K. Akhmedov and M. Frigerio, Interplay of type I and type II seesaw contributions to neutrino mass. *JHEP*, **01**, 043 (2007) [arXiv:hep-ph/0609046](#).
- [127] E. K. Akhmedov, M. Blennow, T. Hallgren, T. Konstandin and T. Ohlsson, Stability and leptogenesis in the left-right symmetric seesaw mechanism. *JHEP*, **04**, 022 (2007) [arXiv:hep-ph/0612194](#).
- [128] D. Chang, R. N. Mohapatra and M. K. Parida, Decoupling parity and $SU(2)_R$ breaking scales: A new approach to left-right symmetric models. *Phys. Rev. Lett.*, **52**, 1072 (1984).
- [129] J. Goldstone, Field theories with superconductor solutions. *Nuovo. Cimento.*, **19**, 154 (1961).
- [130] J. Goldstone, A. Salam and S. Weinberg, Broken symmetries. *Phys. Rev.*, **127**, 965 (1962).
- [131] G. Passarino and M. Veltman, One loop corrections for e^+e^- annihilation into $\mu^+\mu^-$ in the Weinberg model. *Nucl. Phys. B*, **160**, 151 (1979).
- [132] S. Antusch, M. Drees, J. Kersten, M. Lindner and M. Ratz, Neutrino mass operator renormalization revisited. *Phys. Lett. B*, **519**, 238 (2001) [arXiv:hep-ph/0108005](#).
- [133] W. Grimus and L. Lavoura, Renormalization of the neutrino mass operators in the multi-Higgs-doublet Standard Model. *Eur. Phys. J. C*, **39**, 219 (2005) [arXiv:hep-ph/0409231](#).
- [134] S. Antusch, M. Drees, J. Kersten, M. Lindner and M. Ratz, Neutrino mass operator renormalization in two Higgs doublet models and the MSSM. *Phys. Lett. B*, **525**, 130 (2002) [arXiv:hep-ph/0110366](#).
- [135] F. Staub, SARAH 4 : A tool for (not only SUSY) model builders. *Comput. Phys. Commun.*, **185**, 1773 (2014) [arXiv:1309.7223 \[hep-ph\]](#).
- [136] F. Lyonnet, I. Schienbein, F. Staub and A. Wingerter, PyR@TE: Renormalization group equations for general gauge theories. *Comput. Phys. Commun.*, **185**, 1130 (2014) [arXiv:1309.7030 \[hep-ph\]](#).
- [137] M. E. Machacek and M. T. Vaughn, Two loop renormalization group equations in a general quantum field theory. 1. Wave function renormalization. *Nucl. Phys. B*, **222**, 83 (1983).
- [138] M. E. Machacek and M. T. Vaughn, Two loop renormalization group equations in a general quantum field theory. 2. Yukawa couplings. *Nucl. Phys. B*, **236**, 221 (1984).

- [139] M. E. Machacek and M. T. Vaughn, Two loop renormalization group equations in a general quantum field theory. 3. Scalar quartic couplings. *Nucl. Phys. B*, **249**, 70 (1985).
- [140] M. Schwartz, *Quantum Field Theory and the Standard Model*. Cambridge University Press, 2013.
- [141] A. Denner, Techniques for the calculation of electroweak radiative corrections at the one-loop level and results for W -physics at LEP200. *Fortschr. Phys.*, **41**, 307 (1993) [arXiv:0709.1075 \[hep-ph\]](#).
- [142] J. Kersten, Renormalization group evolution of neutrino masses. *Diploma Thesis* (2001).
- [143] A. Denner, H. Eck, O. Hahn and J. Küblbeck, Feynman rules for fermion number violating interactions. *Nucl. Phys. B*, **387**, 467 (1992).

Appendix A

The Standard Model (SM) and the Left-Right Symmetric Model (LRSM)

A.1 Particle Contents of the SM

	$SU(3)_C$	$SU(2)_L$	$U(1)_Y$
Quarks			
Q_L	3	2	$\frac{1}{3}$
u_R	3	1	$\frac{4}{3}$
d_R	3	1	$-\frac{2}{3}$
Leptons			
ℓ_L	1	2	-1
e_R	1	1	-2
Gauge bosons			
G^a	8	1	0
W^i	1	3	0
B	1	1	0
Higgs			
ϕ	1	2	1

Table A.1: The particle contents of the SM.

The SM particle contents and their transformation properties under the gauge group $SU(3)_C \times SU(2)_L \times U(1)_Y$ are summarized in Tab. A.1. The electric charge Q of a particle is related to its weak isospin T_3 and its hypercharge Y by

$$Q = T_3 + \frac{Y}{2}. \quad (\text{A.1})$$

As we see, all the particles are $SU(3)_C$ singlets except quarks and gluons. For fermions (leptons and quarks), the LH particles are $SU(2)_L$ doublets, while the RH ones are $SU(2)_L$ singlets. Gauge interactions are mediated by the gauge bosons. There are twelve of them, including eight $SU(3)_C$ gauge bosons G_μ^a ($a = 1, \dots, 8$) responsible for the strong interaction, three $SU(2)_L$ gauge bosons W_μ^i ($i = 1, 2, 3$) and one $U(1)_Y$ gauge boson B_μ responsible for the electroweak interaction. The Higgs particle is responsible for generating masses for the fermions and the gauge bosons via the Higgs mechanism.

A.2 Particle Contents of the LRSM

	$SU(3)_C$	$SU(2)_L$	$SU(2)_R$	$U(1)_{B-L}$
Fermion sector				
Q_L	3	2	1	$\frac{1}{3}$
Q_R	3	1	2	$\frac{1}{3}$
ℓ_L	1	2	1	-1
ℓ_R	1	1	2	-1
Higgs sector				
Φ	1	2	2	0
Δ_L	1	3	1	2
Δ_R	1	1	3	2
Gauge boson sector				
G^a	8	1	1	0
W_L^i	1	3	1	0
W_R^i	1	1	3	0
A	1	1	1	0

Table A.2: The particle contents of the LRSM.

The particle contents of the minimal LRSM, including the fermion sector, the Higgs sector and the gauge boson sector, are summarized in Tab. A.2. Due to the introduction of the $SU(2)_R$ gauge group, both the LH and RH fermions are now doublets under $SU(2)$. There are also additional $SU(2)_R$ gauge bosons $W_{R\mu}^i$ ($i = 1, 2, 3$). The conserved charge related to the $U(1)$ symmetry is $B - L$, which is related to the electric charge Q by

$$Q = T_{3L} + T_{3R} + \frac{B - L}{2}. \quad (\text{A.2})$$

A_μ is the $U(1)_{B-L}$ gauge boson, analogous to the $U(1)_Y$ gauge boson B_μ in the SM. The Higgs sector in the LRSM contains three different Higgses, a bi-doublet Φ , an $SU(2)_L$ triplet Δ_L , and an $SU(2)_R$ triplet Δ_R . They transform according to the following relations:

$$\begin{aligned}
\Phi &\rightarrow U_L \Phi U_R^\dagger, & \tilde{\Phi} &\rightarrow U_L \tilde{\Phi} U_R^\dagger, \\
\Delta_L &\rightarrow U_L \Delta_L U_L^\dagger, & \Delta_L^\dagger &\rightarrow U_L \Delta_L^\dagger U_L^\dagger, \\
\Delta_R &\rightarrow U_R \Delta_R U_R^\dagger, & \Delta_R^\dagger &\rightarrow U_R \Delta_R^\dagger U_R^\dagger,
\end{aligned} \quad (\text{A.3})$$

where $U_{L,R}$ are the $SU(2)_{L,R}$ unitary transformations.

Appendix B

Dimensional Regularization

B.1 Feynman Parameters

Feynman parameters are based on some easily verifiable mathematical identities, which allow us to “complete the square” in the denominator for the convenience of later calculations. Some useful identities are

$$\frac{1}{AB} = \int_0^1 dx \frac{1}{[xA + (1-x)B]^2}, \quad (\text{B.1a})$$

$$\frac{1}{A^\alpha B^\beta} = \frac{\Gamma(\alpha + \beta)}{\Gamma(\alpha)\Gamma(\beta)} \int_0^1 dx \frac{x^{\alpha-1}(1-x)^{\beta-1}}{[xA + (1-x)B]^{\alpha+\beta}}, \quad (\text{B.1b})$$

$$\frac{1}{ABC} = 2 \int_0^1 dx \int_0^1 dy \frac{y}{[xyA + (1-x)yB + (1-y)C]^3}, \quad (\text{B.1c})$$

$$\frac{1}{A_1 A_2 \cdots A_n} = \int_0^1 dx_1 \cdots dx_n \delta\left(\sum_i x_i - 1\right) \frac{(n-1)!}{[x_1 A_1 + x_2 A_2 + \cdots + x_n A_n]^n}, \quad (\text{B.1d})$$

where $\Gamma(z)$ is the Gamma function, which is the natural continuation of the factorial from integers to complex numbers. It is defined as

$$\Gamma(z) \equiv \int_0^\infty dt e^{-t} t^{z-1}, \quad \forall z \in \mathbb{C}, \text{Re}(z) > 0. \quad (\text{B.2})$$

It clearly satisfies

$$\Gamma(z+1) = z\Gamma(z), \quad \Gamma(1) = 1. \quad (\text{B.3})$$

$\Gamma(z)$ diverges at 0 and at all the negative integers, which are called the “poles”. We usually expand it around the pole at $z = 0$:

$$\Gamma(\epsilon) = \frac{1}{\epsilon} - \gamma_E + \mathcal{O}(\epsilon), \quad (\text{B.4})$$

where $\gamma_E \simeq 0.577$ is the Euler-Mascheroni constant. In a more general form, the expansion around the poles is

$$\Gamma(-n + \epsilon) = \frac{(-1)^n}{n!} \left[\frac{1}{\epsilon} + \psi(n+1) + \mathcal{O}(\epsilon) \right], \quad (\text{B.5})$$

where

$$\psi(n+1) = \sum_{k=1}^n \frac{1}{k} - \gamma_E = \frac{\Gamma'(z)}{\Gamma(z)}. \quad (\text{B.6})$$

B.2 Wick Rotations

After introducing the Feynman parameters to complete the square, the one-loop integrals often appear as

$$\int \frac{d^4 k}{(2\pi)^4} \frac{1}{(k^2 - \Delta + i\varepsilon)^n}. \quad (\text{B.7})$$

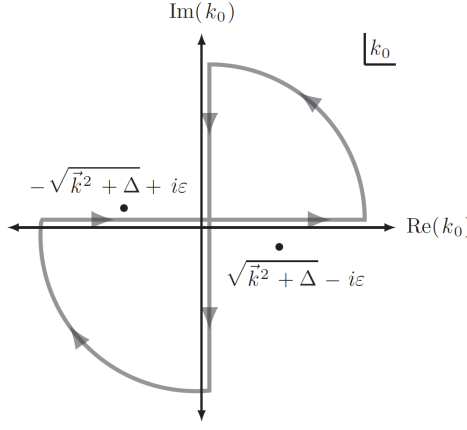


Figure B.1: An illustration of Wick rotations. The two poles are shown as dots. Integrating over the real axis is equivalent to integrating over the imaginary axis. Figure from [140].

Assuming $\Delta > 0$, such an integral has poles at $k_0 = \pm(\sqrt{\vec{k}^2 + \Delta} - i\varepsilon)$, as shown in Fig. B.1. Since the poles are in the top-left and bottom-right quadrants of the k_0 complex plane, the integral over the contour shown in the figure must vanish. This then implies that the integrals over the real axis and the imaginary axis are equal and opposite. Therefore, if we make the substitution $k_0 \rightarrow ik_0$, then

$$k^2 \rightarrow -k_0^2 - \vec{k}^2 \equiv -k_E^2, \quad (\text{B.8})$$

where $k_E^2 = k_0^2 + \vec{k}^2$ is the Euclidean momentum. This is known as the Wick rotation. Using this technique, the integral (B.7) can be written as

$$\int \frac{d^4 k}{(2\pi)^4} \frac{1}{(k^2 - \Delta + i\varepsilon)^n} = i \int \frac{d^4 k_E}{(2\pi)^4} \frac{1}{(k_E^2 + \Delta)^n}. \quad (\text{B.9})$$

Hence, by performing the Wick rotation, the poles in the original integral no longer exist.

B.3 Dimensional Regularization

The key observation of DR is that an integral such as

$$\int \frac{d^d k}{(2\pi)^d} \frac{1}{(k^2 - \Delta + i\varepsilon)^2} \quad (\text{B.10})$$

is divergent only if $d \geq 4$. If $d < 4$, it is convergent. To evaluate such an integral, the first step is generally to perform Wick rotation. After that, we go to the spherical coordinates, that is,

$$\int d^d k = \int d\Omega_d \int dk k^{d-1}, \quad (\text{B.11})$$

where $d\Omega_d$ denotes the differential solid angle of the d -dimensional unit sphere. Note that d is the dimension of the solid volume, not the surface, which has dimension $d - 1$. The $(d - 1)$ -dimensional surface areas of a ball of radius 1 in integer dimensions are

$$\Omega_2 = \int d\Omega_2 = 2\pi \text{ (circle)}, \quad (\text{B.12a})$$

$$\Omega_3 = \int d\Omega_3 = 4\pi \text{ (sphere)}, \quad (\text{B.12b})$$

$$\Omega_4 = \int d\Omega_4 = 2\pi^2 \text{ (3-sphere) etc.} \quad (\text{B.12c})$$

For non-integer dimensions, the surface area formula can be derived using the Gaussian integrals

$$(\sqrt{\pi})^d = \left(\int_{-\infty}^{\infty} dx e^{-x^2} \right)^d = \int d\Omega_d \int_0^{\infty} dr r^{d-1} e^{-r^2} = \frac{1}{2} \Gamma\left(\frac{d}{2}\right) \int d\Omega_d. \quad (\text{B.13})$$

So we have

$$\Omega_d = \int d\Omega_d = \frac{2\pi^{d/2}}{\Gamma(\frac{d}{2})}. \quad (\text{B.14})$$

Then the integrals over the Euclidean k_E are straightforward,

$$\int dk_E \frac{k_E^a}{(k_E^2 + \Delta)^b} = \Delta^{\frac{a+1}{2}-b} \frac{\Gamma(\frac{a+1}{2}) \Gamma(b - \frac{a+1}{2})}{2\Gamma(b)}. \quad (\text{B.15})$$

In summary, some useful d -dimensional integrals for DR are:

$$\int \frac{d^d k}{(2\pi)^d} \frac{1}{(k^2 - \Delta + i\varepsilon)^n} = i \frac{(-1)^n}{(4\pi)^{d/2}} \frac{\Gamma(n - \frac{d}{2})}{\Gamma(n)} \left(\frac{1}{\Delta}\right)^{n-d/2} \quad (\text{B.16a})$$

$$\int \frac{d^d k}{(2\pi)^d} \frac{k^2}{(k^2 - \Delta + i\varepsilon)^n} = -i \frac{d}{2} \frac{(-1)^n}{(4\pi)^{d/2}} \frac{\Gamma(n - 1 - \frac{d}{2})}{\Gamma(n)} \left(\frac{1}{\Delta}\right)^{n-1-d/2} \quad (\text{B.16b})$$

$$\int \frac{d^d k}{(2\pi)^d} \frac{k_\mu k_\nu}{(k^2 - \Delta + i\varepsilon)^n} = -\frac{i}{2} \eta_{\mu\nu} \frac{(-1)^n}{(4\pi)^{d/2}} \frac{\Gamma(n - 1 - \frac{d}{2})}{\Gamma(n)} \left(\frac{1}{\Delta}\right)^{n-1-d/2} \quad (\text{B.16c})$$

$$\int \frac{d^d k}{(2\pi)^d} \frac{(k^2)^2}{(k^2 - \Delta + i\varepsilon)^n} = i \frac{d(d+2)}{4} \frac{(-1)^n}{(4\pi)^{d/2}} \frac{\Gamma(n - 2 - \frac{d}{2})}{\Gamma(n)} \left(\frac{1}{\Delta}\right)^{n-2-d/2} \quad (\text{B.16d})$$

$$\int \frac{d^d k}{(2\pi)^d} \frac{k_\mu k_\nu k_\rho k_\sigma}{(k^2 - \Delta + i\varepsilon)^n} = \frac{i}{4} (\eta_{\mu\nu} \eta_{\rho\sigma} + \eta_{\mu\rho} \eta_{\nu\sigma} + \eta_{\mu\sigma} \eta_{\nu\rho}) \frac{(-1)^n}{(4\pi)^{d/2}} \frac{\Gamma(n - 2 - \frac{d}{2})}{\Gamma(n)} \left(\frac{1}{\Delta}\right)^{n-2-d/2}. \quad (\text{B.16e})$$

By symmetry, the integrals over odd powers of k_μ in the numerator vanishes,

$$\int \frac{d^d k}{(2\pi)^d} k_\mu f(k^2) = 0. \quad (\text{B.17})$$

Moreover, we can transform integrals containing $k_\mu k_\nu$ into those involving only k^2 by using

$$\int \frac{d^d k}{(2\pi)^d} k_\mu k_\nu f(k^2) = \frac{1}{d} \eta_{\mu\nu} \int \frac{d^d k}{(2\pi)^d} k^2 f(k^2), \quad (\text{B.18})$$

where we have used the property of the Minkowski metric tensor in d dimensions,

$$\eta_{\mu\nu} \eta^{\mu\nu} = d. \quad (\text{B.19})$$

At the end of DR, we set $d = 4$ and go back to the usual 4-dimensional spacetime.

B.4 Passarino-Veltman Functions

The Passarino-Veltman functions [131] are very useful in loop calculations because their divergent parts have been identified and one can refer to these functions when calculating loop diagrams and quickly determine the divergences. In the calculations involved in this thesis, we mainly use the Passarino-Veltman functions to determine the divergent parts of the loop diagrams.

The one-point function A_0

The one-point function is defined as

$$A_0(m^2) \equiv \frac{\mu^\epsilon}{i\pi^2} \int d^d k \frac{1}{k^2 - m^2}. \quad (\text{B.20})$$

Remember that μ is the renormalization scale introduced to make the coupling in the vertex function dimensionless and $\epsilon = 4 - d$. This can be evaluated using the formulas given previously:

$$\begin{aligned} A_0(m^2) &= (2\pi)^d \frac{\mu^\epsilon}{i\pi^2} \int \frac{d^d k}{(2\pi)^d} \frac{1}{k^2 - m^2} \\ &\stackrel{(\text{B.16a})}{=} -m^2 \pi^{-\epsilon/2} \Gamma\left(-1 + \frac{\epsilon}{2}\right) \left(\frac{\mu^2}{m^2}\right)^{\epsilon/2} \\ &\stackrel{(\text{B.5})}{=} m^2 \left[1 - \frac{\epsilon}{2} \ln \pi + \mathcal{O}(\epsilon^2)\right] \left[\frac{2}{\epsilon} + \psi(2) + \mathcal{O}(\epsilon)\right] \left[1 + \frac{\epsilon}{2} \ln \frac{\mu^2}{m^2} + \mathcal{O}(\epsilon^2)\right] \\ &\stackrel{(\text{B.6})}{=} m^2 \left(\frac{2}{\epsilon} - \ln \pi - \gamma_E + 1 + \ln \frac{\mu^2}{m^2}\right) + \mathcal{O}(\epsilon). \end{aligned} \quad (\text{B.21})$$

The terms proportional to ϵ and higher orders of ϵ are irrelevant because they vanish as $\epsilon \rightarrow 0$, i.e. $d \rightarrow 4$. Therefore, the one-point function can be written as a sum of the divergent and finite parts,

$$A_0(m^2) = \frac{2}{\epsilon} m^2 + \text{UV finite}. \quad (\text{B.22})$$

The two-point function B

The two-point functions are defined as

$$B_0(p^2, m_1^2, m_2^2) \equiv \frac{\mu^\epsilon}{i\pi^2} \int d^d k \frac{1}{(k^2 - m_1^2) [(k+p)^2 - m_2^2]}, \quad (\text{B.23a})$$

$$B_\mu(p^2, m_1^2, m_2^2) \equiv \frac{\mu^\epsilon}{i\pi^2} \int d^d k \frac{k_\mu}{(k^2 - m_1^2) [(k+p)^2 - m_2^2]}, \quad (\text{B.23b})$$

$$B_{\mu\nu}(p^2, m_1^2, m_2^2) \equiv \frac{\mu^\epsilon}{i\pi^2} \int d^d k \frac{k_\mu k_\nu}{(k^2 - m_1^2) [(k+p)^2 - m_2^2]}. \quad (\text{B.23c})$$

The last two functions B_μ and $B_{\mu\nu}$ can be expressed in terms of the external momentum p and further scalar functions,

$$B_\mu = p_\mu B_1, \quad (\text{B.24a})$$

$$B_{\mu\nu} = \eta_{\mu\nu} B_{00} + p_\mu p_\nu B_{11}, \quad (\text{B.24b})$$

where B_1 , B_{00} and B_{11} are all divergent functions. Similar, their divergences can be evaluated in a similar fashion to the one-point function. For simplicity, we will not perform explicit calculations here and they are listed in Tab. [B.1](#).

The three-point function C

The three-point functions are functions

$$C = C(p^2, (p-q)^2, q^2, m_1^2, m_2^2, m_3^2) \quad (\text{B.25})$$

that are defined as

$$C_0 \equiv \frac{\mu^\epsilon}{i\pi^2} \int d^d k \frac{1}{(k^2 - m_1^2) [(k+p)^2 - m_2^2] [(k+q)^2 - m_3^2]}, \quad (\text{B.26a})$$

$$C_\mu \equiv \frac{\mu^\epsilon}{i\pi^2} \int d^d k \frac{k_\mu}{(k^2 - m_1^2) [(k+p)^2 - m_2^2] [(k+q)^2 - m_3^2]}, \quad (\text{B.26b})$$

$$C_{\mu\nu} \equiv \frac{\mu^\epsilon}{i\pi^2} \int d^d k \frac{k_\mu k_\nu}{(k^2 - m_1^2) [(k+p)^2 - m_2^2] [(k+q)^2 - m_3^2]}, \quad (\text{B.26c})$$

$$C_{\mu\nu\rho} \equiv \frac{\mu^\epsilon}{i\pi^2} \int d^d k \frac{k_\mu k_\nu k_\rho}{(k^2 - m_1^2) [(k+p)^2 - m_2^2] [(k+q)^2 - m_3^2]}. \quad (\text{B.26d})$$

Again, the integrals with a tensor structure can be reduced to expressions containing tensor coefficient functions, that is,

$$C_\mu = p_\mu C_1 + q_\mu C_2, \quad (\text{B.27a})$$

$$C_{\mu\nu} = \eta_{\mu\nu} C_{00} + p_\mu p_\nu C_{11} + q_\mu q_\nu C_{22} + (p_\mu q_\nu + q_\mu p_\nu) C_{12}, \quad (\text{B.27b})$$

$$\begin{aligned} C_{\mu\nu\rho} = & (\eta_{\mu\nu} p_\rho + \eta_{\nu\rho} p_\mu + \eta_{\mu\rho} p_\nu) C_{001} + (\eta_{\mu\nu} q_\rho + \eta_{\nu\rho} q_\mu + \eta_{\mu\rho} q_\nu) C_{002} \\ & + (p_\mu p_\nu q_\rho + p_\mu q_\nu p_\rho + q_\mu p_\nu p_\rho) C_{112} + (q_\mu q_\nu p_\rho + q_\mu p_\nu q_\rho + p_\mu q_\nu q_\rho) C_{122} \\ & + p_\mu p_\nu p_\rho C_{111} + q_\mu q_\nu q_\rho C_{222}. \end{aligned} \quad (\text{B.27c})$$

From power counting, we find that C_0 and C_μ are finite, while $C_{\mu\nu}$ and $C_{\mu\nu\rho}$ contain divergences in ϵ . They are again summarized in Tab. B.1.

Of course, one can also define the four-point functions which contain 8 powers of k in the denominator of the integrand. Since they are not used in our calculations, we do not list them here.

Summary of the divergences

Integral	Divergent part
$A_0(m^2)$	$\frac{2}{\epsilon} m^2$
$B_0(p^2, m_1^2, m_2^2)$	$\frac{2}{\epsilon}$
$B_1(p^2, m_1^2, m_2^2)$	$-\frac{1}{\epsilon}$
$B_{00}(p^2, m_1^2, m_2^2)$	$-\frac{1}{6\epsilon} (p^2 - 3m_1^2 - 3m_2^2)$
$B_{11}(p^2, m_1^2, m_2^2)$	$\frac{2}{3\epsilon}$
C_{00}	$\frac{1}{2\epsilon}$
C_{001}	$-\frac{1}{6\epsilon}$
C_{002}	$-\frac{1}{6\epsilon}$

Table B.1: The divergent parts of the one-, two-, and three-point Passarino-Veltman functions [141].

Appendix C

Seesaw Mechanisms in Feynman Diagrams

Here, we consider the Feynman diagrams of the type-I and type-II seesaw mechanisms and derive the effective coupling of the Weinberg operator using the relevant Feynman rules.

In the type-I seesaw mechanism, due to the introduction of the RH neutrinos N_R , the new Yukawa coupling arises, which is given by

$$\mathcal{L}_Y = -\overline{N_R} y_N \tilde{\phi}^\dagger \ell_L - \overline{\ell_L} \tilde{\phi} y_N^\dagger N_R. \quad (\text{C.1})$$

Then the process of integrating out the RH neutrinos can be understood by considering the corresponding Feynman diagrams:

$$\text{Diagram 1} + \text{Diagram 2} \xrightarrow{p^2 \ll M_N^2} \text{Effective Vertex } \kappa \quad (\text{C.2})$$

The two Feynman diagrams on the left correspond to two possible topologies of the interaction vertices arisen from the Yukawa couplings among the RH neutrinos, the Higgs doublet and the lepton doublet, corresponding to the Lagrangian (C.1). At an energy scale much lower than the RH neutrino masses, that is, when all the particles' momenta are much smaller than the RH neutrino masses, $p^2 \ll M_N^2$, N_R are effectively integrated out. This means that the propagator line of N_R in the Feynman diagram can be ignored, resulting the effective vertex joining two Higgs doublets and two lepton doublets together, as shown in the Feynman diagram on the right. This effective interaction is characterized by the effective coupling κ . It can be determined by evaluating the Feynman diagrams above using the Feynman rules given in [142]

$$\begin{aligned} & \text{Diagram 1} + \text{Diagram 2} \\ &= [-i(y_N^T)_{\beta\gamma}\varepsilon_{cd}P_L] \frac{i(\not{p} + M_N)}{p^2 - M_N^2} [-i(y_N)_{\gamma\alpha}(\varepsilon^T)_{ab}P_L] + \\ & \quad [-i(y_N^T)_{\beta\gamma}\varepsilon_{ca}P_L] \frac{i(\not{p} + M_N)}{p^2 - M_N^2} [-i(y_N)_{\gamma\alpha}(\varepsilon^T)_{db}P_L] \\ & \xrightarrow{p^2 \ll M_N^2} i \cdot 2(y_N^T M_N^{-1} y_N)_{\beta\alpha} \cdot \frac{1}{2}(\varepsilon_{cd}\varepsilon_{ba} + \varepsilon_{ca}\varepsilon_{bd})P_L. \end{aligned} \quad (\text{C.3})$$

On the other hand, the Feynman rule of the effective vertex is given by

$$\begin{array}{c} \phi_d \\ \swarrow \\ \text{---} \end{array} \begin{array}{c} \ell_{Lc}^\beta \\ \nearrow \\ \text{---} \end{array} \begin{array}{c} \kappa \\ \square \end{array} \begin{array}{c} \ell_{Lb}^\alpha \\ \swarrow \\ \text{---} \end{array} \begin{array}{c} \phi_a \\ \searrow \\ \text{---} \end{array} = i\kappa_{\beta\alpha} \cdot \frac{1}{2}(\varepsilon_{cd}\varepsilon_{ba} + \varepsilon_{ca}\varepsilon_{bd})P_L. \quad (\text{C.4})$$

Matching this to the analytical expression in (C.3), we identify

$$\kappa = 2y_N^T M_N^{-1} y_N, \quad (\text{C.5})$$

which agrees with Eq. (3.43).

In the case of the type-II seesaw mechanism, the new interactions due to the addition of the $SU(2)_L$ scalar triplet Δ are given by

$$\mathcal{L}_I = -\Lambda(\phi^T i\tau_2 \Delta^\dagger \phi) - f_\Delta(\ell_L^T C i\tau_2 \Delta \ell_L) + \text{h.c.} \quad (\text{C.6})$$

There is only one Feynman diagram in the full theory that contributes to the effective operator at low energies

$$\begin{array}{c} \phi_d \\ \swarrow \\ \text{---} \end{array} \begin{array}{c} \ell_{Lc}^\beta \\ \nearrow \\ \text{---} \end{array} \begin{array}{c} \Lambda \\ \bullet \end{array} \begin{array}{c} \Delta_k \\ \text{---} \end{array} \begin{array}{c} f_\Delta \\ \bullet \end{array} \begin{array}{c} \ell_{Lb}^\alpha \\ \swarrow \\ \text{---} \end{array} \begin{array}{c} \phi_a \\ \searrow \\ \text{---} \end{array} \xrightarrow{q^2 \ll M_\Delta^2} \begin{array}{c} \phi_d \\ \swarrow \\ \text{---} \end{array} \begin{array}{c} \ell_{Lc}^\beta \\ \nearrow \\ \text{---} \end{array} \begin{array}{c} \kappa \\ \square \end{array} \begin{array}{c} \ell_{Lb}^\alpha \\ \swarrow \\ \text{---} \end{array} \begin{array}{c} \phi_a \\ \searrow \\ \text{---} \end{array} \quad (\text{C.7})$$

$$= [(f_\Delta)_{\beta\alpha}(\tau_2 \tau_k)_{cb}] \frac{i}{q^2 - M_\Delta^2} [\Lambda(\tau_2 \tau_k)_{ad}] \xrightarrow{q^2 \ll M_\Delta^2} -i \cdot 2 \frac{\Lambda}{M_\Delta^2} (f_\Delta)_{\beta\alpha} \cdot \frac{1}{2}(\varepsilon_{cd}\varepsilon_{ba} + \varepsilon_{ca}\varepsilon_{bd}).$$

Again, by matching this analytical expression to the effective vertex expression (C.4), we obtain the effective coupling for the type-II seesaw mechanism,

$$\kappa = -2 \frac{\Lambda}{M_\Delta^2} f_\Delta, \quad (\text{C.8})$$

which agrees with Eq. (3.51).

Appendix D

Summary of the Relevant Feynman Rules

Here we list the Feynman rules for a general n Higgs doublet model that were used in the calculations involved in this thesis. Following [143], we introduce the notion of fermion flow, which is indicated by a gray arrow in the diagrams. If the lepton number is conserved, it coincides with the lepton number flow. However, due to the presence of Majorana spinors, the lepton number is violated by 2. Thus, for leptons, the fermion flow may be parallel or antiparallel to the lepton number flow. As baryon number is conserved in our model, we do not need fermion flow for the quarks.

Propagators

For simplicity, we define the Majorana spinors $N^\alpha \equiv N_R^\alpha + (N_R^\alpha)^c$ to describe the heavy neutrinos.

$$\begin{array}{c} \text{---} \xrightarrow{\text{gray}} \text{---} \\ N^\alpha \quad N^\beta \end{array} : iS_N(p) = \frac{i(\not{p} + M_\alpha)}{p^2 - M_\alpha^2 + i\varepsilon} \delta_{\beta\alpha} \quad (\text{D.1a})$$

$$\begin{array}{c} \text{---} \xrightarrow{\text{gray}} \text{---} \\ \ell_{La}^\alpha \quad \ell_{Lb}^\beta \end{array} : iS_{\ell_L}(p) = \frac{i\not{p}}{p^2 + i\varepsilon} \delta_{\beta\alpha} \delta_{ba} \quad (\text{D.1b})$$

$$\begin{array}{c} \text{---} \xrightarrow{\text{gray}} \text{---} \\ e_R^\alpha \quad e_R^\beta \end{array} : iS_{e_R}(p) = \frac{i\not{p}}{p^2 + i\varepsilon} \delta_{\beta\alpha} \quad (\text{D.1c})$$

$$\begin{array}{c} \text{---} \xleftarrow{\text{gray}} \text{---} \\ \ell_{La}^\alpha \quad \ell_{Lb}^\beta \end{array} : iS_{\ell_L}(-p) = \frac{-i\not{p}}{p^2 + i\varepsilon} \delta_{\beta\alpha} \delta_{ba} \quad (\text{D.1d})$$

$$\begin{array}{c} \text{---} \xleftarrow{\text{gray}} \text{---} \\ e_R^\alpha \quad e_R^\beta \end{array} : iS_{e_R}(-p) = \frac{-i\not{p}}{p^2 + i\varepsilon} \delta_{\beta\alpha} \quad (\text{D.1e})$$

$$\begin{array}{c} \text{---} \xrightarrow{\text{gray}} \text{---} \\ Q_{La}^\alpha \quad Q_{Lb}^\beta \end{array} : iS_{Q_L}(p) = \frac{i\not{p}}{p^2 + i\varepsilon} \delta_{\beta\alpha} \delta_{ba} \quad (\text{D.1f})$$

$$\begin{array}{c} \text{---} \xrightarrow{\text{gray}} \text{---} \\ u_R^\alpha \quad u_R^\beta \end{array} : iS_{u_R}(p) = \frac{i\not{p}}{p^2 + i\varepsilon} \delta_{\beta\alpha} \quad (\text{D.1g})$$

$$\begin{array}{c} \text{---} \xrightarrow{\text{gray}} \text{---} \\ d_R^\alpha \quad d_R^\beta \end{array} : iS_{d_R}(p) = \frac{i\not{p}}{p^2 + i\varepsilon} \delta_{\beta\alpha} \quad (\text{D.1h})$$

$$\begin{array}{c} \text{---} \xrightarrow{\text{gray}} \text{---} \\ \phi_{ai} \quad \phi_{bj} \end{array} : iS_\phi(p) = (U^\dagger)_{ik} \frac{i}{p^2 - d_{kk}^2 + i\varepsilon} U_{kj} \delta_{ba} \quad (\text{D.1i})$$

$$\begin{array}{c} \text{---} \xrightarrow{\text{gray}} \text{---} \\ \Delta_a \quad \Delta_b \end{array} : iS_\Delta(p) = \frac{i}{p^2 - M_\Delta^2 + i\varepsilon} \delta_{ba} \quad (\text{D.1j})$$

$$\begin{array}{c} \text{~~~~~} \\ B^\mu \quad B^\nu \end{array} : iD_B^{\mu\nu}(p) = i \frac{-\eta^{\mu\nu} + (1 - \xi_1) \frac{p^\mu p^\nu}{p^2}}{p^2 + i\varepsilon} \quad (\text{D.1k})$$

$$\begin{array}{c} \text{~~~~~} \\ W^{s\mu} \quad W^{t\nu} \end{array} : iD_{W^s}^{\mu\nu}(p) = i \frac{-\eta^{\mu\nu} + (1 - \xi_2) \frac{p^\mu p^\nu}{p^2}}{p^2 + i\varepsilon} \delta_{st} \quad (\text{D.1l})$$

Gauge boson - lepton interactions

$$\begin{array}{c} \ell_{Lb}^\beta \\ \uparrow \\ \ell_{La}^\alpha \end{array} \begin{array}{c} B_\mu \\ \text{---} \end{array} : \frac{i}{2} \mu^{\frac{\epsilon}{2}} g_1 \delta_{\beta\alpha} \delta_{ba} \gamma_\mu P_L \qquad \begin{array}{c} \ell_{Lb}^\beta \\ \downarrow \\ \ell_{La}^\alpha \end{array} \begin{array}{c} B_\mu \\ \text{---} \end{array} : -\frac{i}{2} \mu^{\frac{\epsilon}{2}} g_1 \delta_{\alpha\beta} \delta_{ab} \gamma_\mu P_R \quad (\text{D.2a})$$

$$\begin{array}{c} \ell_{Lb}^\beta \\ \uparrow \\ \ell_{La}^\alpha \end{array} \begin{array}{c} W_\mu^s \\ \text{---} \end{array} : -\frac{i}{2} \mu^{\frac{\epsilon}{2}} g_2 \delta_{\beta\alpha} \tau_{ba}^s \gamma_\mu P_L \qquad \begin{array}{c} \ell_{Lb}^\beta \\ \downarrow \\ \ell_{La}^\alpha \end{array} \begin{array}{c} W_\mu^s \\ \text{---} \end{array} : \frac{i}{2} \mu^{\frac{\epsilon}{2}} g_2 \delta_{\alpha\beta} (\tau^{sT})_{ba} \gamma_\mu P_R \quad (\text{D.2b})$$

$$\begin{array}{c} e_R^\beta \\ \uparrow \\ e_R^\alpha \end{array} \begin{array}{c} B_\mu \\ \text{---} \end{array} : i \mu^{\frac{\epsilon}{2}} g_1 \delta_{\beta\alpha} \gamma_\mu P_R \qquad \begin{array}{c} e_R^\beta \\ \downarrow \\ e_R^\alpha \end{array} \begin{array}{c} B_\mu \\ \text{---} \end{array} : -i \mu^{\frac{\epsilon}{2}} g_1 \delta_{\alpha\beta} \gamma_\mu P_L \quad (\text{D.2c})$$

Gauge boson - Higgs interactions

In the 2HDM, the Higgs Lagrangian is given by

$$\mathcal{L}_\phi = (D_\mu \phi_i)^\dagger (D^\mu \phi_i) - m_{ij}^2 \phi_i^\dagger \phi_j - \frac{1}{4} \lambda_{ijkl} (\phi_i^\dagger \phi_j) (\phi_k^\dagger \phi_l). \quad (\text{D.3})$$

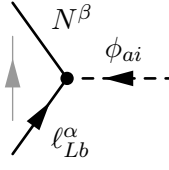
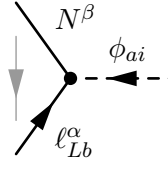
Hence, we see that the kinetic term is diagonal in the Higgs flavor space. The Feynman rules are then given by

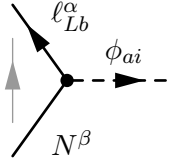
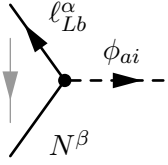
$$\begin{array}{c} \phi_{bj} \\ q \\ \nearrow \\ p \\ \searrow \\ \phi_{ai} \end{array} \begin{array}{c} B_\mu \\ \text{---} \end{array} : -\frac{i}{2} \mu^{\frac{\epsilon}{2}} g_1 (p_\mu + q_\mu) \delta_{ba} \delta_{ji} \quad (\text{D.4a})$$

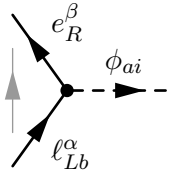
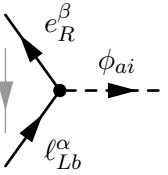
$$\begin{array}{c} \phi_{bj} \\ q \\ \nearrow \\ p \\ \searrow \\ \phi_{ai} \end{array} \begin{array}{c} W_\mu^s \\ \text{---} \end{array} : -\frac{i}{2} \mu^{\frac{\epsilon}{2}} g_2 (p_\mu + q_\mu) \tau_{ba}^s \delta_{ji} \quad (\text{D.4b})$$

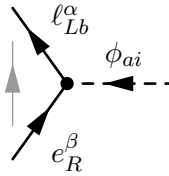
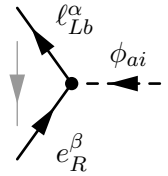
where p and q are the momenta of the Higgses. The quartic couplings between the gauge bosons and Higgses also exist but are not shown here because they are not used in this thesis.

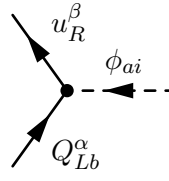
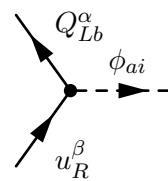
Yukawa interactions

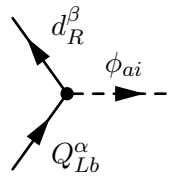
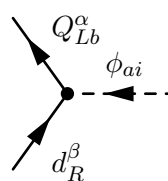

 $: -i\mu^{\frac{\epsilon}{2}}(Y_\nu^i)_{\beta\alpha}(\varepsilon^T)_{ab}P_L \quad (D.5a)$


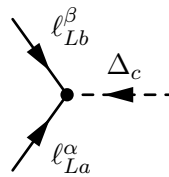
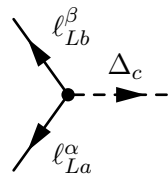

 $: -i\mu^{\frac{\epsilon}{2}}(Y_\nu^{i\dagger})_{\alpha\beta}\varepsilon_{ba}P_R$

 $: -i\mu^{\frac{\epsilon}{2}}(Y_\nu^{i*})_{\beta\alpha}(\varepsilon^T)_{ab}P_R \quad (D.5b)$


 $: -i\mu^{\frac{\epsilon}{2}}(Y_e^i)_{\beta\alpha}\delta_{ab}P_L$

 $: -i\mu^{\frac{\epsilon}{2}}(Y_e^{iT})_{\alpha\beta}\delta_{ab}P_L \quad (D.5c)$


 $: -i\mu^{\frac{\epsilon}{2}}(Y_e^{i\dagger})_{\alpha\beta}\delta_{ab}P_R$

 $: -i\mu^{\frac{\epsilon}{2}}(Y_e^{i*})_{\beta\alpha}\delta_{ab}P_R \quad (D.5d)$

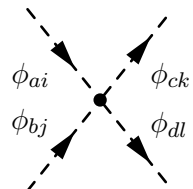

 $: -i\mu^{\frac{\epsilon}{2}}(Y_u^i)_{\beta\alpha}(\varepsilon^T)_{ab}P_L$

 $: -i\mu^{\frac{\epsilon}{2}}(Y_u^{i\dagger})_{\alpha\beta}\varepsilon_{ba}P_R \quad (D.5e)$


 $: -i\mu^{\frac{\epsilon}{2}}(Y_d^i)_{\beta\alpha}\delta_{ab}P_L$

 $: -i\mu^{\frac{\epsilon}{2}}(Y_d^{i\dagger})_{\alpha\beta}\delta_{ba}P_R \quad (D.5f)$


 $: \mu^{\frac{\epsilon}{2}}(Y_\Delta)_{\beta\alpha}(\tau_2\tau_c)_{ba}P_L$

 $: -\mu^{\frac{\epsilon}{2}}(Y_\Delta^\dagger)_{\alpha\beta}(\tau_c\tau_2)_{ab}P_R \quad (D.5g)$

Higgs-Higgs interactions

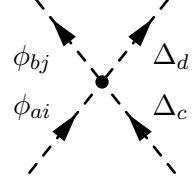
The Feynman rule for the quartic interaction between the Higgses is derived from the last term in Lagrangian (D.3). It is given by


 $: -i\mu^\epsilon \frac{1}{2}(\lambda_{kilj}\delta_{ca}\delta_{db} + \lambda_{kjli}\delta_{cb}\delta_{da}) \quad (D.6)$

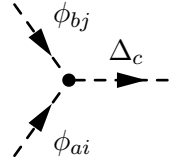
For the Higgs-Higgs interactions involving the $SU(2)_L$ scalar triplet Δ and the Higgs doublets ϕ_i , we derive the Feynman rules from the following Lagrangian:

$$\mathcal{L}_{(\Delta,\phi)} = -\Lambda_1^{ij} \phi_i^\dagger \phi_j \text{Tr}(\Delta^\dagger \Delta) - \Lambda_2^{ij} \phi_i^\dagger [\Delta^\dagger, \Delta] \phi_j - \left[\frac{\Lambda_3^{ij}}{\sqrt{2}} \phi_i^T i\tau_2 \Delta^\dagger \phi_j + \text{h.c.} \right] \quad (\text{D.7})$$

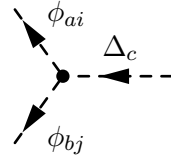
Then the Feynman rules are given by



$$: -i\mu^\epsilon \left[\Lambda_1^{ij} \delta_{ba} \delta_{dc} + \Lambda_2^{ij} i\varepsilon_{dcm} (\tau_m)_{ba} \right] \quad (\text{D.8a})$$

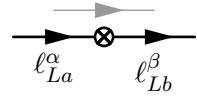


$$: \Lambda_3^{ij} \mu^{\frac{\epsilon}{2}} (\tau_2 \tau_c)_{ba} \quad (\text{D.8b})$$

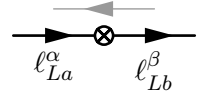


$$: -\Lambda_3^{ij*} \mu^{\frac{\epsilon}{2}} (\tau_c \tau_2)_{ab} \quad (\text{D.8c})$$

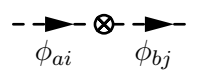
Counterterms for the two-point functions



$$: i\not{p} (\delta Z_{\ell_L})_{\beta\alpha} P_L \delta_{ba} \quad (\text{D.9a})$$

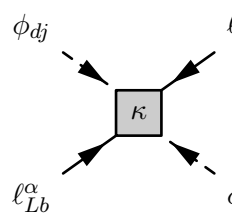


$$: -i\not{p} (\delta Z_{\ell_L})_{\beta\alpha} P_L \delta_{ba} \quad (\text{D.9b})$$

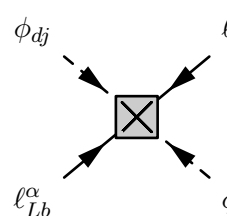


$$: i[p^2 (\delta Z_\phi)^{ij} - \delta m_{ij}^2] \delta_{ba} \quad (\text{D.9c})$$

Effective vertex and its counterterm



$$: i\mu^\epsilon \frac{1}{2} \left(\kappa_{\beta\alpha}^{ji} \varepsilon_{cd} \varepsilon_{ba} + \kappa_{\beta\alpha}^{ij} \varepsilon_{ca} \varepsilon_{bd} \right) \quad (\text{D.10a})$$



$$: i\mu^\epsilon \frac{1}{2} \left(\delta \kappa_{\beta\alpha}^{ji} \varepsilon_{cd} \varepsilon_{ba} + \delta \kappa_{\beta\alpha}^{ij} \varepsilon_{ca} \varepsilon_{bd} \right) \quad (\text{D.10b})$$

Acronyms

Here is the list of common acronyms that are used throughout the thesis in alphabetical order.

2HDM	Two Higgs doublet model
CMB	Cosmic microwave background
CP	Charge-parity
DR	Dimension regularization
EFT	Effective field theory
GUT	Grand unified theory
GWS theory	Glashow-Weinberg-Salam theory
IO	Inverted ordering
LH	Left-handed
LR	Left-right
LRSM	Left-right symmetric model
MS	Minimal subtraction
$\overline{\text{MS}}$	Modified minimal subtraction
NO	Normal ordering
PMNS matrix	Pontecorvo-Maki-Nakagawa-Sakata matrix
QED	Quantum electrodynamics
QFT	Quantum field theory
RH	Right-handed
RG	Renormalization group
RGE	Renormalization group equation
SM	Standard Model
UV	Ultraviolet
VEV	Vacuum expectation value